

The Multi-Step Activation of the Proprotein Convertase Furin

by

Eric David Anderson

A DISSERTATION

Presented to the Department of Cell and Developmental Biology

and the Oregon Health Sciences University

School of Medicine

in partial fulfillment of

the requirements for the degree of

Doctor of Philosophy

August 1999

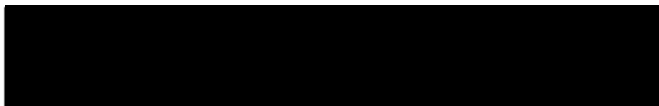
School of Medicine
Oregon Health Sciences University

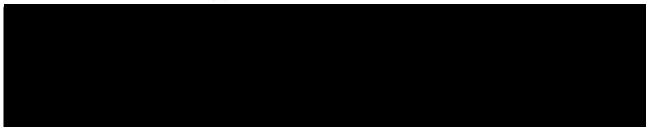
CERTIFICATE OF APPROVAL

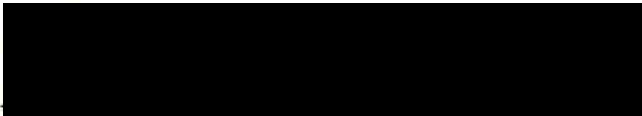
This is to certify that the Ph.D. thesis of


Eric David Anderson

has been approved


Professor in charge of thesis


Member


Member


Member

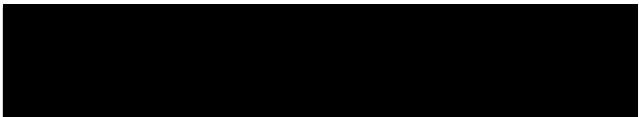

Associate Dean for Graduate Studies

TABLE OF CONTENTS

INTRODUCTION	1
I. Protein Folding in the Endoplasmic Reticulum	1
II. Quality Control in the Secretory Pathway	5
III. Intramolecular Chaperones	7
IV. Furin and the Proprotein Convertases.....	10
 CHAPTER ONE	21
Abstract.....	22
Introduction	23
Materials and Methods.....	25
Results.....	30
Discussion.....	34
Acknowledgements	38
Figures.....	39
 CHAPTER TWO	51
Abstract.....	52
Introduction	53
Materials and Methods.....	56
Results.....	61
Discussion.....	67
Acknowledgements	71
Figures and Table	72
 SUMMARY AND CONCLUSIONS	90
 REFERENCES	92

TABLE OF FIGURES AND TABLES

Introduction

Figure 1: Folding and Trafficking of Proteins in the Early Secretory Pathway	13
Figure 2: IMC-mediated Protease Folding	14
Figure 3: Structures of the Eukaryotic Proprotein Convertases	15
Figure 4: Furin Processing Compartments and <i>in vivo</i> furin substrates.....	17
Figure 5: Functional Domains of Furin	19

Chapter One

Figure 1: Schematic of furin constructs.....	39
Figure 2: Expression, immunoreactivity and <i>in vitro</i> activity of furin constructs.....	41
Figure 3: <i>In vitro</i> activation of ER-retained furin by low pH and calcium	42
Figure 4: Effect of pH on furin activation and time course of activation at pH 6.0	43
Figure 5: Limited trypsinization releases inhibition of furin at neutral pH	44
Figure 6: Inhibition of furin <i>in trans</i> by its propeptide	45
Figure 7: Fate of the propeptide during furin activation	46
Figure 8: MALDI-TOF mass spectra of propeptide cleavage products ..	47
Figure 9: Activation of R ₇₀ A:fur/f/haΔtc-k and R ₇₅ A:fur/f/haΔtc-k <i>in vitro</i>	48
Figure 10: Model of furin activation <i>in vivo</i>	49

Chapter Two

Figure 1: Schematic of furin constructs.....	72
Figure 2: Expression, immunoreactivity and <i>in vitro</i> activity of furin constructs	74
Figure 3: Glycosylation analysis of furin constructs	75

Figure 4: Retention of fur/f Δ pro and fur/fD ₁₅₃ N in the early secretory pathway.....	76
Figure 5: <i>In trans</i> restoration of activity and trafficking to fur/f Δ pro by the furin propeptide.	78
Figure 6: Autoproteolytic, intramolecular activation of furin.	80
Table I: Furin processing of native and mutant propeptide cleavage motifs.....	81
Figure 7: <i>In vivo</i> furin activation.	83
Figure 8: Furin•propeptide localization and propeptide dissociation.	84
Figure 9: Antibody uptake and internal propeptide cleavage	86
Figure 10: V ₇₂ R: fur/f/ha subcellular localization.....	88

ABBREVIATIONS

The following is a list of abbreviations used in this thesis:

BFA	Brefeldin A
BiP	Heavy Chain Binding Protein
BIVS	BFA-induced vesicular structures
CFTR	Cystic Fibrosis Transmembrane Conductance Regulator
CGN	<i>Cis</i> -Golgi Network
ER	Endoplasmic Reticulum
ERGIC	ER/Golgi Intermediate Compartment
FITC	Fluorescein Isothiocyanate
HA	Hemagglutinin
IMC	Intramolecular Chaperone
mAb	Monoclonal Antibody
MHC	Major Histocompatibility Complex
PC	Proprotein Convertase
PDI	Proline Disulfide Isomerase
PPI	Peptidyl-Prolyl Isomerase
RER	Rough Endoplasmic Reticulum
SBTI	Soy Bean Trypsin Inhibitor
SDS-PAGE	Sodium Dodecyl Sulfate Polyacrylamide Gel Electrophoresis
TGN	<i>Trans</i> -Golgi Network
TxRd	Texas Red
VSV G	Vesicular Stomatitis Virus

ACKNOWLEDGMENTS

I would like to thank a number of people who have inspired me and contributed to this project. I would like to thank members of the Gary Thomas laboratory at the Vollum Institute of Oregon Health Sciences University. Special thanks go to Gary Thomas, whose teaching and mentoring has been invaluable, not only with this thesis, but with my undergraduate thesis as well. I would like to thank both Gary and Steve Arch of Reed College for easing the transition from undergraduate to graduate study of biology and for being first-rate teachers and mentors. Thanks also go to Ms. German, my biology teacher at Moses Brown High School in East Providence, Rhode Island, for inspiring my interest in biology in the first place, and to my parents, Jim and Diana Anderson. Finally, and most importantly, I would like to thank my wife, Rebecca Rix. Without her support I would not have even started this dissertation, let alone been able to finish it.

ABSTRACT

Furin, a serine endoprotease of the proprotein convertase family, is localized to the *trans*-Golgi network (TGN)/endosomal system where it cleaves/activates many precursor secretory proteins at the consensus site -Arg-X-Lys/Arg-Arg[↓]-. Synthesized as an inactive zymogen with an 83-amino acid N-terminal propeptide, furin's activation requires ER-localized autoproteolytic excision of its propeptide at -Arg-Thr-Lys-Arg₁₀₇[↓]- [Leduc et al. 1992. *J. Biol. Chem.* 267:14304-14308]. While propeptide excision is necessary for furin activation, it is not sufficient: activation also requires exposure to late secretory pathway compartments [Molloy et al. 1994. *EMBO J.* 13:18-33; Vey et al. 1994. *J. Cell Biol.* 127:1829-1842]. This thesis identifies i) the steps necessary for furin activation following propeptide excision and ii) a potential role for the propeptide in furin folding by a combination of *in vitro* and *in vivo* analysis. The first chapter describes an *in vitro* study in which it was found that furin undergoes a multi-step pH-dependent process of activation. Following propeptide excision, the furin propeptide remains non-covalently bound to the enzyme, acting as an autoinhibitor ($K_{0.5}$ =14 nM). Exposure of the inactive furin•propeptide complex to a mildly acidic (pH 6.0) and calcium-containing (low millimolar) environment characteristic of the TGN results in a second cleavage within the propeptide at -Arg₇₀-Gly-Val-Thr-Lys-Arg₇₅[↓]-. Concomitant with internal cleavage, the propeptide fragments dissociate from furin, permitting the enzyme to cleave substrates *in trans*. These *in vitro* findings suggest a model in which furin specifically becomes active within the TGN, the enzyme's compartment of residence. In the second chapter we i) explored the possibility that the propeptide might act as an 'intramolecular chaperone' (IMC) responsible for mediating the folding of furin, and ii) verified that our model of *in vitro* furin activation accurately represented the *in vivo* process. Consistent with the role of the furin propeptide as an IMC we found that i) a furin mutant lacking the propeptide is ER-localized and inactive, ii) co-expression of the propeptide *in trans* partially restored both trafficking and activity and iii) failure of furin to excise the propeptide at -Arg₁₀₇[↓]- results in ERGIC/CGN-localization of furin, suggesting incomplete folding and selective retention by the quality control system. Further, consistent with the prediction made from our *in vitro* experiments, we found that following folding, propeptide excision, and transport to the late secretory pathway, furin autoproteolytically and predominantly intramolecularly cleaves its propeptide at -Arg₇₅[↓]-. Selective, pH-sensitive cleavage of the internal propeptide cleavage site sequence was demonstrated *in vitro* using synthetic peptide substrates. Unlike propeptide excision, blocking cleavage at -Arg₇₅[↓]- *in vivo* does not result in a detectable trafficking defect. Unexpectedly, the integrity of the P1/P6 Arg internal cleavage site motif

is essential to correct furin folding. Introduction of a P4 Arg into the site of internal propeptide cleavage (-Arg-Gly-Val₇₂-Thr-Lys-Arg₇₅- → -Arg-Gly-**Arg**₇₂-Thr-Lys-Arg₇₅-) in order to generate an -Arg-X-Lys/Arg-Arg[↓]- consensus cleavage motif, blocks propeptide excision and prevents exit from the ER. A speculative model for the folding of furin, based on differential access of these two propeptide cleavage sites to furin's substrate binding pockets, is discussed.

INTRODUCTION

The correct folding of secretory proteins is essential to cellular homeostasis. Genetic mutations resulting in secretory proteins with folding defects have been demonstrated or implicated as causative agents in disorders as diverse as Alzheimer's disease [aggregation of β -amyloid (Lansbury, 1999)], cystic fibrosis [misfolding of CFTR (reviewed in Kopito, 1999)], hereditary blindness [misfolding of rhodopsin (Kaushal and Khorana, 1994)], inheritable emphysema [misfolding of α_1 -antitrypsin (Qu et al., 1996)], and Marfan's syndrome [misfolding of fibrillin (Ramirez, 1996)], among others (reviewed Kuznetsov and Nigam, 1998; Thomas et al., 1995b). Further, when the mammalian nervous system protein PrP undergoes a specific conformational change ($\text{PrP}^{\text{sen}} \rightarrow \text{PrP}^{\text{res}}$), it becomes a 'prion,' the causative agent of the transmissible human neurodegenerative disorder Creutzfeldt-Jakob disease (reviewed in Johnson and Gibbs, 1998; Prusiner, 1998; Prusiner et al., 1998).

Many secretory proteins are initially synthesized as larger inactive precursors that, following folding, undergo selective proteolytic cleavage in the late secretory pathway to yield smaller, biologically active products. A ubiquitous eukaryotic endoprotease involved in this process is furin, a member of the 'proprotein convertase' (PC) family (reviewed in Molloy et al., 1999). Furin, like other PCs, is produced from a larger, inactive precursor with an N-terminal propeptide. Furin undergoes a compartment-specific, pH-dependent process of folding and activation involving coordinated autoproteolytic propeptide cleavages (Anderson et al., 1997). This activation process, including the possible role of the propeptide in the folding of furin, is the focus of the research presented in this dissertation. This introduction provides information necessary for placing this research in the context of previous work on protein folding and maturation *in vivo*. The information divided into four sections as follows: Section I) how proteins in the secretory pathway fold, Section II) how a system of 'quality control' in the secretory pathway retains and degrades proteins that do not fold correctly, Section III) how certain endoproteases, including a bacterial homologue of furin, undergo a propeptide-mediated folding process, and Section IV) an overview of relevant research on furin.

I. Protein Folding in the Endoplasmic Reticulum

Our understanding of furin folding is informed by the current model for global, hierarchic protein folding (reviewed in Dobson and Karplus, 1999; Eaton, 1999; Onuchic et al., 1995;

Radford and Dobson, 1999).¹ In this model i) a protein's amino acid sequence contains all of the information necessary for attainment of the native state (Anfinsen, 1973), and ii) the process of folding can be represented as an energy 'funnel' consisting of decreasing numbers of folding intermediates of decreasing energy, with the lowest-energy native state at the bottom. Beginning as a random coil, a folding protein rapidly undergoes a 'hydrophobic collapse' in which hydrophobic residues interact with one another to prevent interactions with the aqueous solvent (Duan and Kollman, 1998; Eaton et al., 1997). Hydrophobic collapse results in a 'compact intermediate,' which has some native-like secondary structure caused by the strength of local interactions, but little or no fixed tertiary structure (reviewed in Baldwin and Rose, 1999a; Baldwin and Rose, 1999b; Fink, 1995). The amount of native secondary and tertiary structure incrementally increases while the protein passes through numerous short-lived intermediates of decreasing energy (Baldwin and Rose, 1999a; Baldwin and Rose, 1999b; Matthews, 1993). These intermediates typically have exposed hydrophobic surfaces, which persist until folding is complete (Broglia et al., 1998). The folding process may be facilitated by the appearance of specific sub-domains of entirely native structure that act as 'nuclei' around which the rest of the protein folds (Shakhnovich et al., 1996; Shakhnovich, 1997). As folding progresses, the number of intermediates accessible to the protein decreases, and some proteins are observed to pass through long-lived folding intermediates due to kinetic constraints (Matthews, 1993). Whether these intermediates speed (Wagner and Kiefhaber, 1999) or slow (Fersht, 1995; Fersht, 1997) folding is unclear. It has been proposed that all proteins pass through the 'molten globule' intermediate near the end of the folding process (Ptitsyn et al., 1990). The 'molten globule' is proposed to be less compact than the native state, and to have native-like secondary structure, but no rigid tertiary structure (Ptitsyn et al., 1990). Ultimately, the folding protein finds the minimum-energy native state through the correct formation of many non-covalent interactions (reviewed in Dobson and Karplus, 1999; Eaton, 1999; Onuchic et al., 1995; Radford and Dobson, 1999).

In mammalian cells, secretory proteins, such as furin, are translated by cytosolic ribosomes and are typically co-translationally translocated into the lumen of the endoplasmic reticulum (ER) (Rapoport et al., 1996), the compartment in which they fold (see Figure 1). Translocation into the ER occurs by passage of the nascent protein through the heterotrimeric sec61p pore of the macromolecular complex called the 'translocon' (reviewed in Matlack et al., 1998; Rapoport et al., 1996). The ER's lumen provides an optimal environment for protein folding and oligomerization as its pH is ~7 (Kim et al., 1998) and it is an oxidizing environment relative to the cytoplasm due primarily to high concentrations of oxidized glutathione (Hwang et al., 1992), thus facilitating the formation of disulfide bonds (Huppa and Ploegh, 1998).

¹ Recently, a model for non-hierarchic folding has been proposed ('nucleation condensation'; Fersht, 1997), although its significance is disputed (Baldwin and Rose, 1999a; Baldwin and Rose, 1999b).

In the ER lumen, secretory protein folding can be accelerated and/or modified in several ways. For example, folding may be accelerated by 'folding catalysts' that assist in specific, rate limiting folding steps. Examples include peptidyl-prolyl isomerase (PPI), which assists in correct proline isomerization (Freskgard et al., 1992), and protein disulfide isomerase (PDI), which assists in correct disulfide bond formation (Ferrari and Soling, 1999). Further, glycosylation and subsequent carbohydrate modifications influence protein folding and assembly both directly (Jaenicke, 1991; Marquardt and Helenius, 1992) and indirectly (Gahmberg and Tolvanen, 1996; Helenius, 1994). This is of great significance, as >90% of known secretory proteins are glycosylated (Gahmberg and Tolvanen, 1996).

There are two very significant *in vivo* difficulties that must be overcome for a secretory protein to fold correctly. First, the N-terminus of a domain of a translocating protein would, in the absence of intervening factors, begin to fold in the ER lumen before the C-terminus of that domain had been synthesized (see Helenius et al., 1992; Netzer and Hartl, 1997; Rothman, 1989). This could lead to misfolding and aggregation, as protein domains typically need the entirety of their sequence to fold correctly (Jaenicke, 1987). Thus, protein folding occurs in a vectorial fashion *in vivo*, not globally as it is often studied *in vitro* (see Netzer and Hartl, 1997; Fedorov and Baldwin, 1997). Second, in the lumen of the ER a folding secretory protein encounters protein concentrations that may be in excess of 100 mg/ml (Koch, 1987), which could result in many intermolecular interactions. These interactions could result in aggregation, as hydrophobic patches on folding intermediates can bind intermolecularly (Broglia et al., 1998). If not prevented, intermolecular binding can lead to heterotypic (Sawyer et al., 1994) or homotypic (DeFelippis et al., 1993; Oberg et al., 1994) aggregation.

Because of these *in vivo* complications, many proteins require the assistance of 'molecular chaperones' to fold without aggregating (reviewed in Ellis and Hartl, 1999). A molecular chaperone is a protein that stabilizes an otherwise unstable conformer of another protein by cycles of controlled binding and release (Hartl, 1996).² Molecular chaperones in the ER prevent nascent proteins from folding until translation and translocation are complete, and effectively create conditions of 'infinite dilution' that prevent folding intermediates from aggregating. By cyclically binding and releasing the exposed hydrophobic residues of their 'substrate', chaperones prevent non-productive intra- and inter-molecular hydrophobic interactions (Rothman, 1989). Molecular chaperones do not guide the 'substrate' along a specific folding pathway, nor do they impart any steric information; rather, chaperones serve to keep the protein on a pathway of spontaneous

² There are conflicting definitions of 'molecular chaperone' (Hartl, 1996). In one definition, a molecular chaperone is any protein that aids in the self-assembly of another protein, but is not part of the native, functional state (Ellis and Hartl, 1999). By this definition, both PPI and PDI are molecular chaperones. I have chosen to use the definition of molecular chaperone that excludes PPI and PDI.

folding (Baker and Agard, 1994; Ellis and Hartl, 1999). Hence, molecular chaperones have been referred to as 'non-steric chaperones' (Ellis, 1998). It is worth pointing out that molecular chaperones do not increase the rate of protein folding, but rather increase the yield of properly folded protein (thus distinguishing them from folding catalysts). The fundamental importance of molecular chaperones is underscored by several observations: i) chaperones are ubiquitous (Hartl, 1996), ii) they are one of the major protein components of the cell and may outnumber their 'substrates', iii) genetic knockouts of certain chaperones are lethal (Helenius et al., 1997), iv) there are currently 20 known families of chaperone proteins (Ellis, 1999) and v) expression of these already abundant proteins is upregulated greatly when cells are stressed (reviewed in Chapman et al., 1998; Kim and Arvan, 1998; Pahl and Baeuerle, 1997; Sidrauski et al., 1998).

The best studied ER chaperones are BiP and calnexin (Helenius et al., 1997; Kim and Arvan, 1998; Krause and Michalak, 1997). BiP (a member of the HSP70 family) is a 78 kDa soluble ER-retained protein that cyclically binds and releases exposed hydrophobic residues in an ATP-dependent fashion (reviewed in Bukau and Horwich, 1998). BiP carries out this function in conjunction with co-factors *in vivo* such as J proteins which regulates BiP's substrate specificity (Misselwitz et al., 1998). BiP prefers to bind 7-8 residue primary sequences containing certain aromatic and hydrophobic residues (Blond-Elguindi et al., 1993; Flynn et al., 1991; Fourie et al., 1994). In addition to its role in protein folding, BiP is essential for the translocation of proteins into the ER (Lyman and Schekman, 1997) by acting as a 'molecular ratchet' (Matlack et al., 1999) as demonstrated by *in vitro* reconstitution experiments with yeast.

In contrast to BiP, the 65 kDa, ER-localized chaperone calnexin, the only known membrane-anchored chaperone, depends on its 'substrate's' glycosylation state for binding (reviewed in Helenius et al., 1997; Kim and Arvan, 1998). Translocating proteins with the consensus sequence for the addition of N-linked glycans (Asn-X-Thr/Ser) in many cases have a core glycan moiety added *en bloc* to the Asn residue, an antenna of which ends in three glucose residues. These glucose residues are removed in a stepwise fashion by glucosidase I (terminal glucose) and glucosidase II (two remaining glucoses). The enzyme UDP-Glc:glycoprotein glucosyl transferase (UGTR) can counteract the action of glucosidase II by adding back a single glucose residue to the completely deglycosylated species. UGTR only monoglucosylates proteins that are in non-native states (Sousa and Parodi, 1995). Calnexin cyclically binds the short-lived monoglucosylated intermediate allowing for further 'monitoring' by UGTR (Zapun et al., 1997). Calnexin may make protein/protein interactions with its 'substrates,' although this is a matter of considerable dispute (reviewed in Helenius et al., 1997). It is therefore unclear precisely how calnexin carries out its chaperone function. Like BiP, calnexin interacts with translocating proteins (Bergeron et al., 1994; Chen et al., 1995; Kim and Arvan, 1995), and calnexin's cytoplasmic tail

binds to membrane bound ribosomes (Chevet et al., 1999). Both observations suggest a direct role for calnexin in preventing the misfolding of translocating proteins.

The correct folding of a single polypeptide chain may be assisted by multiple chaperones. It is a matter of debate whether i) a folding protein interacts with a single chaperone, or defined linear sequence of chaperones, until it completes folding (the 'pathway model'), or ii) a folding protein interacts with any of a number of simultaneously competing chaperones in different combinations (the 'network' model) (reviewed in Ellis, 1999). Experimental evidence exists to support both hypotheses (Buchberger et al., 1996; Farr et al., 1997; Helenius et al., 1997; Kim and Arvan, 1995; Melnick et al., 1994). It is clear, however, that some chaperones have overlapping specificity. For example, the MHC class I, which ordinarily requires calnexin for assembly (Jackson et al., 1994), is able to assemble without calnexin in a cell line that has upregulated BiP expression (Balow et al., 1995).

II. Quality Control in the Secretory Pathway

Eukaryotic cells carefully monitor secretory protein folding. If a protein misfolds, it is retained in the ER for eventual degradation in a process called 'quality control' (Bonifacino and Weissman, 1998; Hammond and Helenius, 1995; Helenius et al., 1992; Hurtley and Helenius, 1989; Kim and Arvan, 1998). This 'quality control' system retains misfolded proteins primarily either by persistent chaperone binding, or selective exclusion of misfolded protein aggregates from transport vesicles budding from the ER (reviewed in Kim and Arvan, 1998). It should be noted that there are additional, as yet poorly defined, mechanisms for the ER retention and for the post-ER/pre-Golgi localization of misfolded proteins (discussed below).

The ER is the primary site of oligomerization in the secretory pathway, and oligomerization is often required for ER exit (Hurtley and Helenius, 1989). Therefore, the quality control system monitors the quaternary structures of secretory proteins in addition to secondary and tertiary structures. In some instances, incompletely assembled subunits of macromolecular complexes are retained in the ER through chaperone binding [e.g. thrombospondin (Prabakaran et al., 1996)]. Additionally, some proteins with exposed free thiol residues, which are often used for covalently linking protein subunits, are retained in the ER [rather than retrieved (Isidoro et al., 1996)] even if these subunits are otherwise properly folded [e.g. IgM μ H chain (reviewed in Reddy and Corley, 1998)]. The molecular mechanism(s) responsible for free-thiol binding are poorly understood.

Some misfolded proteins escape the ER-quality control system, but encounter post-ER quality control mechanisms that prevent them from progressing to the late secretory pathway (reviewed in Hammond and Helenius, 1995). For example, at prolonged high levels of

expression, a misfolded VSV G mutant can escape the ER only to be retrieved in the ERGIC/CGN (Hammond and Helenius, 1994). A mechanism for retrieval was suggested based on the finding that post-ER, misfolded VSV G is bound to BiP (Hammond and Helenius, 1994). Hammond and Helenius (1994) proposed that post-ER misfolded VSV G•BiP may be retrieved when BiP is bound and retrieved by the KDEL receptor, thus bringing the VSV G along with it. Similarly, unassembled MHC class I molecules are retrieved from the CGN and brought back to the ER (Hsu et al., 1991), although the mechanism of retrieval is unknown. Further, proteins with uncleaved glycosphosphatidyl inositol membrane anchor attachment signals have been suggested to accumulate in the ERGIC/CGN (Field et al., 1994; Moran and Caras, 1992). The nature of this retention mechanism is also unknown.

Misfolded, ER-retained secretory proteins are degraded following a variable lag period (reviewed in Bonifacino and Weissman, 1998; Cresswell and Hughes, 1997; Kopito, 1999; Plemper and Wolf, 1999; Sommer and Wolf, 1997). Most commonly, both membrane anchored and soluble misfolded proteins undergo retrograde translocation, or 'dislocation' via the heterotrimeric sec61p pore (Pilon et al., 1997; Plemper et al., 1997; Wiertz et al., 1996), in association with other translocon components (Plemper et al., 1997). Once in the cytosol these proteins are deglycosylated, ubiquitinated in most cases, and rapidly degraded by the proteasome (reviewed in Bonifacino and Weissman, 1998). The signal for triggering degradation appears to be (at least in part) prolonged chaperone association (Beggah et al., 1996; Knittler et al., 1995; Qu et al., 1996), and blocking this association protects misfolded proteins from degradation (Beggah et al., 1996; Liu et al., 1999; McCracken and Brodsky, 1996).

In addition to dislocation and proteosomal degradation, there are alternate pathways for degrading misfolded ER-retained proteins. For instance, there is morphological evidence that regions of ER membrane containing aggregated proteins are directly converted into lysosomes (Noda and Farquhar, 1992). There is also accumulating evidence for the existence of ER localized cysteine proteases that degrade HMG-CoA reductase (Moriyama et al., 1998) and apolipoprotein B (Adeli et al., 1997; Wu et al., 1997).

If a secretory proteins folds/assembles correctly, it is exported from the ER in coated transport vesicles (see Figure 1). These vesicles are suggested to be coated with COPII, although this is still a controversial issue (see Gaynor et al., 1998). In some cases export may be preceded by specific sorting and concentration of the protein (reviewed in Mellman and Warren, 1999; Nishimura et al., 1999; Teasdale and Jackson, 1996). Further, export of certain proteins may be mediated by 'transport receptors' (Herrmann et al., 1999) that provide information required for entry into the transport vesicles [e.g. ERGIC-53's action on coagulation factors V and VII (Nichols et al., 1998) and cathepsin C (Vollenweider et al., 1998)]. Once packaged into COPII coated transport vesicles (Scales et al., 1997), a secretory protein move from the ER to the ER-

Golgi Intermediate Compartment (ERGIC; see Bannykh et al., 1998; Farquhar and Palade, 1998; Kaiser and Ferro-Novick, 1998 for reviews). It is currently unclear if the ERGIC is i) a static compartment or ii) a transient intermediate composed of fused vesicles. The best studied ERGIC marker is ERGIC-53, which cycles between the ER and the Golgi, but is concentrated in the ERGIC (reviewed in Itin et al., 1995). From the ERGIC, COPI coated vesicular structures containing secretory proteins (Scales et al., 1997) move to the *cis*-Golgi Network (CGN). The CGN is defined as the *cis*-most Golgi cisternae and numerous associated vesicles. Like the ERGIC, it is unclear if the CGN is a static compartment or the result of the fusion of transport intermediates (reviewed in Bannykh et al., 1998). The exact relationship/distinction between the ERGIC and CGN has not been clearly defined (Kaiser and Ferro-Novick, 1998), although the CGN has been shown to have several distinct marker proteins [e.g. the Golgi calcium binding protein CALNUP (Lin et al., 1998; Lin et al., 1999) and the microtubule binding protein GMAP-210 (Infante et al., 1999)]. From the CGN, secretory proteins pass through the Golgi and TGN to the late secretory pathway.

III. Intramolecular Chaperones

Furin has been proposed to fold in a process mediated by its 83 residue N-terminal propeptide (see Section IV). This proposal is informed by the finding that many evolutionarily unrelated classes of protease (e.g. serine-, aspartyl-, cysteinyl- and metallo-proteases) have a type of propeptide called an 'intramolecular chaperone' (IMC) that guides the folding of its cognate protease (reviewed in Baker et al., 1993) (see Figure 2). Following IMC-mediated folding, IMC propeptides are autoproteolytically excised and (sometimes autoproteolytically) degraded, leaving the protease in its native state. IMC-mediated folding is ideal for a protease that has to be stable in a harsh environment surrounded by other proteases (reviewed in Baker, 1998; Baker et al., 1993). Since even local protein breathing may result in degradation, these proteases have a large kinetic barrier to unfolding that keeps the enzyme 'locked' in its native state. This kinetic barrier must be overcome late during the process of folding. IMC propeptides serve to increase the folding rate of their cognate proteases by lowering this kinetic barrier late in the folding pathway by means of stabilizing a high-energy folding intermediate (reviewed in Baker, 1998; Baker et al., 1992b; Shinde and Inouye, 1993). Thus, in contrast to molecular chaperones, which suppress off-pathway folding reactions (i.e. aggregation), IMCs increase the rate of the forward folding reaction. For that reason, IMC-mediated folding has been described as being under 'kinetic control' (Baker, 1998; Baker and Agard, 1994; Baker et al., 1992b).

The most thoroughly investigated examples of IMC-mediated protease folding are those of the secreted bacterial endoproteases α -lytic protease and subtilisin. Alpha-lytic protease and subtilisin have 166 / 198 residue and 77 / 275 residue pro / catalytic domains, respectively. Both degradative endoproteases fold in the periplasmic space and subsequently excise their N-terminal propeptides by single cleavages (Fujishige et al., 1992; Power et al., 1986). Propeptide excision triggers conformational changes that have been proposed to mark the end of the folding process (Anderson et al., 1999; Shinde et al., 1999). Failure to excise the propeptide results in a zymogen folding intermediate with exposed hydrophobic surfaces (Anderson et al., 1999; Shinde et al., 1999), and this intermediate is retained in the periplasmic space *in vivo* (Fujishige et al., 1992; Power et al., 1986). The propeptides of both subtilisin and α -lytic protease are required for correct folding of their catalytic domains and facilitate this process both *in vitro* and *in vivo* (Ikemura and Inouye, 1988; Power et al., 1986; Silen et al., 1989; Zhu et al., 1989). IMC-mediated folding of subtilisin and α -lytic protease can be guided by non-covalently linked propeptide *in trans* (Baker et al., 1992a; Eder et al., 1993b; Silen et al., 1989; Strausberg et al., 1993). Thus, energy liberated from propeptide excision is not required for the folding of either protease.

Following excision, the propeptides of subtilisin and α -lytic protease remain non-covalently associated with their cognate enzymes, acting as tight binding autoinhibitors (Baker et al., 1992a; Li et al., 1995). Crystal structures reveal that the propeptide's C-terminal residues occupy the cognate proteases' substrate-binding clefts, while the rest of the propeptide is folded into a separate domain bound at a distance from the active site (Bryan et al., 1995; Gallagher et al., 1995; Sauter et al., 1998). Thus, propeptide mediated inhibition is caused by the propeptide cleavage site sequence sterically occluding the active site (Sohl et al., 1997). Interestingly, Peters and co-workers (1998) have demonstrated a critical role for these C-terminal IMC residues in the folding of α -lytic protease. This group found that removal or mutagenesis of the four residues at the propeptide excision site could greatly diminish propeptide folding activity *in trans* (up to $>10^6$ fold) (Peters et al., 1998). Work on subtilisin has yielded comparable results (Li et al., 1995), suggesting that the use of these C-terminal residues for IMC action may be a general mechanism for propeptide mediated folding. These residues may be directly involved in the folding of the active site (Baker, 1998).

Given that IMCs bind and inhibit their cognate proteases, these propeptides must be degraded for enzyme activation. In the cases of subtilisin and α -lytic protease, the propeptides are rapidly degraded following folding. Degradation of the subtilisin propeptide has been speculated to be an intermolecular, autoproteolytic event, with an already active-subtilisin molecule cleaving a methionine-rich site in the propeptide of an inactive subtilisin•propeptide complex (Bryan et al., 1995). By contrast, the propeptide of α -lytic protease has been suggested to be degraded *in trans* by an unknown protease(s) *in vivo* (Sauter et al., 1998). The rapidity of propeptide degradation

for both bacterial enzymes has prevented rigorous study of the importance of this process to folding and activation (Bryan et al., 1995).

The specific molecular mechanisms by which the subtilisin and α -lytic protease propeptides guide folding is of great interest. It is currently believed that a significant kinetic barrier to folding exists very late in the folding process, and that further folding requires that the propeptide stabilizes a high-energy folding intermediate (reviewed in Baker, 1998). In subtilisin, the propeptide-stabilized folding barrier is believed to involve the formation of an α - β - α substructure (Bryan et al., 1995; Gallagher et al., 1995), while in α -lytic protease it appears to be the formation of a β -hairpin (Sauter et al., 1998). Once formed, these structures may act as folding nuclei around which the rest of the protease folds (Bryan et al., 1995; Gallagher et al., 1995). Folding intermediates that have reached this late kinetic barrier have been characterized for both α -lytic protease and subtilisin. Following denaturation and subsequent removal of denaturant in the absence of the propeptide, both subtilisin and α -lytic protease adopt an inactive, partially folded state called the 'I state' (Baker et al., 1992b; Eder et al., 1993b). The I state is extremely stable and has the characteristics of a molten globule folding intermediate, as it is less compact than the native state and it contains significant secondary structure with little or no organized tertiary structure (Baker et al., 1992b). This intermediate does not interconvert with the native state on a biologically relevant time scale [$t_{1/2} > 2,000$ years in the case of α -lytic protease (Sauter et al., 1998)] illustrating the difficulty of overcoming this kinetic folding barrier in the absence of the propeptide.

In order to reach its native state, protease in the I state must undergo a conformational change via a high energy folding intermediate (reviewed in Baker, 1998). This intermediate is 'native-like' in structure and is stabilized by the propeptide. The addition of cognate propeptide *in trans* to either subtilisin or α -lytic protease in the I state causes rapid conversion to the native state (Baker et al., 1992b; Eder et al., 1993b; Strausberg et al., 1993). The role of the propeptide in stabilizing a 'native-like' folding intermediate is supported by the binding of propeptides to the native states of their cognate enzymes resulting in enzyme inhibition (reviewed in Baker and Agard, 1994; Sohl et al., 1997). It should be noted, however, that propeptides probably bind to the 'native-like' folding intermediate more strongly than to the native state itself (Peters et al., 1998; Sohl et al., 1998).

Given the strong kinetic character of IMC-mediated folding, it was speculated that some IMC-folded proteases might be metastable (Baker and Agard, 1994), rather than being at the global energy minimum as suggested by the standard model of protein folding (see Section I). Recent experimentation has demonstrated that this is indeed the case for α -lytic protease: in the absence of the propeptide, the molten globule I state is thermodynamically more stable than the native species (Sohl et al., 1998). The metastability of α -lytic protease suggests the possibility of 'protein memory' (Baker and Agard, 1994). In theory, there could be numerous kinetically trapped

'native' states for a protease that could be accessed by different IMC sequences. Hence, the protease could 'remember' steric information from the IMC that mediated its folding even after that IMC had been degraded.

The existence of protein memory was demonstrated experimentally using subtilisin (Shinde et al., 1997). A subtilisin propeptide containing a specific point mutation causes subtilisin to fold into a kinetically stable 'altered' conformation. This 'altered' conformation displays biophysical and enzymatic properties different than subtilisin folded with the wild-type propeptide (Shinde et al., 1997), and the 'imprinting' of this information occurs late in the folding process (Shinde et al., 1999). Since IMCs convey steric information to their cognate proteases, in marked contrast to molecular chaperones, they have been termed 'steric chaperones' (Ellis, 1998).

IV. Furin and the Proprotein Convertases

Following folding, many secretory proteins are proteolytically modified in late secretory pathway compartments. Single or multiple endoproteolytic cleavages of these proteins result in the release of smaller, bioactive products. A class of endoproteases in eukaryotes responsible for cleavage at sites containing oligo basic amino acids are the proprotein convertases (PCs; see Figure 3). These calcium-dependent serine endoproteases are homologous to bacterial subtilisin. Members of the PC family include Kex2p, which catalyzes the activation of α -mating pheromone in yeast, and many Kex2p homologues expressed in higher eukaryotes including PC1/3, PC2, PC4, PC5/6, LPC/PC7/8, PACE-4 and furin (see Molloy et al., 1999; Nakayama, 1997; Seidah and Chretien, 1997; Steiner, 1998 for reviews).

Furin is a 794 amino acid, type I membrane protein localized to the trans-Golgi network (TGN)/endosomal system, where it cleaves many precursor proteins at the consensus site -Arg-X-Lys/Arg-Arg[↓]- (Bresnahan et al., 1990; Hatsuzawa et al., 1992a; Matthews et al., 1994a; Molloy et al., 1992; Molloy et al., 1994) (see Figure 4). Known functional regions within furin are shown in Figure 5. Furin substrates include proproteins cleaved in both the exocytic and endocytic pathways, as furin cycles between the cell surface and the TGN via endosomal compartment(s) (Figure 3; Molloy et al., 1994; Schafer et al., 1995; Voorhees et al., 1995). Movement of furin between two local cycling loops, one at the TGN and the other at the cell surface, is mediated by a cycle of phosphorylation/dephosphorylation of the furin cytoplasmic tail by casein kinase II and phosphatase 2A, respectively (Jones et al., 1995; Molloy et al., 1994; Wan et al., 1998). Furin's dwell time at the cell surface is modulated by association with ABP-280 (Liu et al., 1997). Further, furin is cleaved prior to the transmembrane domain in the late secretory pathway (Wan et al., 1998), resulting in the release of soluble, active furin from the cell (Molloy et al., 1994; Vey et

al., 1994; Vidricaire et al., 1993). Shed furin may be responsible for the cleavage of extracellular substrates (see Figure 4).

Furin substrates include a wide variety of endogenous proteins, as well as exogenous pathogen molecules including viral envelope glycoproteins and bacterial toxins (see Figure 4). Indeed, the specific furin inhibitor α_1 -PDX has been shown to have potent anti-pathogenic properties. This recombinant protein inhibitor blocks HIV-1 gp160 proteolytic maturation (Anderson et al., 1993), measles infection (Watanabe et al., 1995), *Pseudomonas* exotoxin A-mediated cell killing (Jean et al., 1998) and cytomegalovirus infection (F. Jean and G. Thomas, unpublished results) in tissue culture systems.

Furin is synthesized as an inactive zymogen with an N-terminal propeptide, similar to its homologue bacterial subtilisin. That the 83 residue propeptide plays a significant role in furin folding is suggested by the finding that propeptide truncation abolishes enzyme activity (Rehemtulla et al., 1992). Furin's propeptide is autoproteolytically excised within the ER by cleavage at the site -Arg-Thr-Lys-Arg₁₀₇[↓]- ($t_{1/2} < 10$ minutes) (Creemers et al., 1995; Leduc et al., 1992; Molloy et al., 1994; Vey et al., 1994). This cleavage is unaffected by the fungal metabolite brefeldin A (Molloy et al., 1994; Thomas et al., 1995a), but is blocked by depletion of intracellular calcium stores with the ionophore A23187 (Vey et al., 1994). Further, mutation of the catalytic triad or the P1 or P4 residues of the propeptide excision site blocks propeptide excision and enzyme activation (Creemers et al., 1995; Leduc et al., 1992) as well as transport out of the early secretory pathway (Creemers et al., 1995; Molloy et al., 1994 and this dissertation).

Furin is not enzymatically active immediately following ER-localized propeptide excision. Rather, activation requires exposure of the endoprotease to post-ER compartments (Molloy et al., 1994; Vey et al., 1994). The studies undertaken for this dissertation determined why this is the case. We initially speculated that furin activation might involve the gradients of pH, and possibly calcium, that exist within the secretory pathway. The pH of the ER is roughly neutral (Kim et al., 1998) whereas the pH of the TGN is ~6.0 (Demaurex et al., 1998; Seksek et al., 1995), and some endosomal compartments are acidic as well (Clague, 1998; Mellman et al., 1986). Further, many studies have suggested that the concentration of available calcium in the ER is relatively low (perhaps in the micromolar range; reviewed in Meldolesi and Pozzan, 1998), and while the calcium concentration in the TGN is not firmly established, it has been suggested to be in the low millimolar range (Chanat and Huttner, 1991; Chandra et al., 1991; Kendall et al., 1994; Roos, 1988; Sambrook, 1990; Song and Fricker, 1995).

An *in vitro* study by our group found that furin undergoes a multi-step, pH-dependent process of activation following propeptide excision (Chapter 1). After excision, the propeptide remains non-covalently bound to furin, acting as an autoinhibitor, much like the subtilisin propeptide (Li et al., 1995). Exposure of the inactive furin•propeptide complex to a mildly acidic

(pH 6.0) and calcium-containing (low millimolar) environment suggested to be characteristic of the TGN results in a second cleavage within the propeptide at -Arg-Gly-Val-Thr-Lys-Arg₇₅[↓]-. Following internal cleavage, the propeptide fragments dissociate from furin, permitting the enzyme to cleave substrates *in trans*. These *in vitro* findings were interpreted to suggest that furin becomes active *in vivo* within the TGN, the enzyme's primary compartment of residence (Molloy et al., 1994).

In a second set of studies we sought to determine if the model generated by our *in vitro* work indeed reflected furin activation *in vivo* (Chapter 2). We also explored the relationship between furin's activation state and the secretory pathway quality control system. We found that a furin construct lacking the propeptide is inactive and ER-localized, suggesting misfolding. Co-expression of the propeptide *in trans* partially restored trafficking and activity, consistent with the putative role of the furin propeptide as an IMC. Further, failure of furin to excise its propeptide at -Arg-Thr-Lys-Arg₁₀₇[↓]- results in ERGIC/CGN localization, suggesting selective retention by the quality control system. Consistent with predictions made in light of our *in vitro* studies, furin autoproteolytically and intramolecularly cleaves its propeptide at -Arg-Gly-Val-Thr-Lys-Arg₇₅[↓]- in the late secretory pathway ($t_{1/2}$ = 105 minutes). The pH-modulated cleavage of this site was demonstrated by the use of synthetic peptide substrates. Unlike excision, preventing propeptide cleavage at -Arg-Gly-Val-Thr-Lys-Arg₇₅[↓]- does not result in a trafficking defect. Interestingly, introduction of a P4 Arg into the site of internal propeptide cleavage (-Arg-Gly-Val₇₂-Thr-Lys-Arg₇₅- → -Arg-Gly-Arg₇₂-Thr-Lys-Arg₇₅-), so that it resembles the site of propeptide excision, i) blocks propeptide excision and ii) prevents exit of furin from the ER, both of which suggest misfolding. These data demonstrate that the integrity of the P1/P6 Arg internal propeptide cleavage motif is essential for furin activation. A possible model for furin folding that is consistent with this result is discussed.

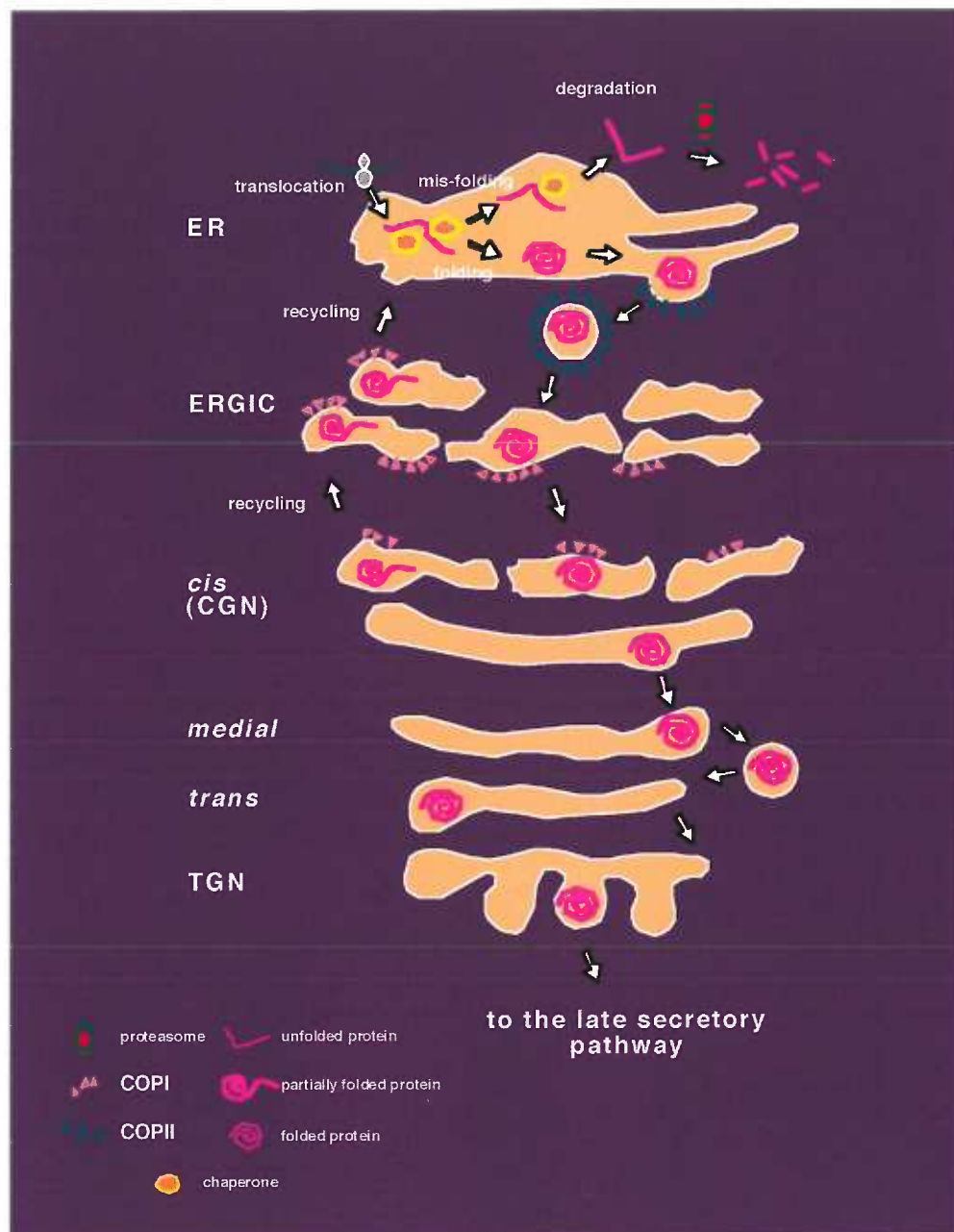


Figure 1: Folding and trafficking of proteins in the early secretory pathway.

Nascent proteins enter the ER via the translocon. In the ER lumen they undergo folding/assembly, often with the assistance of molecular chaperones. Misfolded proteins are retained in the ER by the quality control system, and are subsequently degraded, usually by the proteasome. Secretory proteins enter COPII coated vesicles and transit to the ERGIC. Proteins then move in COPI coated structures to the CGN. From the CGN they pass through the *cis*-, *medial*-, and *trans*-Golgi to the TGN and the other compartments of the late secretory pathway. Some partially- or mis-folded proteins are recycled to the ER from the ERGIC or CGN.

After Farquhar and Palade, 1998.

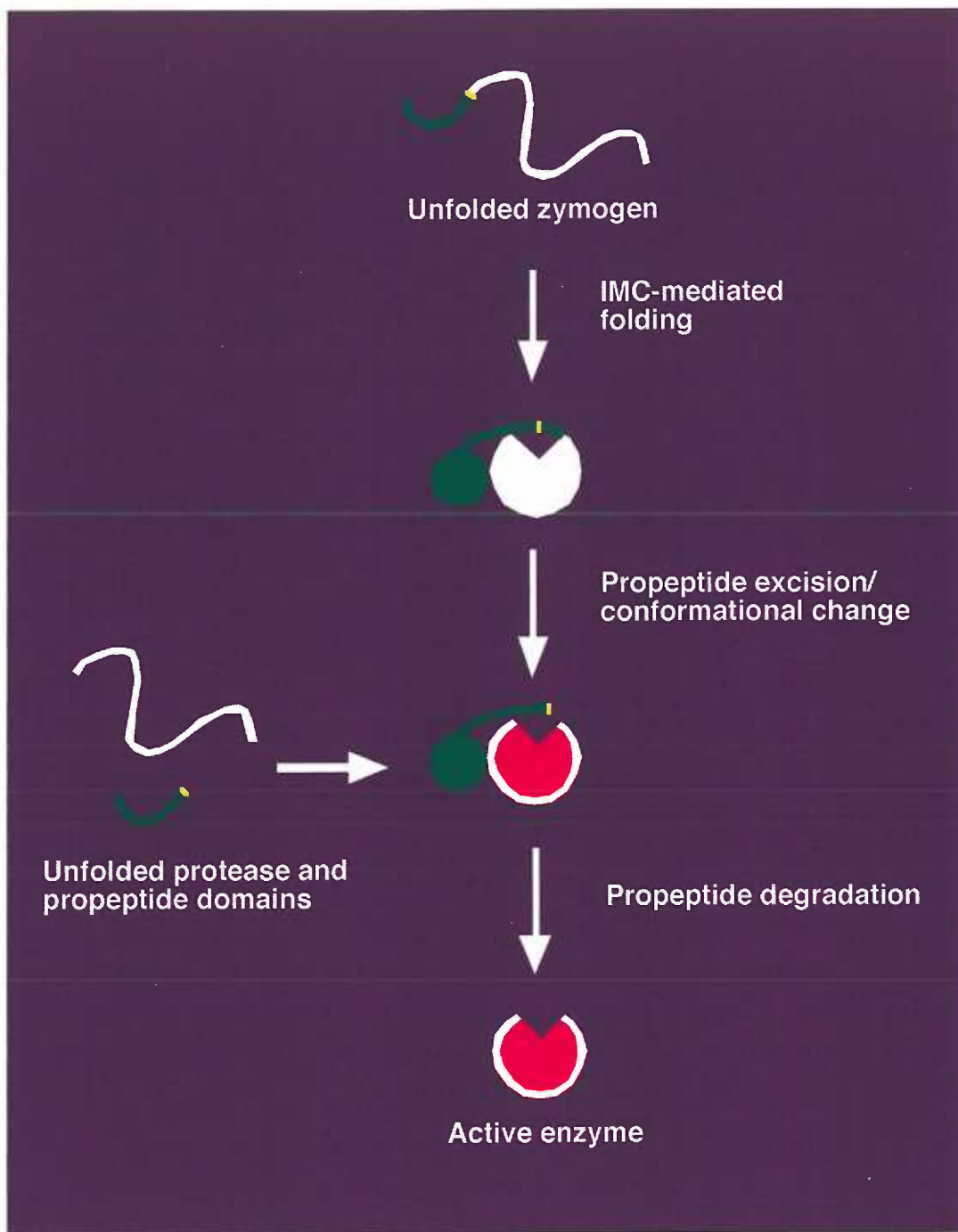


Figure 2: IMC-mediated protease folding. Starting as an unfolded polypeptide chain, the catalytic domain (*white*) folds in a process mediated by the IMC (*green*). The propeptide is then autoproteolytically and intramolecularly excised (*yellow cleavage site*), triggering a conformational change that is believed to mark the end of the folding process. The propeptide transiently remains associated with the protease, acting as a potent autoinhibitor until its subsequent degradation. Degradation is sometimes an autoproteolytic process, as in the case of subtilisin. Interestingly, covalent linkage of the IMC and catalytic domains is not required for folding, as mixing of the two unfolded domains *in trans* results in active enzyme.

Figure 3: Structures of the eukaryotic proprotein convertases (PCs).

The functional domains of the PCs presented here are indicated. Kex2p is found in *S. cerevisiae*, and dKLIP-1 is found in *D. melanogaster*. The other PCs shown are found in mammals.

This figure was made by Gary Thomas.

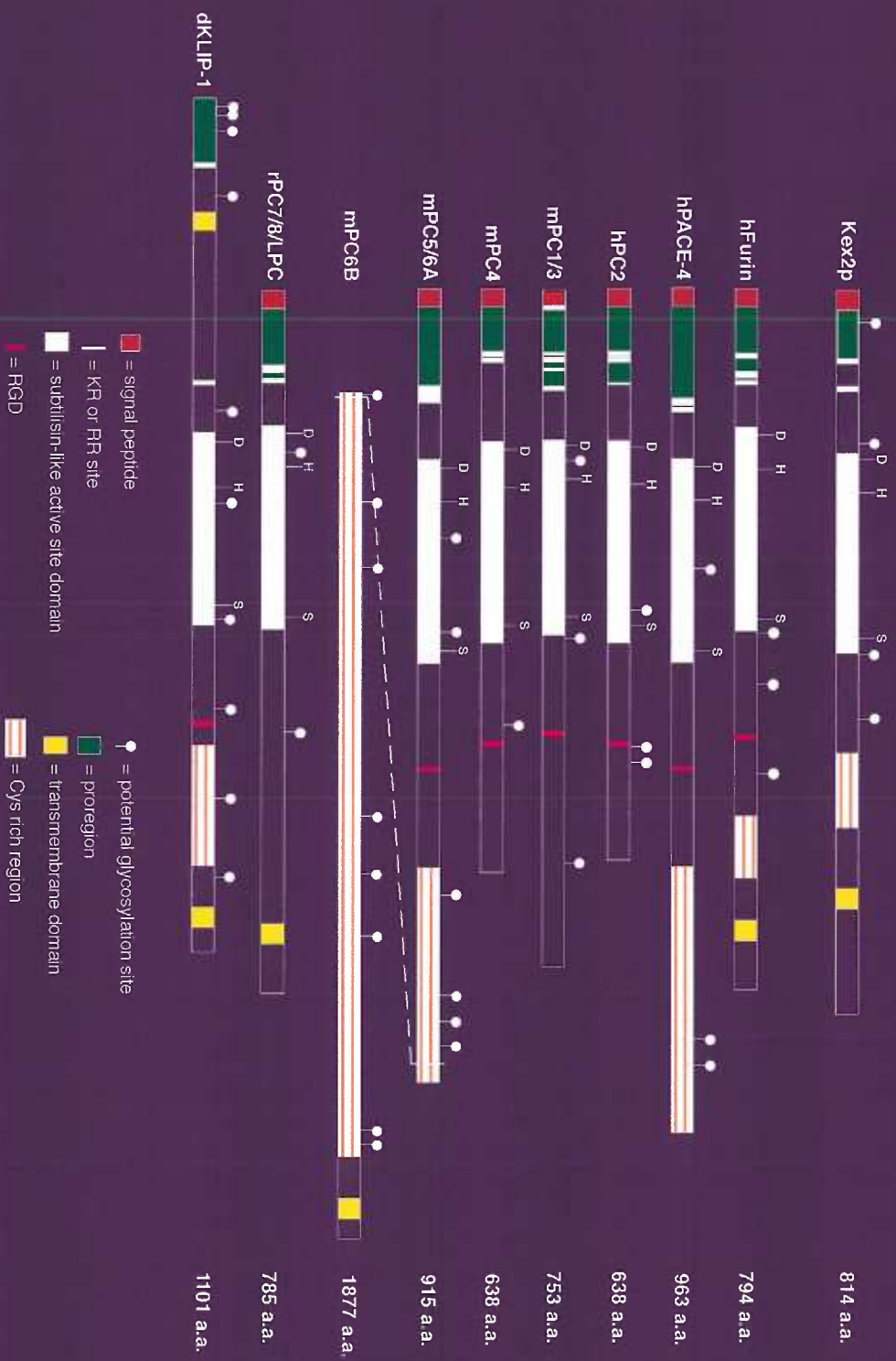


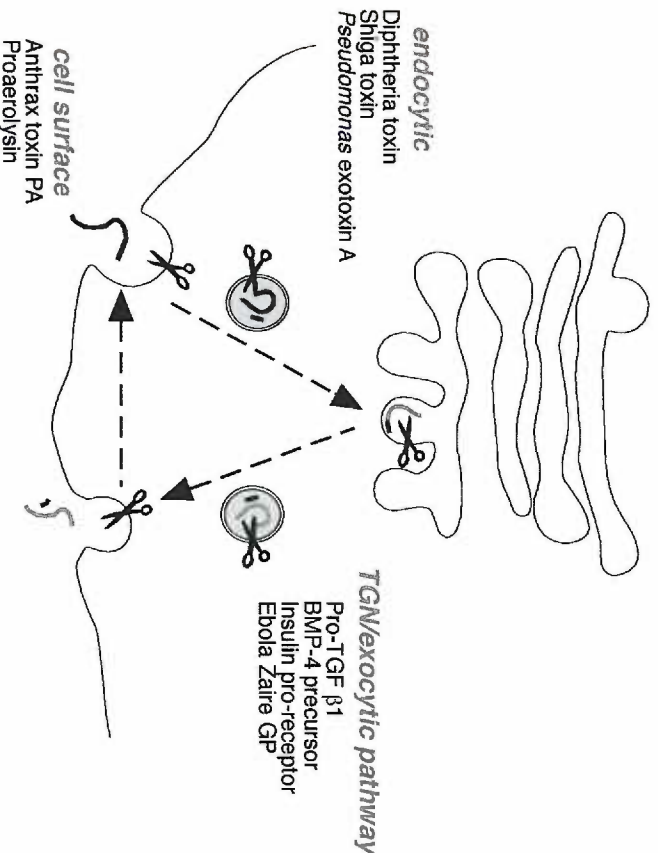
Figure 4: Furin processing compartments and *in vivo* furin substrates.

(Inset) Furin (*scissors*) can cleave substrates in multiple cellular compartments, including the TGN/endosomal system and the cell surface. Representative furin substrates processed in each designated compartment are shown. Further, a truncated, active form of furin is shed from the cell, and may participate in the proteolytic maturation of extracellular substrates. The P6-P2' cleavage site sequences for a selected list of proposed furin substrates are shown. Basic P1/P4 residues constituting the minimal furin cleavage site are highlighted in purple, while the additional basic P2 residue generating the consensus furin site is highlighted in blue. Basic residues in the P6 position that are necessary for the alternate furin cleavage site are highlighted in green. Note that some substrates have not only a consensus furin cleavage site but also a P6 basic residue (e.g. profibrillin). a) Misumi, Y. *et al.* 1991. *J. Biol. Chem.* 266:16954-16959 and Brennan, S. O. Nakayama, K. 1994. *FEBS Lett.* 338:147-151, b) Wasley, L. C. *et al.* 1993. *J. Biol. Chem.* 268:8458-8465, c) Drews, R. *et al.* 1995. *Proc. Natl. Acad. Sci. U.S.A.* 92:10462-10466, d) van de Ven, W. J. *et al.* 1990. *Mol. Biol. Rep.* 14:265-275 and Wise, R. J. *et al.* 1990. *Proc. Natl. Acad. Sci. U.S.A.* 87:9378-9382, e) Bresnahan, P. A. *et al.* 1990. *J. Cell Biol.* 111:2851-2859, f) Cui, Y. *et al.* 1998. *EMBO J.* 17: 4735-4743, g) Sawada, Y. *et al.* 1997. *J. Biol. Chem.* 272:20545-20554, h) Hendy, G. N. *et al.* 1995. *J. Biol. Chem.* 270:9517-9525, i) Adams, R. H. *et al.* 1997. *EMBO J.* 16:6077-6086, j) Dubois, C. M. *et al.* 1995. *J. Biol. Chem.* 270:10618-106124, k) Mondino, A. *et al.* 1991. *Mol. Cell Biol.* 11:6084-6092 and Bravo, D. A. *et al.* 1994. *J. Biol. Chem.* 269:25830-25837, l) Logeat, F. *et al.* 1998. *Proc. Natl. Acad. Sci. U.S.A.* 95:8108-8112, m) Komada, M. *et al.* 1993. *FEBS Lett.* 328: 25-29, n) Kozyraki, R. *et al.* 1998. *Blood* 91:3593-3600, o) Paquet, L. *et al.* 1994. *J. Biol. Chem.* 269:19279-19285, p) Kessler, E. *et al.* 1996. *Science* 271:360-362, q and r) Kramer, J. M. and Johnson, J. J. 1993. *Genetics* 135:1035-1045, s) Sato, H. *et al.* 1996. *FEBS Lett.* 393:101-104, t) Lehmann, M. *et al.* 1996. *Biochem. J.* 317:803-809, u) Milewicz, D. M. *et al.* 1995. *J. Clin. Invest.* 95:2373-2378, v) Pei, D. and Weiss, S.J. 1995. *Nature* 375:244-247, w) Yang, M. *et al.* 1997. *J. Biol. Chem.* 272:13527-13533, x and y) Epifano, O. *et al.* 1995. *Development* 121:1947-1956, z) Yurewicz, E. C. *et al.* 1993. *Biochim. Biophys. Acta* 1174:211-214, aa) Klimpel, K. R. *et al.* 1992. *Proc. Natl. Acad. Sci. U.S.A.* 89:10277-10281 and Molloy, S. S. *et al.* 1992. *J. Biol. Chem.* 267:16396-16402, bb) Gordon, V. M. *et al.* 1997. *Infect. Immun.* 65:4130-4134, cc) Tsuneoka, M. *et al.* 1993. *J. Biol. Chem.* 268:26461-26465, dd) G. van der Goot, pers. comm, ee) Moehring, J. M. *et al.* 1993. *J. Biol. Chem.* 268:2590-2594, ff) Garred, Ø. *et al.* 1995. *J. Biol. Chem.* 270:10817-10821, gg) Subbarao, K. *et al.* 1998. *Science* 279:393-396, hh) Richt, J. A. *et al.* 1998. *J. Virol.* 72:4528-4533, ii) Spaete, R. R. *et al.* 1988. *Virology* 167:207-225, jj) Volchkov, V. E. *et al.* 1998. *Proc. Natl. Acad. Sci. U.S.A.* 95:5762-5767, kk) Pellett, P. E. *et al.* 1985. *J. Virol.* 56:807-813, ll) Hallenberger, S. *et al.* 1992. *Nature* 360:358-361 and Decroly, E. *et al.* 1994. *J. Biol. Chem.* 269:12240-12247, mm) Cavanagh, D. *et al.* 1986. *Virus Res.* 4:133-143, nn) Sumiyoshi, H. *et al.* 1986. *Gene* 48:195-201, oo) Richardson, C. *et al.* 1986. *Virology* 155:508-523, pp) Collins, P. L. *et al.* 1984. *Proc. Natl. Acad. Sci. U.S.A.* 81:7683-7687, qq) Schwartz, D. E. *et al.* 1983. *Cell* 32:853-869, rr) Rice, C. M. *et al.* 1985. *Science* 229:726-733.

Adapted from Molloy *et al.*, 1999.

This figure was made by Eric Anderson and Gary Thomas.

	P6	P4	P2	P1	↓	P1'	P2'	Ref.
Serum proteins								
Proalbumin	R L R S	G N S I	V F P L S	R R R R	D Y D S	A N T L	a b c d	
Pro-factor IX								
Pro-protein C								
Pro-von Willebrand Factor								
Hormones and growth factors								
Pro-β-nerve growth factor	T R T T	I R L S R S	S A A K T I	R R R R	S S S S	S P P V D L	e f g h i	
BMP-4 precursor	T R T T	I R L S R S	S A A K T I	R R R R	S S S S	S P P V D L	e f g h i	
Pro-BNP	T R T T	I R L S R S	S A A K T I	R R R R	S S S S	S P P V D L	e f g h i	
Pro-parathyroid hormone	T R T T	I R L S R S	S A A K T I	R R R R	S S S S	S P P V D L	e f g h i	
Pro-semaphorin D (PCS 1)	T R T T	I R L S R S	S A A K T I	R R R R	S S S S	S P P V D L	e f g h i	
Pro-TGF β1	T R T T	I R L S R S	S A A K T I	R R R R	S S S S	S P P V D L	e f g h i	
Cell surface receptors								
Insulin pro-receptor	P G E L	S G K Q	K Q K Q	R R R R	S E S S	L L T I	k i m n	
Notch1 receptor	P G E L	S G K Q	K Q K Q	R R R R	S E S S	L L T I	k i m n	
Scatter factor receptor	P G E L	S G K Q	K Q K Q	R R R R	S E S S	L L T I	k i m n	
Vitamin B12 pro-receptor	P G E L	S G K Q	K Q K Q	R R R R	S E S S	L L T I	k i m n	
"Helper" protein/chaperone								
Pro-7B2	Q R R R	K R R R	R R R R	R R R R	S V		o	
Extracellular matrix proteins								
BMP-1	R S S S	S N K V	S V V R R R	R R R R	A Q Q Y	A Q Y A L T	p q r s t u v w x y z	
<i>C. elegans</i> rol-6	R S S S	S N K V	S V V R R R	R R R R	A Q Q Y	A Q Y A L T	p q r s t u v w x y z	
<i>C. elegans</i> sqt-1	R S S S	S N K V	S V V R R R	R R R R	A Q Q Y	A Q Y A L T	p q r s t u v w x y z	
Human MT-MMP1	R S S S	S N K V	S V V R R R	R R R R	A Q Q Y	A Q Y A L T	p q r s t u v w x y z	
Integrin α3-chain	R S S S	S N K V	S V V R R R	R R R R	A Q Q Y	A Q Y A L T	p q r s t u v w x y z	
Profibillin	R S S S	S N K V	S V V R R R	R R R R	A Q Q Y	A Q Y A L T	p q r s t u v w x y z	
Stromelysin-3	R S S S	S N K V	S V V R R R	R R R R	A Q Q Y	A Q Y A L T	p q r s t u v w x y z	
<i>Xenopus laevis</i> XMMP	R S S S	S N K V	S V V R R R	R R R R	A Q Q Y	A Q Y A L T	p q r s t u v w x y z	
ZP1	R S S S	S N K V	S V V R R R	R R R R	A Q Q Y	A Q Y A L T	p q r s t u v w x y z	
ZP2	R S S S	S N K V	S V V R R R	R R R R	A Q Q Y	A Q Y A L T	p q r s t u v w x y z	
ZP3α	R S S S	S N K V	S V V R R R	R R R R	A Q Q Y	A Q Y A L T	p q r s t u v w x y z	
Bacterial toxins								
Anthrax toxin PA	N K G R A	S R R N V I S	K G V R Q V A	R R R R	S S S S	T V V V W A	aa bb cc dd ee	
<i>Clostridium septicum</i> α-toxin	N K G R A	S R R N V I S	K G V R Q V A	R R R R	S S S S	T V V V W A	aa bb cc dd ee	
Diphtheria toxin	N K G R A	S R R N V I S	K G V R Q V A	R R R R	S S S S	T V V V W A	aa bb cc dd ee	
Proaerolysin	N K G R A	S R R N V I S	K G V R Q V A	R R R R	S S S S	T V V V W A	aa bb cc dd ee	
<i>Pseudomonas</i> exotoxin A	N K G R A	S R R N V I S	K G V R Q V A	R R R R	S S S S	T V V V W A	aa bb cc dd ee	
Shiga toxin	N K G R A	S R R N V I S	K G V R Q V A	R R R R	S S S S	T V V V W A	aa bb cc dd ee	



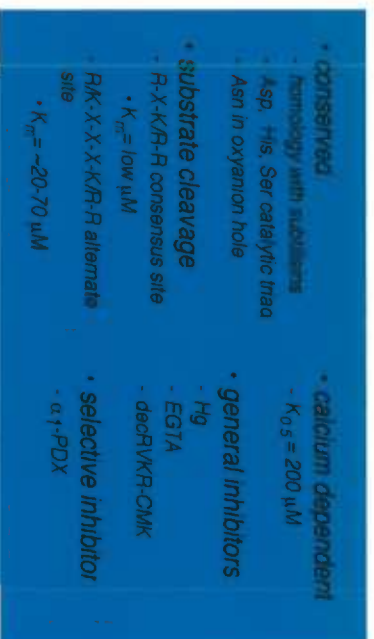
	P6	P4	P2	P1	↓	P1'	P2'	Ref.
Viral coat proteins								
Avian influenza HA (H5N1)	R L T G	R K H R R R	R R R R R R	R R R R	G D S E	L T T A V	gg hh ii jj kk ll mm nn oo pp qq	
Borna Disease virus	R L T G	R K H R R R	R R R R R R	R R R R	G D S E	L T T A V	gg hh ii jj kk ll mm nn oo pp qq	
Cytomegalovirus gB	R L T G	R K H R R R	R R R R R R	R R R R	G D S E	L T T A V	gg hh ii jj kk ll mm nn oo pp qq	
Ebola Zaire GP	R L T G	R K H R R R	R R R R R R	R R R R	G D S E	L T T A V	gg hh ii jj kk ll mm nn oo pp qq	
Epstein-Barr virus gB	R L T G	R K H R R R	R R R R R R	R R R R	G D S E	L T T A V	gg hh ii jj kk ll mm nn oo pp qq	
HIV-1 gp160	R L T G	R K H R R R	R R R R R R	R R R R	G D S E	L T T A V	gg hh ii jj kk ll mm nn oo pp qq	
Infectious bronchitis virus E2	R L T G	R K H R R R	R R R R R R	R R R R	G D S E	L T T A V	gg hh ii jj kk ll mm nn oo pp qq	
Japan B encephalitis M	R L T G	R K H R R R	R R R R R R	R R R R	G D S E	L T T A V	gg hh ii jj kk ll mm nn oo pp qq	
Measles virus F0	R L T G	R K H R R R	R R R R R R	R R R R	G D S E	L T T A V	gg hh ii jj kk ll mm nn oo pp qq	
Respiratory-syncytial virus F	R L T G	R K H R R R	R R R R R R	R R R R	G D S E	L T T A V	gg hh ii jj kk ll mm nn oo pp qq	
Rous sarcoma virus env	R L T G	R K H R R R	R R R R R R	R R R R	G D S E	L T T A V	gg hh ii jj kk ll mm nn oo pp qq	
Yellow fever virus M	R L T G	R K H R R R	R R R R R R	R R R R	G D S E	L T T A V	gg hh ii jj kk ll mm nn oo pp qq	

Figure 5. Functional domains of furin.

The human pre-profurin sequence (EC[#] 3.4.21.85) contains a 24 residue signal peptide (sp) and an 83 residue propeptide (pro) which mediates compartment-specific activation. Furin is a serine endoprotease (it has an Asp, His, Ser catalytic triad), and its ~330 residue catalytic domain is homologous to the bacterial subtilisins. Modeling studies of the catalytic domain, based on the crystal structure of bacterial subtilisins, predict S1, S2, S4 and S6 binding pockets (Siezen et al., 1994b). Also predicted are high- and middle-affinity calcium binding sites (Ca1 and Ca2, respectively). The ~140 residue 'P domain' is necessary for the activity of furin and other PCs (Zhou et al., 1998). P domains may have evolved to enable PCs to be active at mildly acidic pH (unlike bacterial subtilisins) and to stabilize the highly acidic catalytic- and pro-domains (Lipkind et al., 1998). The ~115 residue Cys-rich region (Cys-RR) has no established role. The 23 residue transmembrane domain is followed by a 56 residue cytosolic domain (cd) that contains furin's intracellular sorting information (reviewed in Molloy et al., 1999).

Adapted from Molloy et al., 1999.

This figure was made by Sean Molloy and Linda Cordilia.



• unknown function



- Possibly an intramolecular chaperone
- autoproteolytic cleavage
 - ▼ R-T-K-R₁₀₇ ▼ R-G-V-T-K-R₇₆
- autoinhibitory domain
- $IC_{50} = 14 \text{ nM}$

- necessary for activity
- modulates pH and calcium sensitivity
- cell adhesion/ integrin binding motif (RGD)
- not found in bacterial subtilisins

RS¹GS²FRG³GV⁴TY⁵TD⁶RGL⁷IS⁸YK⁹GL¹⁰PE¹¹AM¹²Q¹³EE¹⁴CP¹⁵S¹⁶₁¹⁷₃DS¹⁸₇¹⁹₇EE²⁰DE²¹G²²R²³GR²⁴ET²⁵AF²⁶IK²⁷D²⁸QS²⁹AL

- (-) • multiple internalization signals
- (-) • cell surface tethering signal
- (-) • acidic cluster motif

- directs TGN localization
- phosphorylated by CKII
- phosphorylation state directs trafficking

CHAPTER 1

Activation of the Furin Endoprotease is a Multiple-Step Process: Requirements for Acidification and Internal Propeptide Cleavage

Eric D. Anderson^{1,2}, Judy K. VanSlyke², Craig D. Thulin³, François Jean¹ and Gary Thomas^{1,4}

Vollum Institute and ¹Department of Cell and Developmental Biology, Oregon Health Sciences University, 3181 SW Sam Jackson Park Road, Portland, OR 97201-3098

²contributed equally to the study

³Current Address: Department of Zoology, Brigham Young University, Provo, UT 84601

⁴corresponding author

The manuscript that comprises this chapter was published in the *EMBO Journal* (1997) 16:1508-1518. The experiments for Figures 2, 3, 4, 5, 6 and 9 were performed by Eric Anderson. The experiment for Figure 7 was performed by Judy K. VanSlyke. The experiment for Figure 8 was performed by Craig D. Thulin.

ABSTRACT

Activation of furin requires autoproteolytic cleavage of its 83-amino acid propeptide at the consensus furin site, -Arg-Thr-Lys-Arg₁₀₇[↓]- [Leduc et al. 1992. *J. Biol. Chem.* 267:14304-14308]. This RER-localized cleavage is necessary but not sufficient for enzyme activation. Rather, full activation of furin requires exposure to, and correct routing within, the TGN/endosomal system [Molloy et al. 1994. *EMBO J.* 13:18-33; Vey et al. 1994. *J. Cell Biol.* 127:1829-1842]. Here, we identify the steps in addition to the initial propeptide cleavage necessary for activation of furin. Exposure of membrane preparations containing an inactive RER-localized soluble furin construct to either i) an acidic and calcium containing environment characteristic of the TGN or ii) mild trypsinization at neutral pH, resulted in the activation of the endoprotease. Together these results suggest that the pH drop facilitates the removal of a furin inhibitor. Consistent with these findings, following cleavage in the RER, the furin propeptide remains associated with the enzyme and functions as a potent inhibitor of the endoprotease. Co-immunoprecipitation studies coupled with analysis by mass spectrometry show that release of the propeptide at acidic pH, and hence activation of furin, requires a second cleavage within the autoinhibitory domain at a site containing a P6 arginine (-Arg₇₀-Gly-Val-Thr-Lys-Arg₇₅[↓]-). The significance of this cleavage in regulating the compartment-specific activation of furin, and the relationship of the furin activation pathway to those of other serine endoproteases are discussed.

INTRODUCTION

Biosynthesis of proteins destined for residence within, or routing through, the secretory pathway requires an orchestrated series of events, including one or more proteolytic cleavages to yield the mature and functional molecule. The primary translation product for many bioactive proteins (*e.g.* growth modulators, receptors, peptide hormones and proteinases) contains, in addition to the active region, a propeptide, that is typically an amino-terminal extension of the mature protein. The functions of propeptides appear to be manifold. In the case of several precursors of growth modulators [*e.g.* nerve growth factor and amphiregulin] the propeptides are required for stability or secretion of the active factor (Suter et al., 1991; Thorne and Plowman, 1994), whereas the propeptide of transforming growth factor- β participates in formation of latent complexes (Miyazono et al., 1988). The propeptide of the yeast enzyme carboxypeptidase Y is required for the receptor-mediated sorting to the vacuole (Valls et al., 1990). Finally, propeptides are important for the activation of all classifications of proteinases (*i.e.* serine-, aspartyl-, cysteinyl- and metallo-proteinases; reviewed in Baker et al., 1993).

Perhaps the most thoroughly investigated examples of propeptide-mediated proteinase activation are those of the bacterial serine proteinases, subtilisin and α -lytic protease. The N-terminal propeptides of both enzymes are required for the correct folding of their catalytic domains and can facilitate the refolding of denatured enzyme *in vitro* (Ikemura and Inouye, 1988; Power et al., 1986; Silen et al., 1989; Zhu et al., 1989). Following translation of the nascent chain into the periplasmic space and folding of the zymogen, the amino-terminal propeptides of both bacterial endoproteases are cleaved by an intramolecular reaction (Power et al., 1986; Silen et al., 1989). The propeptides remain associated with the catalytic domains through non-covalent interactions and act as potent autoinhibitors (Baker et al., 1992a; Li et al., 1995). Structural and biochemical analyses have shown that the subtilisin propeptide binds to the enzyme primarily through multiple non-polar interactions, with the C-terminus extending into the active site of the enzyme, thus acting as a competitive inhibitor (Bryan et al., 1995; Gallagher et al., 1995; Li et al., 1995; Li and Inouye, 1994). When subtilisin E propeptide is degraded, by an as yet uncharacterized pathway, the enzyme is free to act on substrates *in trans* (Ikemura and Inouye, 1988).

The bacterial subtilisins are evolutionarily related to the eukaryotic proprotein convertases, a family of calcium-dependent serine endoproteases. The convertases catalyze the proteolytic maturation, and hence activation, of precursor proteins within the secretory pathway by cleavage at oligo-basic amino acid sequences (Smeekens, 1993; Steiner et al., 1992). Members of the proprotein convertase family include the yeast convertase Kex2p, which catalyzes the activation of α -mating pheromone, and a number of Kex2p homologues expressed in metazoa including furin, PC1/3, PC2, PC4, PC5/6, LPC/PC7/8 (hereafter termed PC7) and PACE-4 (see Bruzzaniti et al.,

1996; Meerabux et al., 1996; Seidah et al., 1996; Smeekens, 1993; Steiner et al., 1992).

Like the bacterial subtilisins, the proprotein convertases are synthesized as inactive precursors that require proteolytic cleavage of their amino-terminal propeptides. This was first established for furin, a type I membrane protein concentrated in the TGN/endosomal system (Jones et al., 1995; Molloy et al., 1994; Schafer et al., 1995; Takahashi et al., 1995; Voorhees et al., 1995) that cleaves a large number of proprotein molecules at the consensus furin site -Arg-X-Lys/Arg-Arg- in both the biosynthetic and endocytic pathways (see Bresnahan et al., 1993; Leduc et al., 1992; Van de Ven et al., 1993 for reviews). The furin zymogen undergoes autocatalytic cleavage of its 83 amino acid N-terminal propeptide at the C-terminal side of the consensus furin site -Arg-Thr-Lys-Arg₁₀₇[↓]- soon after deposition of the molecule into the RER ($t_{1/2} < 10$ minutes) (Creemers et al., 1995; Leduc et al., 1992; Molloy et al., 1994; Vey et al., 1994). Not only is the RER-localized propeptide cleavage a necessary step for activation of furin, it is also required for export of the protein from this compartment (Creemers et al., 1995; Molloy et al., 1994). However, this cleavage alone is not sufficient for enzymatic activation of furin. Rather, furin activation also requires exposure of the endoprotease to post-RER compartments (Molloy et al., 1994; Vey et al., 1994). For example, a furin construct unable to be exported from the RER undergoes autoproteolytic cleavage of its propeptide, but remains proteolytically inactive against substrates *in trans* (Molloy et al., 1994).

To begin identification of the additional steps comprising the furin activation pathway, we have developed a simple *in vitro* system to study this process under defined conditions. Here, using this approach, we report the discovery of an ordered series of steps required for the activation of furin. The relationship of these steps to the compartment-dependent activation of furin in the secretory pathway is discussed.

MATERIALS AND METHODS

Materials

The protease inhibitors PMSF, pepstatin-A, and soybean trypsin inhibitor (SBTI) were obtained from the Sigma Chemical Company (St. Louis, MO). E-64 was obtained from Boehringer-Mannheim Biochemicals (Indianapolis, IN). The peptide substrate Boc-Arg-Val-Arg-Arg-4-methyl-coumaryl-7-amide was from Peptides International (Louisville, KY). The internally quenched substrate Q1, Abz-Arg-Val-Lys-Arg-Gly-Leu-Ala-Tyr(NO₂)-Asp-OH, was a gift from Dr. Herbert Anglikar (Friedrich Miescher-Institut, Basel). The secreted soluble furin construct Fur713t was purified as described previously (Molloy et al., 1992). Alkaline phosphatase- and horseradish peroxidase- conjugated goat anti-mouse secondary antibody were obtained from Southern Biotechnology Associates (Birmingham, AL). The mAb 12CA5 directed against the HA epitope was obtained from Boehringer-Mannheim Biochemicals. Purified mAbs M1 and M2 directed against the FLAG epitope were obtained from Kodak-IBI (Rochester, NY).

Cell Culture

BSC-40 Cells were maintained in minimal essential medium (MEM; GIBCO BRL, Gaithersburg, MD) containing 10% fetal bovine serum (FCS; HyClone, Logan, Utah) and 25 µg/ml gentamycin as described previously (Bresnahan et al., 1990; Thorne et al., 1989).

Furin Constructs and Vaccinia Virus (VV) Expression

The FLAG epitope tagged furin construct fur/f was generated previously (Molloy et al., 1994). HA tagged furin constructs were based on the EcoRI/KpnI fragment of furin in Bluescript (SK-) as a template, and generated by single-primer (Kunkel) mutagenesis techniques with the oligonucleotide FURIN/HA (5' - CTG CTA GCA GCT GAT GCT CAA GGA TAC CCC TAC GAC GTG CCC GAC TAC GCC CAG GGC CAG AAG GTC TTC - 3'). Underlined sequences correspond to native furin sequences between Leu₁₉→Ala₂₄ and Gln₂₅→Phe₃₀. This oligonucleotide introduced the sequence encoding QGY[↓]PDV[↓]PDYA (the HA tag is underlined) between the end of the signal sequence and the beginning of the furin propeptide (A₂₄↓Q₂₅G₂₆, see Results section). The additional two residues that are not part of the HA epitope (QG) were introduced to preserve the sequence C-terminal to the signal sequence cleavage site. The full-length furin construct with the HA tag (fur/f/ha) was then generated using the cloning strategy described previously for the construction of fur/f (Molloy et al., 1994). The furin mutants R₇₀A: fur/f/haΔtc-k and R₇₅A: fur/f/haΔtc-k were also generated by single-primer mutagenesis using the primers R70A (5'-

CAC TTC TGG CAT GCA GGA GTG ACG AAG CGG -3' and R75A (5'- GTG ACG AAG GCC TCC CTG TCG -3'). The nucleotides in each oligo that are complementary to the furin sequence are underlined. The R70A mutation introduced a diagnostic SphI site and the R75A mutation introduced a diagnostic StuI site (in boldface type). The ER-retained furin construct fur/fΔtc-k was generated previously (Molloy et al., 1994) and used to construct R₇₀A:fur/f/haΔtc-k and R₇₅A:fur/f/haΔtc-k by swapping the truncated C-terminus with the KDEL sequence from pZVneo:fur/fΔtc-k in place of the full-length furin tail. All furin constructions were ultimately cloned into the pZVneo vector for generating recombinant vaccinia virus by marker transfer as previously described (VanSlyke et al., 1995).

Glutathione-S-Transferase (GST) Fusion Proteins

Sequences encoding the native and HA-tagged furin propeptides were produced by PCR amplification of the appropriate furin construct in pZVneo and inserted between the EcoRI and BamHI sites of pGEX 3X (Pharmacia, Piscataway, NJ). GSTpro was constructed using 5' primer NNAPROG: 5' - GCG GGA TCC AGG GCC AGA AGG TCT TC - 3'. GSTpro/ha was constructed using the 5' primer NHAPROG: 5' - GCG GGA TCC TCT ACC CCT ACG ACG TGC CC - 3'. The 3' primer used for the construction of both GSTpro and GSTpro/ha was CPROG: 5' - GCG GAA TTC ACC GTT TAG TCC GTC GCT T -3'. The sequences complimentary to wild-type or HA-tagged furin are underlined and newly introduced restriction sites are shown in boldface type. GSTpro and GSTpro/ha were expressed in bacteria and purified according to the manufacturer's instructions (Pharmacia).

Cell Fractionation

Crude membrane preparations were made for the analyses of furin constructs by immunoblotting, activation assays, HPLC and mass spectrometry. Confluent BSC-40 cells on 10- or 15-cm plates (1 or 2 x 10⁷ cells per plate, respectively) were infected with recombinant vaccinia virus at a multiplicity of infection (m.o.i.) of 5 and incubated for 14-16 hours at 37°C in a defined serum free medium (MCDB202; McKeehan and Ham, 1977). For harvesting, the plates were placed on ice and the medium aspirated. The cells were then removed with a rubber policeman in 2.5 mls (for 10 cm plates) or 5 mls (for 15 cm plates) of 10 mM HEPES (pH 7.2) supplemented with protease inhibitors (0.2 mM PMSF, 1 mM EDTA and 0.01 mM pepstatin-A, and 5 mM E-64). The cells were lysed by repeated passage through a 25 gauge needle followed by centrifugation at 5,000 x g for 5 minutes at 4°C to remove unbroken cells and nuclei. Membranes were pelleted from 400-500 µl aliquots of the low speed supernatants by centrifugation at 55,000 r.p.m. in either a TLA 100.1

or TLA 100.3 fixed angle rotor (Beckman Instruments, Inc., Fullerton, CA) for 1 h at 4°C. Pellets were resuspended in buffers as indicated.

Furin Activity Assays

All assays were carried out in 100 mM HEPES, pH 7.5, 1 mM 2-mercaptoethanol, 0.5% Triton X-100 and 1 mM CaCl₂. Fluorometric assays with 4-methyl-coumaryl-7-amide-containing peptides (AMC substrate) were performed as described previously (Molloy et al., 1992) except when GSTpro or GSTpro/ha were added as indicated. Assays with the internally quenched Q1 substrate were performed essentially as described previously (Anglikar et al., 1995) except that a 3 ml reaction volume with 3.8 μ M Q1 substrate was used.

Furin Activation Assays

Membrane pellets were resuspended by trituration into 100 μ l of 10 mM Bis-Tris (pH 6.0 or 7.5), 0.5% Triton X-100, 5 mM CaCl₂, 1 mM 2-mercaptoethanol. Protease inhibitors were added as indicated. Appropriate substitutions or omissions were made to this buffer to analyze the effect of pH and calcium on the activation of the ER-retained furin constructs. Following resuspension the samples were transferred to 1.5 ml Eppendorf tubes and pre-incubated in a 30°C water bath for the indicated lengths of time. Following incubation, two 30 μ l aliquots of the samples were assayed for enzymatic activity against the Q1 substrate

Immunoprecipitations and Immunoblotting

A portion of the membrane pellets resuspended in Bis-Tris buffer was diluted with mRIPACa²⁺ buffer (50 mM Tris-HCl, pH 8.0, 150 mM NaCl, 1% NP-40, 1% sodium deoxycholate, 1 mM CaCl₂). The monoclonal antibody M1 was added (50 μ g/ml) and rotated for 2 hours at 4°C. Protein G Sepharose (Zymed, South San Francisco, CA) was added (30 μ l of a 50% slurry) to the immunoprecipitation reactions and incubated one hour. The Sepharose beads were washed four times with mRIPACa²⁺ buffer before resuspending them in SDS-sample loading buffer. Samples were separated on a 15% peptide gel using a SDS-Tris-tricine buffer system (Dayhuff et al., 1992; Schägger and von Jagow, 1987). The proteins were then transferred to nitrocellulose membranes for 30 minutes at 36 volts. The membranes were first blocked in TBST (50 mM Tris-HCl, pH 8.0, 150 mM NaCl, 0.05% TX-100 and 0.01% NaN₃) containing 5% milk and then probed with mAb 12CA5 (0.5 μ g/ml final concentration) overnight at 4°C. The secondary antibody (goat anti-mouse-alkaline phosphatase conjugate) was incubated with the blot for 1 h at room temperature and the

immunostaining pattern was developed with BCIP and NBT solutions (Zymed). When extracts were to be analyzed directly, portions of the membrane preparation suspensions were mixed with SDS-sample loading buffer and subjected to peptide gel electrophoresis and western blot analysis as described above.

Limited Trypsinization of Propeptide

Confluent BSC-40 cells were infected with VV:hFur/fΔtc-k and cell membranes were prepared as described above. Membrane pellets were resuspended by trituration in 100 μl of 100 mM HEPES pH 7.0, 0.5% Triton X-100, 1 mM CaCl₂, 1 mM 2-mercaptoethanol. Controls had no subsequent additives, except when 5 μl of 1 mg/ml soybean trypsin inhibitor (SBTI; final concentration = 2.5 μM) along with 2 μl of 1 μg/ml bovine trypsin (for final concentration of 0.83 nM) were added. Trypsin alone was added to the experimental samples and all samples were incubated 1 hour at 30°C, after which 5 μl of 1 mg/ml SBTI was added to the experimental samples and all samples were incubated a further 30 minutes. Enzymatic activity was determined using the Q1 substrate as described above.

Mass Spectrometry of Propeptide Fragment

Forty 15 cm plates of confluent BSC-40 cells (a total of 8×10^8 cells) were infected at an m.o.i. of 5 with VV:hFur/f/haΔtc-k construct. At eighteen-hours post infection the cells were harvested and a crude membrane preparation made (see above). The membrane preparation was incubated for 8 hours at 30°C in 5 ml of 10 mM Bis-Tris pH 6.0, 5 mM CaCl₂, 0.5% triton X-100, with 0.2 mM PMSF, 0.01 mM pepstatin-A and 5 mM E-64. The clarified supernatant from this incubation was acidified with TFA (final concentration = 0.1%) and run on reversed-phase HPLC using a Vydac C₄ column, developing the following gradient: 16 to 25% B over 2 minutes., 25 to 49% B over 75 minutes., 49 to 90% B over 10 minutes., where buffer A is 0.1% TFA in H₂O and buffer B is 0.1% TFA in 80% acetonitrile, with a flow rate of 1 ml/min. One ml fractions were collected, dried down and resuspended in 100 μl water. Ten μl of each fraction was then run on 15% peptide gel using a SDS-Tris-tricine buffer system which was then transferred to PVDF membrane and immunoblotted using the 12CA5 anti-HA as the primary antibody. Fractions 65, 66, and 67 were found to contain the ~6 kDa fragment of interest. These fractions were acidified with acetic acid (final concentration = 10%). One μl of each was used for MALDI-TOF analysis on a Voyager Elite (PerSeptive Biosystems, Cambridge, MA) in linear mode with the sample embedded in a sinapinic (3,5-dimethoxy-4-hydroxy cinnamic) acid matrix. Electrospray capillary LC/MS was performed on a Perkin Elmer/Sciex API-III triple quadrupole with an ionspray source on 25 μl of

each sample. The capillary column was hand-packed by J. Kowalak (Univ. of Washington) using PerSeptive Biosystems R1 reversed-phase resin. At a flow rate of 15 μ l/min. the chromatography was developed with 0.1% TFA and a gradient of 0 to 60% isopropanol over 60 minutes., followed by 60 to 100% isopropanol over 5 minutes. Masses from MALDI-TOF were used to scan the LC/MS data for multiply charged ions of molecular species in the range of interest. The calculation of expected molecular weights was facilitated with the Sherpa data analysis program written by J. Taylor (Univ. of Washington), and all calculations employed average isotope abundance masses.

RESULTS

To determine the requirements for the activation of furin, a series of epitope-tagged furin constructs was used (Figure 1). Introduction of the FLAG-epitope tag immediately C-terminal to the propeptide cleavage site permits the use of immunologic methods to monitor propeptide cleavage and correlation of this event with enzyme activity. Importantly, the FLAG tag at this position does not affect measurably propeptide cleavage or enzyme activity *in vivo* (Molloy et al., 1994). By employing two FLAG peptide-specific antibodies, mAb M1 and mAb M2, the zymogenic form of furin (which cross-reacts with mAb M2 only) can be distinguished from the mature forms (i.e. propeptide cleaved) of furin generated by autoproteolytic cleavage C-terminal to Arg₁₀₇ (cross-reacts with both mAb M1 and mAb M2).

In initial studies, the importance of propeptide cleavage in furin activation was determined (Figure 2). Replicate plates of BSC-40 cells were either mock-infected (lane 1), or infected with wild-type vaccinia virus (lane 2), with vaccinia recombinants expressing the TGN localized fur/f (lane 3), or one of two furin constructs that are concentrated in the RER; a truncated soluble form of furin containing the RER retrieval signal -Lys-Asp-Glu-LeuCOOH, fur/fΔtc-k (lane 4), or the active site mutant fur/fD₁₅₃N (lane 5). Analysis of crude membrane preparations by western blot (panels A and B) showed that both fur/f and fur/fΔtc-k had undergone the autoproteolytic propeptide cleavage (both recognized by mAb M2 and mAb M1) whereas fur/fD₁₅₃N failed to undergo this step (cross-reactive with mAb M2 only). Each of the samples was then assayed for furin enzymatic activity using the Q1 internally quenched peptide substrate (panel C). Only the membrane sample from cells expressing fur/f was capable of efficiently cleaving the substrate.

The inability of the RER-localized fur/fΔtc-k to cleave *in vitro* the synthetic furin substrate under conditions in which the TGN-localized fur/f construct could is in agreement with our previous work demonstrating that propeptide cleavage is necessary but not sufficient for furin activation (Molloy et al., 1994). Additional factors, including cellular calcium stores, are also important for furin activation. The concentration of available calcium in the RER versus the TGN is not firmly established (see Discussion), however, one measured difference between these compartments is pH. The pH of the RER is neutral (Mellman et al., 1986) whereas the pH of the TGN is approximately 6.2 (Seksek et al., 1995). To determine directly whether calcium and/or the acidification of the TGN contribute to furin activation, fur/fΔtc-k in crude membrane preparations was measured with or without pre-incubation in the presence or absence of 5 mM calcium under neutral (pH 7.5) or acidic (pH 6.0) conditions (Figure 3). Consistent with the data in Figure 2, fur/fΔtc-k failed to be activated at neutral pH irrespective of the presence of calcium. By contrast, exposure of fur/fΔtc-k to a TGN-like acidic and calcium-containing environment resulted in a striking increase in enzyme activity. Importantly, the activation of fur/fΔtc-k required a pre-

incubation under these conditions (compare lanes 1 and 6 to lane 5).

The pH optimum for activation of fur/f Δ tc-k was determined using a range of buffers (Figure 4A). Maximal activation occurred at pH 6.0. A time course of fur/f Δ tc-k activation at pH 6.0 was next determined (Figure 4B). Under these conditions enzyme activity increased linearly for approximately 180 minutes.

The results in Figures 2 and 3 demonstrated a requirement for calcium and an acidic pH for the activation of furin following the autoproteolytic cleavage of its 83-amino acid propeptide. However, because furin undergoes an autoproteolytic cleavage of its amino-terminal propeptide in the RER, the endoprotease must be intrinsically active. These findings suggest that the acidic environment of the TGN facilitates the removal of a furin inhibitor. To examine this possibility, a crude membrane fraction was prepared from BSC-40 cells expressing fur/f Δ tc-k. An aliquot of the membrane sample was then subjected to limited digestion with trypsin to facilitate degradation of the furin inhibitor, followed by an assay for furin activity (Figure 5). A sequential treatment of the sample with trypsin followed by addition of soybean trypsin inhibitor (to block trypsin selectively) resulted in a large increase in furin activity compared to control samples (compare column 3 with columns 1 and 2). These results are consistent with the hypothesis that fur/f Δ tc-k is inactive at neutral pH because of its association with a trypsin-labile inhibitor.

Because the amino-terminal propeptides of the structurally related bacterial subtilisins are potent autoinhibitors, we examined the ability of the furin propeptide to inhibit furin's activity *in vitro*. A GST-fusion protein containing residues encoding the entire furin propeptide (Gln₂₅ → Arg₁₀₇), GSTpro, was prepared. Increasing amounts of the purified fusion protein were then pre-incubated for one hour with furin enzyme *in vitro* prior to addition of an AMC substrate (Figure 6). Furin activity was inhibited with near stoichiometric quantities of added propeptide. The inhibitory effect was specific for sequences within the furin propeptide since GST showed no inhibitory activity.

Together, the results in Figures 2 and 6 argue that the furin propeptide functions as a tightly bound autoinhibitor and suggest that removal of this fragment requires exposure of the complex to an acidic pH. Therefore, to monitor the fate of the furin propeptide during enzyme activation, a dual epitope tag construct was generated (Figure 1). In this construct, fur/f/ha Δ tc-k, the hemagglutinin (HA) epitope tag was inserted by loop-in mutagenesis C-terminal to the predicted signal peptidase cleavage site (Ala₂₄↓Gln₂₅, see Figure 1). Western blot analysis and time course of activation studies showed that fur/f/ha Δ tc-k underwent correct propeptide cleavage and was activated with similar kinetics as fur/f Δ tc-k (data not shown). To show that the HA tag did not affect the furin inhibitory properties of the propeptide, a second GST fusion protein, GSTpro/ha, was constructed containing the HA-tagged furin propeptide. Enzyme inhibition studies showed that GSTpro/ha attenuated furin activity at concentrations very similar to GSTpro (Figure 6).

The potent autoinhibitory properties of the furin propeptide suggest that the lack of activity of fur/f Δ tc-k when incubated at neutral pH may be the result of a tight-binding interaction between the mature enzyme and the cleaved propeptide domain. To demonstrate directly the association of the furin propeptide with the enzyme *in vivo*, a co-immunoprecipitation experiment was performed (Figure 7). Replicate samples of a crude membrane preparation from BSC-40 cells expressing fur/f/ha Δ tc-k were incubated at either pH 7.5 or pH 6.0 and the furin construct was immunoprecipitated with mAb M1 either immediately or following a pre-incubation in either of the two buffers. Analysis of the mAb M1 immunoprecipitates by western blot using the mAb 12CA5 showed that the HA-tagged propeptide is associated with the mature enzyme (panel A). At pH 7.5 the propeptide•enzyme complex remained stable during an extended incubation (panel A, lane 2). By contrast, incubation of the complex at pH 6.0 resulted in a release of propeptide from the endoprotease (panel A, lane 4). The loss of co-immunoprecipitating propeptide was coincident with a marked increase in furin activity (panel B). Interestingly, western blot analysis of the whole extract showed that the propeptide underwent a second proteolytic cleavage, generating an ~6 kDa HA-tagged peptide, that was coincident with its release from the enzyme and furin activation (panel C).

Identification of the ~6 kDa HA-tagged propeptide fragment was accomplished using mass spectrometry (Figure 8). A crude membrane sample prepared from BSC-40 cells expressing fur/f/ha Δ tc-k was incubated at pH 6.0 and the extract was fractionated by reversed-phase HPLC. The column fractions containing the HA-tagged ~6 kDa band (determined by western blot) were then subjected to MALDI-TOF MS and electrospray LC/MS. Analysis by MALDI showed that the ~6 kDa HA-tagged band was composed of three species with masses of i) 7032 ± 2.7 a.m.u., ii) 6878.3 ± 4.1 a.m.u. and iii) 6753.9 ± 3.3 a.m.u. Analysis by LC/MS allowed refinement of the mass measurements for each species to 7035.5 a.m.u. 6880.0 a.m.u. and 6752.0 a.m.u. respectively. Using mass spectrometric methods, we showed that the 83 amino acid was cleaved to generate three distinct N-terminal fragments with masses of 7036, 6880 and 6752 a.m.u. These masses are 17 a.m.u. less than the predicted HA-tagged-Gln₂₅ → Arg₇₅, HA-tagged-Gln₂₅ → Lys₇₄ and HA-tagged-Gln₂₅ → Thr₇₃ respectively. However, because N-terminal glutamine residues readily cyclize, generating products that are 17 a.m.u. smaller than predicted (Krishna and Wold, 1993), we conclude that the N-terminus of profurin initiates at Gln₂₅ which becomes cyclized to pyroglutamic acid (pGlu). Thus these peptides were identified as i) HA-tagged-pGlu₂₅→Arg₇₅, ii) HA-tagged-pGlu₂₅→Lys₇₄ and iii) HA-tagged-pGlu₂₅→Thr₇₃. The identification of these three peptide shows that the internal cleavage of the furin propeptide occurs after the -Lys₇₄-Arg₇₅-doublet and that a carboxypeptidase B-like activity in the extract degrades slightly the carboxyl terminus.

Unlike the initial furin propeptide cleavage site (-Arg-Thr-Lys-Arg₁₀₇-) processed in the RER, the -Lys₇₄-Arg₇₅- doublet is part of a site that lacks a P4 arginine typical of furin substrates yet possesses a P6 arginine (-Arg₇₀-Gly-Val-Thr-Lys-Arg₇₅-). This kind of cleavage site is also present in a subset of furin substrates preferentially cleaved at acidic pH (Brennan and Nakayama, 1994a; Brennan and Nakayama, 1994b). To determine the importance of cleavage of the propeptide at Arg₇₅ in the activation of furin, as well as to assess the contribution of Arg₇₀ to this step, site-directed mutagenesis was employed. Replicate plates of BSC-40 cells were infected with vaccinia recombinants expressing either fur/f/haΔtc-k or constructs containing either Arg₇₅ → Ala (R₇₅A:fur/f/haΔtc-k) or Arg₇₀ → Ala (R₇₀A:fur/f/haΔtc-k) mutations. Crude membrane preparations from each sample were incubated in pH 7.5 or 6.0 buffers, or subjected to limited trypsin proteolysis at pH 7.5 to release the autoinhibitory action of the propeptide (Figure 9). Each construct was proteolytically inactive following incubation at pH 7.5. After incubation at pH 6.0, activation of fur/f/haΔtc-k was observed. By contrast, furin activity was suppressed in samples containing R₇₅A:fur/f/haΔtc-k or, to a slightly lesser extent, R₇₀A:fur/f/haΔtc-k. Following limited trypsinization at neutral pH however, each of the constructs could be activated. These data show that acid pH-dependent cleavage of the -Lys₇₄-Arg₇₅- doublet is necessary for activation of furin. Furthermore, efficient cleavage at this site requires a P6 arginine (Arg₇₀).

DISCUSSION

Earlier studies revealed that activation of furin requires one or more steps subsequent to the initial cleavage of its N-terminal propeptide (Molloy et al., 1994; Rehemtulla et al., 1992; Thomas et al., 1995a; Vey et al., 1994). Here, using an *in vitro* approach, we identify a sequence of events necessary for furin activation (Figure 10A). Following translocation of furin into the RER, and concomitant removal of the signal sequence, the proregion is autoproteolytically cleaved at -Arg-Thr-Lys-Arg₁₀₇[↓]- (Creemers et al., 1995; Leduc et al., 1992; Molloy et al., 1994; Vey et al., 1994). In the neutral environment of the RER, the propeptide remains associated with the endoprotease and functions as an autoinhibitor. Exposure of the furin-propeptide complex to a mildly acidic (pH 6.0) and calcium-containing (low millimolar) environment characteristic of the TGN results in a second cleavage within the propeptide at -Arg₇₀-Gly-Val-Thr-Lys-Arg₇₅[↓]- as determined by mass spectrometry. Mutational analyses showed that both the P1 (Arg₇₅) and P6 (Arg₇₀) residues are essential for the acid pH-dependent activation of furin. Following the internal cleavage of the propeptide, the fragments dissociate from furin permitting the enzyme to cleave substrates *in trans*.

The furin activation pathway determined using the *in vitro* approach reported here is consistent with earlier studies, performed *in vivo*, that described the requirements for activation of this endoprotease (Molloy et al., 1994; Vey et al., 1994). Not only is propeptide cleavage upon entry into the RER a necessary step for activation of the enzyme, it is also a requirement for subsequent export of the membrane-tethered protein (Creemers et al., 1995; Molloy et al., 1994). This requirement suggests that *in vivo* cleavage at Arg₁₀₇ is necessary for folding of the molecule into a transport-competent form or perhaps facilitates the generation of furin oligomers. Nonetheless, this maturation step, which requires calcium and is sensitive to reducing agents, is alone not sufficient for furin activation. Furthermore, treatment of cells with either brefeldin A or monensin show that furin activation requires exposure to a late Golgi compartment (Vey et al., 1994). Our results are consistent in showing the importance of a mildly acid pH to the second site cleavage at -Arg₇₀-Gly-Val-Thr-Lys-Arg₇₅[↓]- and activation of furin. Indeed, by comparing the relative activity of furin constructs containing deletions of the enzyme's cytoplasmic tail, full activation of furin was found to depend on the correct localization and routing within the TGN/endosomal system (Molloy et al., 1994). Whether the need for the correct localization of furin to the TGN is important specifically for the time-dependent internal cleavage, conformational changes in the endoprotease and/or the propeptide, or secondary modification of the protein is not known. However, we have observed that truncated forms of furin are less efficiently sialylated implying that dwell time in the TGN (including possibly transit through communicating endosomal compartments) affects the maturation of furin (S.S. Molloy and G. Thomas, unpublished results).

The ordered, pH-dependent cleavages of the furin propeptide suggests a mechanism for the compartment-specific autoproteolytic activation of furin *in vivo* which is based on furin's cleavage site specificity. The autoproteolytic and RER-specific initial cleavage occurs at the consensus furin site -Arg₁₀₄-Thr-Lys-Arg₁₀₇[↓]- (Leduc et al., 1992). Typical of such sites (-Arg-X-Lys/Arg-Arg-) that are cleaved at either neutral or acidic pH (Hatsuzawa et al., 1992a; Hatsuzawa et al., 1992b; Molloy et al., 1992), both the P1 (Arg₁₀₇) and P4 (Arg₁₀₄) arginine residues are required (Leduc et al., 1992). By contrast, furin is able to cleave some substrates containing the motif -Arg-X-X-X-Lys/Arg-Arg[↓]- only in an acidic environment. For example, proalbumin is cleaved most efficiently at pH 5.5-6.0 at a site requiring both P1 and P6 arginine residues (Brennan and Nakayama, 1994a; Brennan and Nakayama, 1994b). Here we show that the measured pH optimum for furin activation *in vitro* (pH 6.0; Figure 4), by virtue of cleavage of the propeptide at -Arg₇₀-Gly-Val-Thr-Lys-Arg₇₅[↓]-, is in close agreement with the pH of the TGN (pH ~6.2; Seksek et al., 1995). Furthermore, mutation of either the P1 (Arg₇₅) or P6 (Arg₇₀) residues to Ala blocks furin activation by acidification but not by trypsinization (Figure 9), demonstrating that cleavage of the propeptide has been blocked, but folding of the enzyme has not been affected. Taken together, these data suggest that furin autoproteolytically cleaves its propeptide at -Arg₇₅ within the acidic environment of the TGN, either *in trans* by an associating active furin protein or by the cognate furin molecule within the propeptide•enzyme bimolecular complex. Whether another protease(s) may be required, as is the case with carboxypeptidase Y activation (Sorensen et al., 1994), is not currently known.

The acidic environment of the TGN may also promote dissociation of the cleaved propeptide fragments from furin. Comparison of the propeptide sequences of the proprotein convertase family shows the presence of multiple conserved histidine residues (reviewed in Siezen et al., 1995, see also legend to Figure 10B). The histidine residues may coordinate a metal atom necessary for enzyme activation or participate in ionic interactions with the mature domain. The pK_a of the ionizable second amino group on the histidine imidazole ring is ~7.0, although this could vary depending on the local microenvironment within the protein (Creighton, 1993). Regardless, within the neutral environment of the RER, these histidine residues should be neutral, while in the acidic environment of the TGN, they should become positively charged. This suggests that the acidification necessary to activate furin may contribute to changes in ionic interactions between the propeptide and a metal atom or the propeptide and the enzyme. These changes, together with cleavage of the propeptide at Arg₇₅, could lead to the dissociation of the propeptide fragments from furin, thereby unmasking the protease to act on substrates *in trans*.

In addition to the requirement for acidification, activation of furin may also be regulated by changes in calcium concentration. Whereas maximal activation of furin *in vitro* requires millimolar levels of calcium, propeptide cleavage in the structurally related enzyme PC1/3 *in vivo* requires calcium at only micromolar levels (Vey et al., 1994; J.V. and G.T. unpublished results). In the

RER, the concentration of total luminal calcium is 3 mM (Sambrook, 1990), however the free calcium concentration in this compartment is predicted to be approximately 1 μ M (Kendall et al., 1994). By contrast, the free calcium concentration in the TGN is believed to be in the millimolar range (Chanat and Huttner, 1991; Chandra et al., 1991; Roos, 1988; Song and Fricker, 1995). Interestingly, a homology model of furin based on the crystal structures of subtilisin and thermolysin has suggested the presence of a high-affinity calcium-binding site (Ca1) and a medium-affinity binding site (Ca2) (Siezen et al., 1994). It is possible that filling of the Ca1 site alone is required for cleavage at Arg₁₀₇ in the ER, whereas filling of both Ca1 and Ca2 is required for cleavage at Arg₇₅, and hence full activation of furin.

Although activation of the evolutionarily related furin and subtilisin endoproteases shares several properties including a requirement for autoproteolytic cleavage of propeptides, these processes differ significantly in at least three respects. First, furin activation is pH- and thus compartment-dependent, while subtilisin shows no such dependency. The need for this regulation is currently being investigated, but it seems likely that the delay of proteolytic activation prevents the enzyme from cleaving substrates prematurely or inappropriately. Alternatively, the compartment-specific activation of furin may facilitate either the adoption of secondary conformations or oligomerization necessary to the generation of the active species. Second, the fate of the subtilisin propeptide appears to be different from that of furin. The rapid and complete degradation of the subtilisin E propeptide during activation, by an as yet uncharacterized pathway, is likely a result of the broad substrate specificity of this endoprotease. By contrast, we show that dissociation of the furin propeptide is achieved with only limited proteolysis, presumably a result of the restricted cleavage site specificity of this proprotein convertase. Third, the propeptides of proprotein convertases share no sequence similarity with the subtilisin propeptide, despite the homologies among their catalytic domains (Fuller et al., 1989; Seidah et al., 1994; Siezen et al., 1995). This suggests that the roles the furin and subtilisin propeptides play in enzyme maturation may be significantly different. Whether or not the furin propeptide directs folding of the enzyme, as it does with subtilisin, remains to be determined. This role for the propeptide is implied by the finding that truncation of the furin propeptide results in the production of an inactive protease (Rehemtulla et al., 1992).

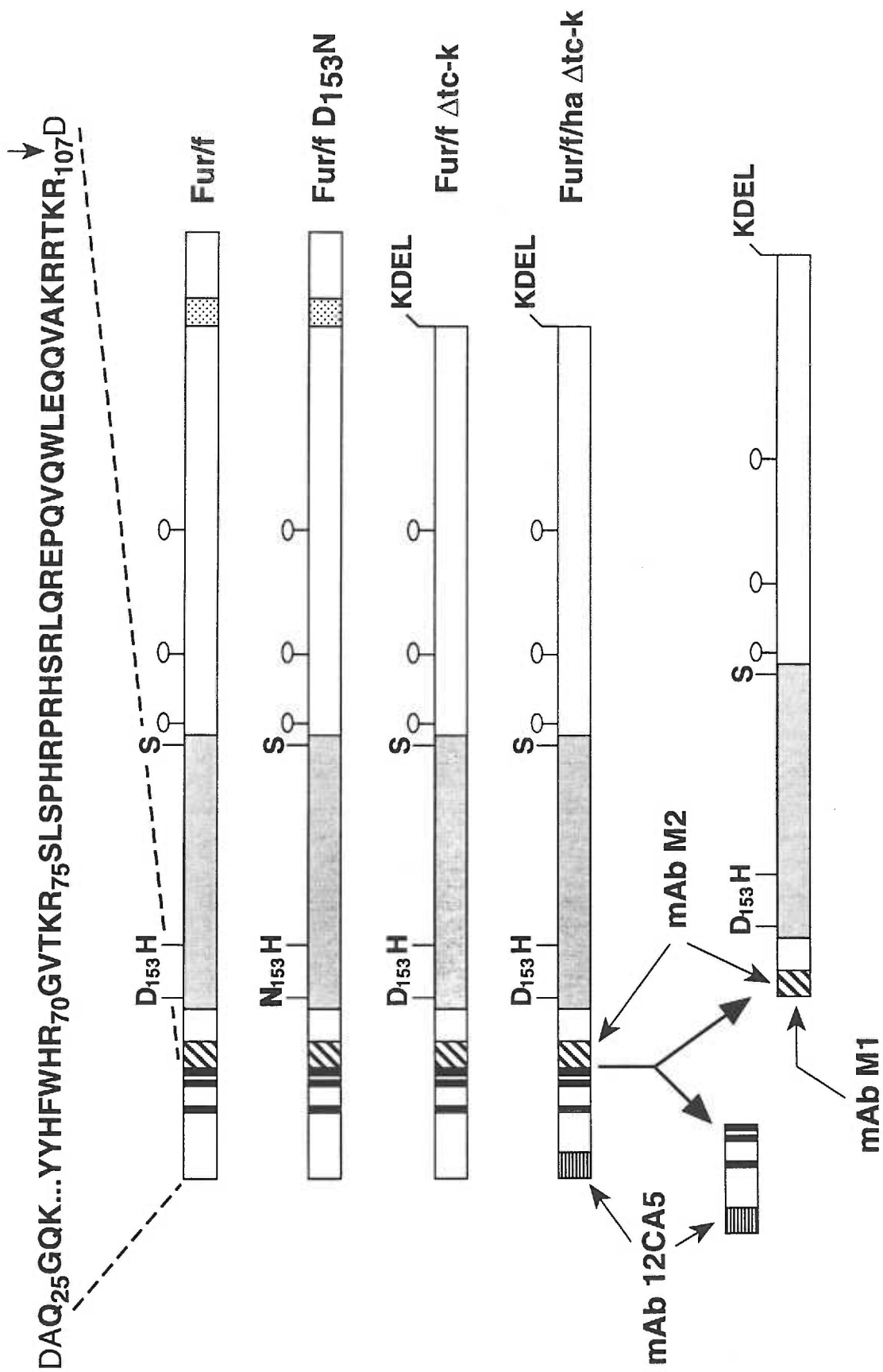
Although the propeptides of members of the convertase family share no sequence similarity with the propeptide of subtilisin, they are similar to one another (Figure 10B; Siezen et al., 1995). Strikingly, the convertase propeptides are highly charged and contain multiple doublets or clusters of basic amino acids in two distinct regions (Siezen et al., 1995). One basic residue cluster (-Arg-X-Lys-Arg⁺-) marks the predicted initial sites of autoproteolytic cleavage of the propeptides (Figure 10B). Indeed, biochemical studies show that, as for furin, the propeptides of Kex2p and PC1/3 are cleaved rapidly at this site following deposition of the recently synthesized proenzymes

into the RER (Gluschankof and Fuller, 1994; Goodman and Gorman, 1994; Lindberg, 1994; Vindrola and Lindberg, 1992). The second cluster of oligo-basic residues present in the propeptides of several other convertases including those for PC1/3, PC2, PC5/6 and PACE-4 can be aligned with the furin internal cleavage site (Figure 10B). This suggests that the multi-step, pH-dependent activation pathway described here for furin may similarly be used by other members of the family. However, not all proprotein convertases are expected to share all features of the furin activation pathway. For instance, the PC4 and PC7 propeptides lack an internal cluster of basic residues marking the second cleavage site, suggesting that these members of the family may be activated by an alternate pathway. Additionally, although proPC2 undergoes multiple cleavages of its proregion, it also requires the participation of an associating proPC2-binding protein, 7B2 for activation (Braks and Martens, 1994; Matthews et al., 1994b). Nonetheless, our results delineating the multi-step activation of furin *in vitro* provide a basis for further work on furin as well as creating a paradigm with which to evaluate the activation pathways of other enzymes in this important converting enzyme family.

ACKNOWLEDGMENTS

We are grateful to L. Thomas for expert technical assistance throughout all stages of this work. We thank H. Angliker for the Q1 substrate. We thank S. Arch and S. Molloy for critical reading of the manuscript and members of the Thomas lab for helpful discussions. This work was supported by NIH grants DK37274, DK44629 and HD30236 (G.T.). E.D.A. was the recipient of a Tartar Trust Fellowship. J.V. is the recipient of fellowship NRSA DK09069. F.J. is the recipient of an MRC (Canada) fellowship. C.D.T. was the recipient of fellowship NRSA DK09370.

Figure 1. Schematic of Furin Constructs. Recombinant furin constructs were generated using loop-in or site-directed mutagenesis. In construct fur/fD₁₅₃N the aspartic acid residue of the catalytic triad has been changed to an asparagine, resulting in inactivation of the protease. The truncated furin constructs fur/fΔtc-k and fur/f/haΔtc-k lack the sequences encoding the furin transmembrane domain (*stippled box*) and cytoplasmic tail, and have the ER-retention/recycling signal KDEL at their C-termini. Fur/f, fur/fD₁₅₃N and fur/fΔtc-k all have the FLAG epitope tag inserted directly after the proregion cleavage site (*diagonal bars*), so the N-terminus of the FLAG sequence is exposed upon autoproteolytic cleavage. The anti-FLAG mAb M2 can recognize either the blocked or exposed form of the FLAG epitope. The anti-FLAG mAb M1 can only recognize the FLAG epitope if it has a free N-terminus, and therefore is only able to detect the mature form of furin. In fur/f/haΔtc-k the HA epitope has been inserted directly after the signal sequence cleavage site (*vertical bars*). This epitope is recognized by the monoclonal antibody 12CA5. The subtilisin-like catalytic domain of furin is denoted by hatchmarks. The residues of the catalytic triad are indicated (*Asp, His, Ser*). Potential glycosylation sides are denoted by 'lollipops'. Pairs of basic amino acids in the proregion are indicated by thick vertical bars.



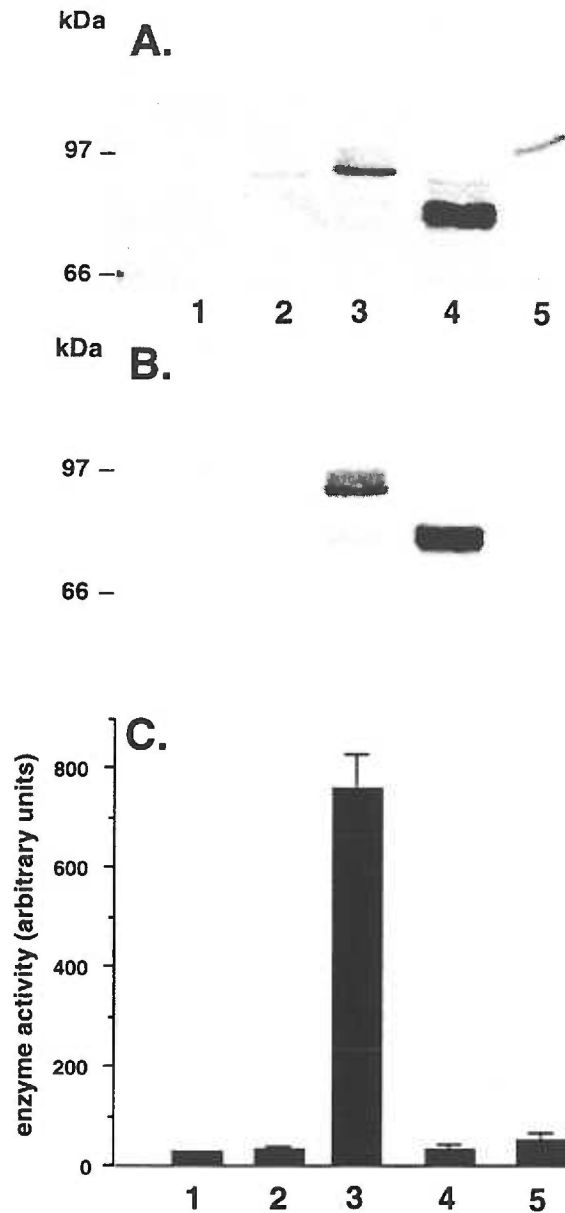


Figure 2. Expression, immunoreactivity and *in vitro* activity of furin constructs. (A and B) Western blot analyses of equivalent amounts of crude membrane samples prepared from BSC-40 cells either mock-infected (*lane 1*) or infected with VV:WT (*lane 2*), VV:hFur/f (*lane 3*), VV:hFur/fΔtc-k (*lane 4*) or VV:hFur/fD₁₅₃N, (*lane 5*). Flag-tagged furin constructs were detected using either mAb M1 (panel A, requires propeptide cleavage) or mAb M2 (panel B). (C) Proteolytic activity from the same membrane preparations were determined with the Q1 substrate (see Materials and Methods). Each reading represents the average of two samples assayed in duplicate. Furin activity is shown in arbitrary units of fluorescence. Bars indicate standard deviations.

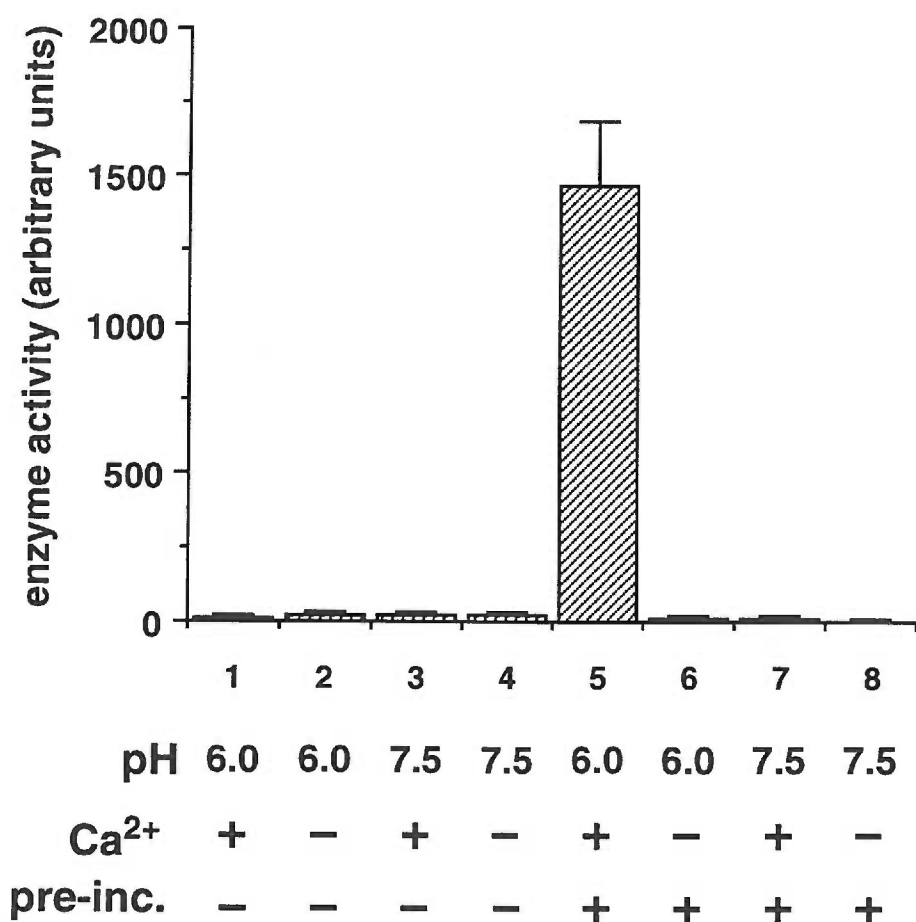


Figure 3. *In vitro* activation of ER-retained furin by low pH and calcium. Crude membrane preparations of BSC-40 cells infected with VV:hFur/fΔtc-k were resuspended in Bis-Tris buffer at pH 6.0 or 7.5, with or without 5 mM CaCl₂ as indicated. These samples were then pre-incubated at 30°C for 0 hours (*columns 1-4*) or for 3 hours (*columns 5-8*). Following pre-incubation, replicate aliquots of each sample was assayed for proteolytic activity using the Q1 substrate. Each reading represents two separate determinations performed in duplicate. Bars indicate standard deviations.

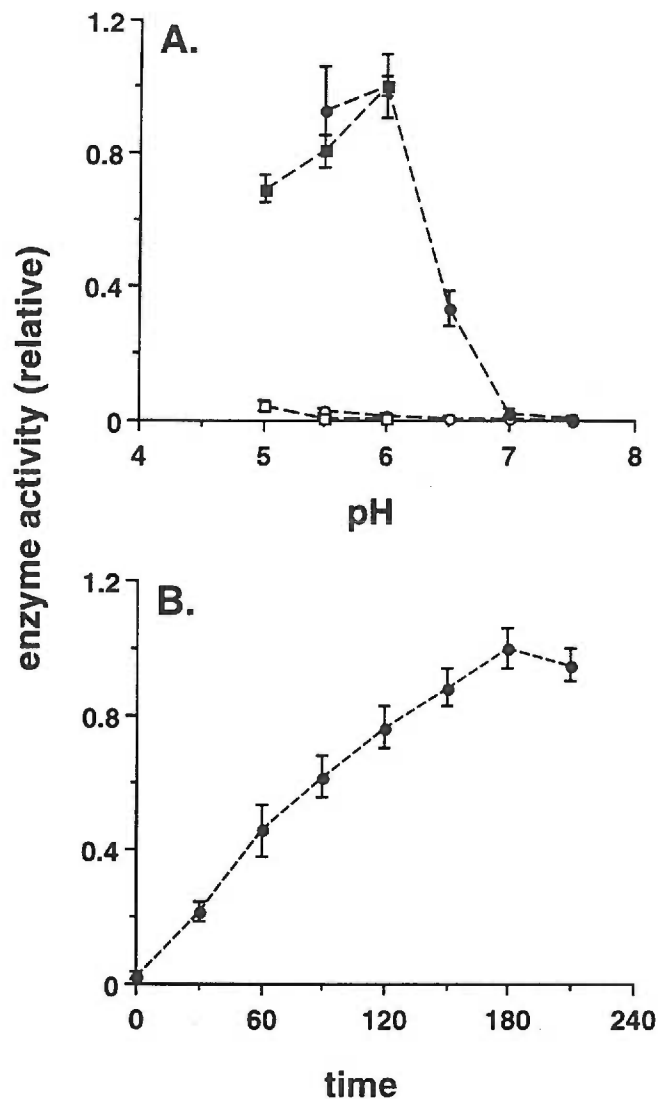


Figure 4. Effect of pH on furin activation and time course of activation at pH 6.0. (A) Replicate samples of crude membrane preparations from BSC-40 cells infected with VV:hFur/fΔtc-k were resuspended in 10 mM Bis-Tris buffer (*circles*) or a 100 mM sodium acetate buffer (*squares*) at the indicated pH. Samples were pre-incubated at 30°C for 0 minutes (*open symbols*) or 150 minutes (*closed symbols*) and assayed for proteolytic activity using the Q1 substrate. The data are normalized to the peak activity at pH 6.0. (B) Crude membrane preparations of BSC-40 cells infected with VV:hFur/fΔtc-k were resuspended in a 10 mM Bis-Tris assay buffer, pH 6.0 and pre-incubated at 30°C for up to 210 minutes. Following pre-incubation the furin activity in each sample was determined using the Q1 substrate. The data were normalized to the peak activity observed at 180 minutes. Each point in both panels represents the average of three separate determinations of samples assayed in quadruplicate. Bars indicate standard deviations.

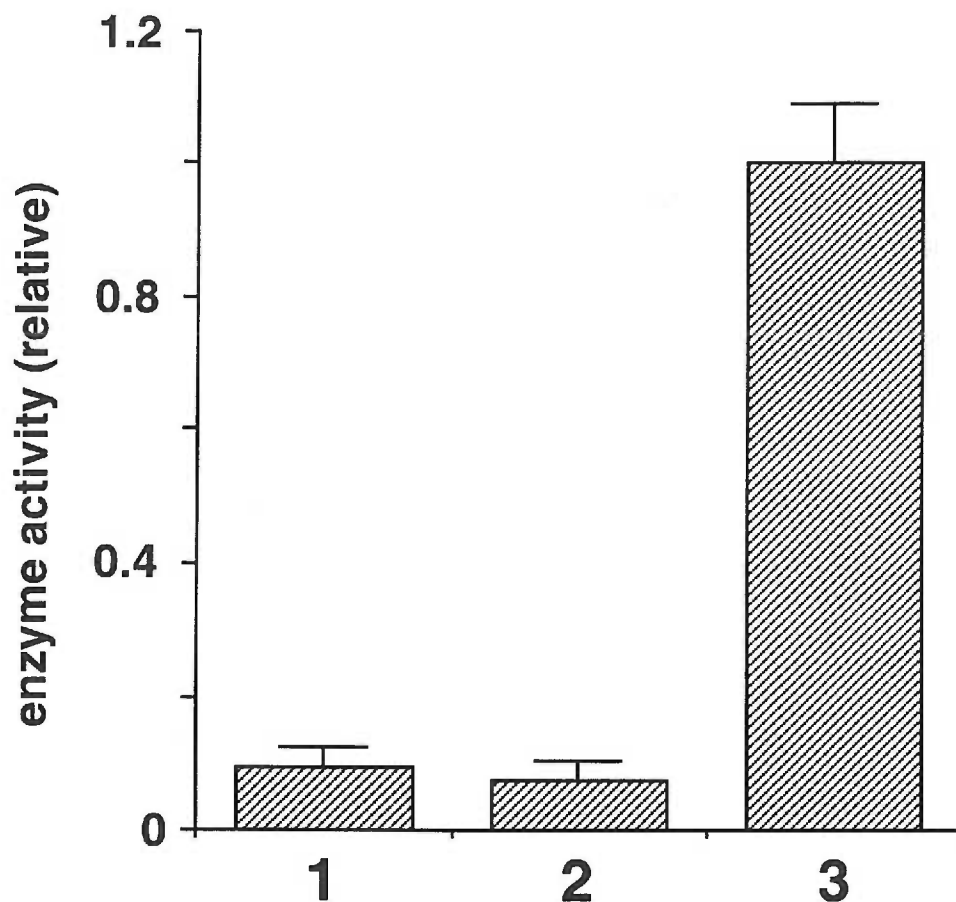


Figure 5. Limited trypsinization releases inhibition of furin at neutral pH. Crude membrane preparations of BSC-40 cells infected with VV:hFur/fΔtc-k were incubated for 1 hour at 30°C at pH 7.5 with no additions (*column 1*), with 2.5 mM soybean trypsin inhibitor and 0.83 nM bovine trypsin added simultaneously for a mock digestion (*column 2*), or with 0.83 nM bovine trypsin alone (*column 3*). Following incubation at 30°C for one 1 hour, 2.5 mM SBTI was added to the latter sample and all samples were incubated an additional 30 minutes at 30°C. Following incubation, the furin activity in all samples was determined using the Q1 substrate. Shown are the normalized means from quadruplicate experiments. Bars indicate standard deviations.

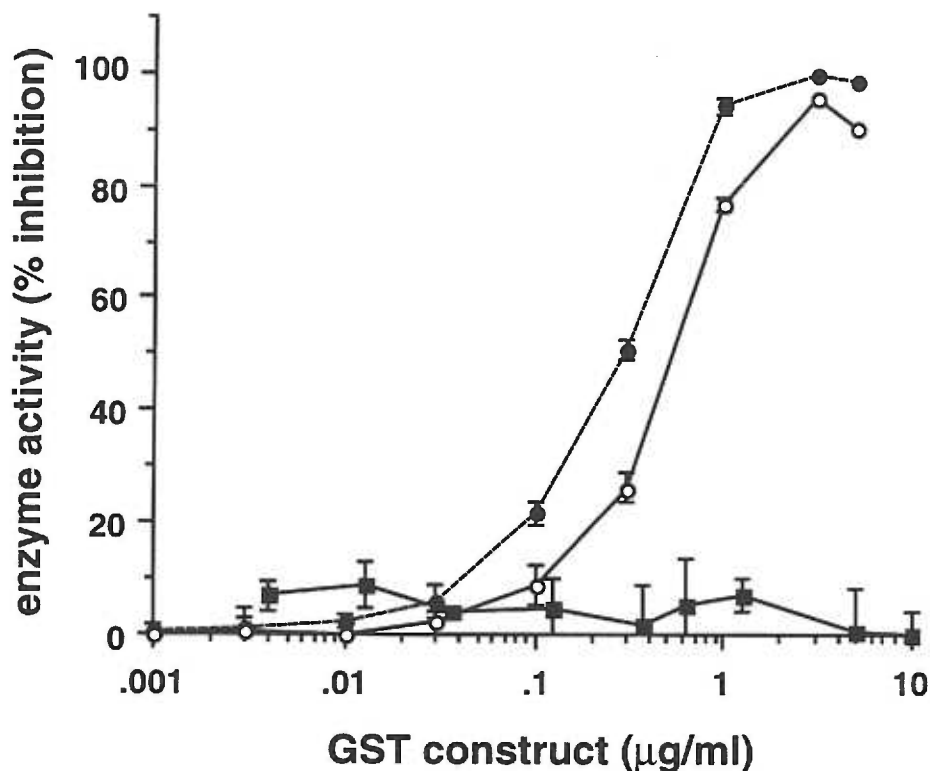


Figure 6. Inhibition of furin *in trans* by its propeptide. The concentration dependence of furin inhibition by GSTpro (*closed circles*) or GSTpro/ha (*open circles*) *in vitro* was determined in 10 mM Bis-Tris assay buffer, pH 7.5 using the fluorescent peptide substrate Boc-Arg-Val-Arg-Arg-4-methyl-coumaryl-7-amide. The $K_{0.5}$ of furin inhibition with GSTpro was 14 nM, and GSTpro/ha was marginally higher. Control samples containing GST alone (*closed squares*) showed no furin inhibition. Each point represents the average of triplicate samples. Bars indicate standard deviations.

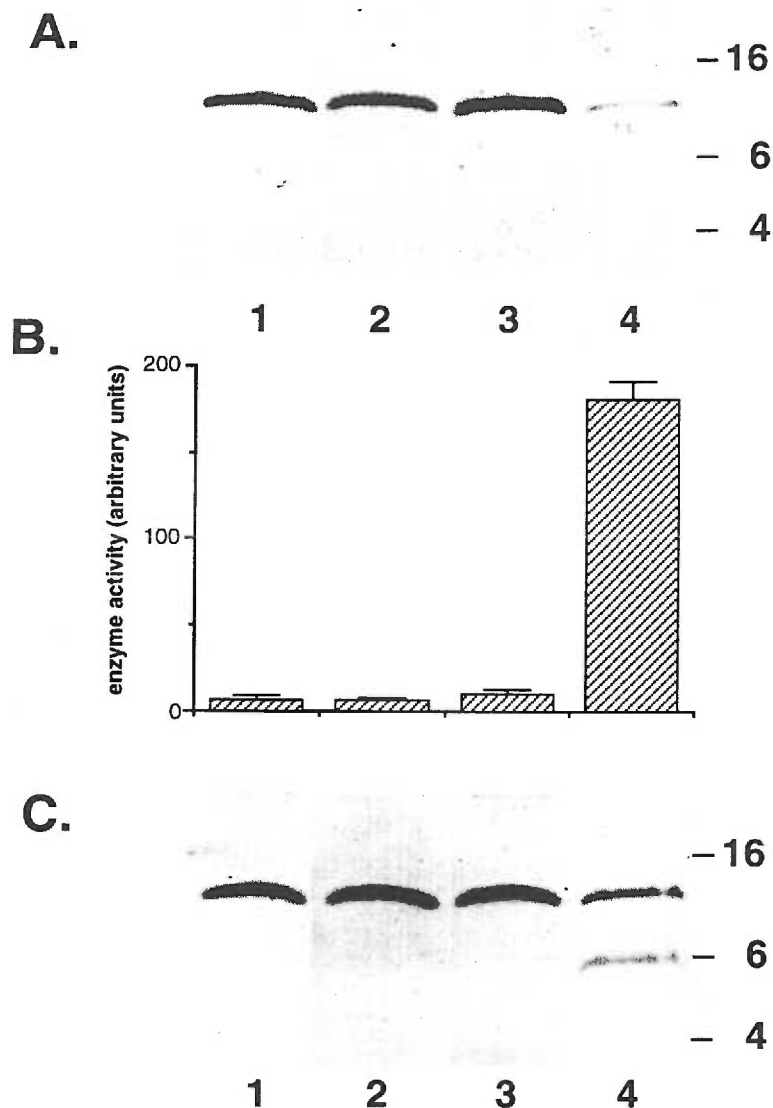


Figure 7. Fate of the Propeptide During Furin Activation. Equivalent amounts of membrane samples from BSC-40 cells expressing fur/f/ha₂tc-k were incubated in 10 mM Bis-Tris assay buffer at pH 7.5 (*lanes 1 and 2*) or pH 6.0 (*lanes 3 and 4*) for 0 hours (*lanes 1 and 3*) or 5 hours (*lanes 2 and 4*). Proportionate amounts of the extracts were then divided and analyzed for furin-associated propeptide, enzymatic activity and total propeptide present (10 μ l). (A) Proteolytically mature recombinant furin was immunoprecipitated with mAb M1, separated on a 15% SDS-peptide gel, transferred to nitrocellulose, and probed with mAb 12CA5 to identify co-immunoprecipitating HA-tagged propeptide. (B) Furin activity of the samples in A was determined using the Q1 substrate. (C) Extracts from the activation assay were analyzed directly by SDS peptide gel electrophoresis, transfer to nitrocellulose, and HA-tagged propeptide immunostaining with mAb 12CA5. Molecular weight markers (labeled in kDa) migrated on gels as indicated at the right of (A) and (B). Bars indicate standard deviation.

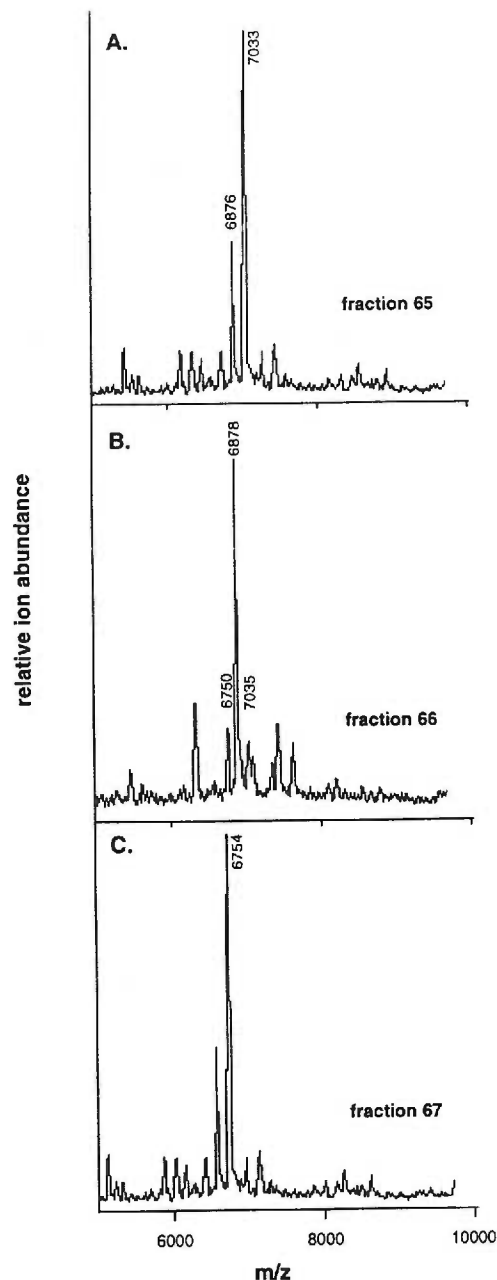


Figure 8. MALDI-TOF mass spectra of propeptide cleavage products. A crude membrane preparation of BSC-40 cells expressing fur/f/haΔtc-k was incubated in 10 mM Bis-Tris assay buffer, pH 6.0 for 8 hours and then fractionated on reversed-phase HPLC. The fractions containing the HA-tagged ~6 kDa band (determined by immunoblotting - data not shown) were subjected to MALDI-TOF MS. In the mass range of this fragment, fraction 65 is seen to contain predominantly the peptide pGlu₂₅→Arg₇₅ (calculated mass = 7036.9), fraction 66 peptide pGlu₂₅→Lys₇₄ (calculated mass = 6880.7), and fraction 67 peptide pGlu₂₅→Thr₇₃ (calculated mass = 6752.5). Electrospray LC/MS of each of these fractions allowed higher precision mass determination as follows: fraction 65 was seen to contain co-eluting species of m/z 1407.9, 1173.7 and 1006.1 (correlating to a mass of 7035.5 a.m.u.); fraction 66 contained co-eluting species of m/z 1377.0, 1147.6, and 983.8 (correlating to a mass of 6880.0 a.m.u.); and fraction 67 contained co-eluting species of m/z 1351.4, 1126.3, and 965.6 (correlating to a mass of 6752.0 a.m.u.).

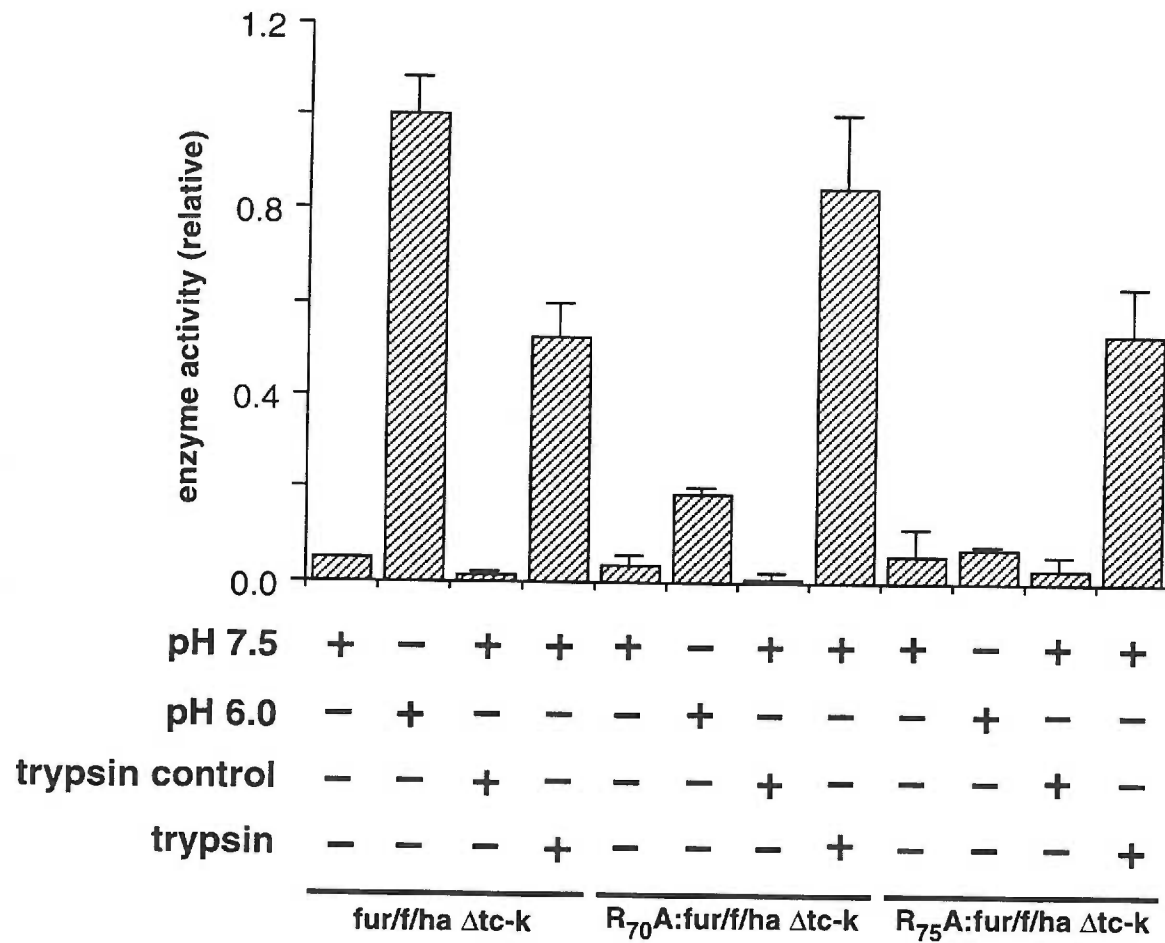
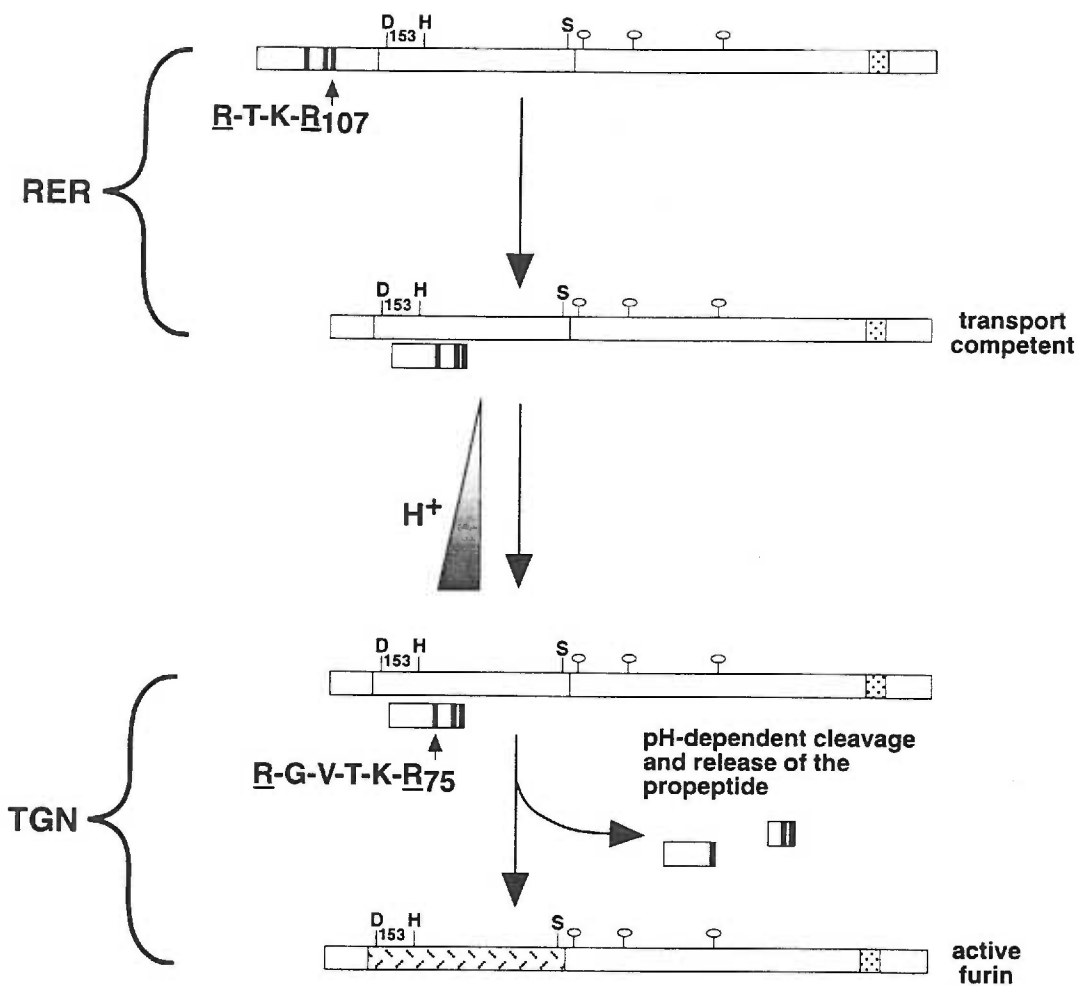


Figure 9. Activation of R₇₀A: fur/f/ha Δ tc-k and R₇₅A: fur/f/ha Δ tc-k *in vitro*. Crude membrane preparations from BSC-40 cells expressing either fur/f/ha Δ tc-k, R₇₀A: fur/f/ha Δ tc-k or R₇₅A: fur/f/ha Δ tc-k were incubated at 30°C in 100 μ l Bis-Tris buffer at pH 7.5 or 6.0 with 1 mM 2-mercaptoethanol, 5 mM CaCl₂, 500 μ M PMSF, 10 μ M pepstatin-A, 20 μ M E-64 and 50 μ g/ml aprotinin for 1.5 h. Alternatively, membrane preparations were incubated with trypsin for 1 h followed by SBTI treatment for 0.5 h or subjected to a mock trypsin digestion (see legend to figure 6). Following treatment the samples were assayed *in vitro* for furin activity against the Q1 substrate. Each point represents the average of three separate assays. Bars indicate standard deviation.

Figure 10. Model of furin activation *in vivo*. (A) The data reported here and in earlier *in vivo* studies (Creemers et al., 1995; Leduc et al., 1992; Molloy et al., 1994; Vey et al., 1994) suggest the following compartment-dependent multi-step model for furin activation. Furin is translocated into the ER and concomitantly the signal sequence is removed at -Ala-Asp-Ala₂₄[↓]-. Following propeptide-mediated folding, furin autoproteolytically cleaves its propeptide at -Arg-Thr-Lys-Arg₁₀₇[↓]-. In the neutral pH and low free calcium environment of the RER, the propeptide remains non-covalently associated and functions as an autoinhibitor. Following this initial propeptide cleavage, the furin•propeptide complex is allowed to exit the RER and transit to the TGN. In the mildly acidic and millimolar free-calcium environment of the TGN, the propeptide is cleaved by furin (either the cognate molecule or *in trans* by an associating furin enzyme) at -Arg-Gly-Val-Thr-Lys-Arg₇₅[↓]-. The propeptide fragments generated by this second cleavage bind less tightly (perhaps aided in part by a weakening of histidine-participatory ionic interactions at the acidic pH) and dissociate from the catalytic domain. Hence furin becomes active to cleave substrates *in trans* (denoted by the highlighting of the catalytic domain) in multiple compartments within the TGN/endosomal system. (B) Partial sequence alignment for the propeptides of several proprotein convertases. The numbering used starts with the proposed initiator methionine residues. The spacing between the primary (*arrow*) and internal (*arrowhead*) cleavage sites is nearly identical for each of the convertases, ranging in size from 28 to 32 residues. Proximal to the internal cleavage sites are a conserved set of histidine residues present in each endoprotease (corresponding to His₆₆, His₆₉ and His₈₄ in furin, refer to Figure 1) that may participate in either metal binding or ionic interactions with furin (see Discussion). Arginine residues shown to be essential for the initial and internal cleavages of the furin propeptide are underlined.

A.



B.

furin	...	R	G	V	T	K	R ₇₅	...	K	R	R	T	K	R ₁₀₇
PC1/3	...	P	R	R	S	R	R ₈₁	...	K	E	R	S	K	R ₁₁₀
PC2	...	K	A	K	R	R	R ₈₁	...	F	D	R	K	K	R ₁₀₉
PC5/6	...	S	R	T	T	K	R ₈₄	...	K	K	R	T	K	R ₁₁₆
PACE-4	...	S	K	T	F	K	R ₁₁₇	...	K	K	R	V	K	R ₁₄₉

CHAPTER 2

The *In Vivo* Activation of Furin: Propeptide Mediated Folding and Compartment Specific Propeptide Cleavage

Eric D. Anderson, François Jean and Gary Thomas

From the Vollum Institute and Department of Cell and Developmental Biology, Oregon Health Sciences University, 3181 SW Sam Jackson Park Road, Portland, OR 97201-3098

Manuscript in Preparation

François Jean synthesized the internally quenched peptide substrates as well as confirming the furin cleavage sites by RP-HPLC and mass spectrometry.

ABSTRACT

Furin is synthesized as an inactive zymogen with an 83-amino acid N-terminal propeptide that has been proposed to be an intramolecular chaperone (IMC). During activation, the propeptide is autoproteolytically excised from furin (-Arg₁₀₄-Thr-Lys-Arg₁₀₇[↓]-) and remains non-covalently bound, acting as a potent autoinhibitor. An *in vitro* study by our group suggested that in the acidic environment of the late secretory pathway, the propeptide is internally cleaved at -Arg-Gly-Val-Thr-Lys-Arg₇₅[↓]- (Anderson et al., 1997). This cleavage results in dissociation of the propeptide, thus allowing furin to act on substrates *in trans*. In this study, we explore the role of the propeptide in mediating the multi-step compartment-specific activation of furin *in vivo* in light of its potential role as an IMC. A furin construct lacking the propeptide, fur/fΔpro, is ER-retained and proteolytically inactive, and co-expression with the propeptide *in trans* partially restores correct trafficking and activity. Further, if the propeptide is not excised, furin is localized to the ERGIC/CGN, suggesting that the quality control system blocks transport of this molecule due to incomplete folding. These results are consistent with the propeptide's role as an IMC. Furin that has undergone propeptide excision proceeds to the acidic compartments of the TGN/endosomal system where it autoproteolytically and intramolecularly cleaves its propeptide at -Arg-Gly-Val-Thr-Lys-Arg₇₅[↓]-, resulting in propeptide dissociation ($t_{1/2}$ = ~105 minutes). Cleavage at -Arg₇₅[↓]- is not required for proper furin trafficking. The pH-modulated cleavage of the internal propeptide cleavage sequence was demonstrated by the use of synthetic peptide substrates. Interestingly, mutagenesis revealed that if the site of internal propeptide cleavage is changed to resemble the canonical -Arg-X-Lys/Arg-Arg[↓]- furin cleavage motif (-Arg-Gly-Val₇₂-Thr-Lys-Arg₇₅- → -Arg-Gly-**Arg**₇₂-Thr-Lys-Arg₇₅-), furin is predominantly ER retained. The implications of this for our understanding of furin folding are discussed.

INTRODUCTION

Following correct folding/assembly, many eukaryotic proteins are proteolytically modified in late secretory pathway compartments. Single or multiple endoproteolytic cleavages of these larger precursors result in the release of smaller, bioactive products. A class of endoproteases in eukaryotes responsible for these cleavage events at sites containing oligo basic amino acids are the proprotein convertases (PCs). These calcium-dependent serine endoproteases are evolutionarily related to bacterial subtilisin. Members of the PC family include Kex2p, which catalyzes the activation of α -mating pheromone in yeast, and many Kex2p homologues are expressed in higher eukaryotes including PC1/3, PC2, PC4, PC5/6, LPC/PC7/8, PACE-4 and furin (see Molloy et al., 1999; Nakayama, 1997; Seidah and Chretien, 1997; Steiner, 1998 for reviews).

Furin is a ubiquitous subtilisin-like serine endoprotease and type I membrane protein localized primarily to the TGN (Bresnahan et al., 1990; Hatsuzawa et al., 1992a; Matthews et al., 1994a; Molloy et al., 1992; Molloy et al., 1994). Furin is not statically retained in this compartment, however; rather, it traffics between two local cycling loops, one at the TGN, the other at the cell surface, by virtue of phosphorylation modulated trafficking signals in its cytoplasmic tail (Jones et al., 1995; Molloy et al., 1994; Schafer et al., 1995; Voorhees et al., 1995; Wan et al., 1998). As it traffics, furin cleaves/activates numerous endogenous and exogenous precursor proteins in both the biosynthetic and endocytic pathways (reviewed in Molloy et al., 1999; Nakayama, 1997; Seidah and Chretien, 1997; Steiner, 1998). Cleavage of these substrates occurs primarily at the consensus furin cleavage site -Arg-X-Lys/Arg-Arg[↓]-, although in some cases furin has been shown to cleave at the motif -Arg-X-X-X-Lys/Arg-Arg[↓]- at acidic pH (Brennan and Nakayama, 1994a; Brennan and Nakayama, 1994b).

Before it can act on its substrates, furin itself must go through a complex process of activation. Furin is translated as an inactive zymogen with an 83 amino acid N-terminal propeptide. Experimental evidence suggests that furin's propeptide may play a role in folding and activation (Anderson et al., 1997; Rehemtulla et al., 1992; Zhou et al., 1995). This is consistent with research that shows that the folding of many evolutionarily unrelated classes of protease (e.g. serine-, aspartyl-, cysteinyl- and metallo-proteases) is mediated by (typically N-terminal) propeptides that act as so-called 'intramolecular chaperones' (IMCs). IMC-mediated folding has been most thoroughly investigated in the secreted bacterial serine endoproteases α -lytic protease and subtilisin. These IMCs have been found to increase the folding rate of their cognate proteases by lowering a specific kinetic barrier very late in the folding pathway by stabilizing a high-energy 'native-like' transition intermediate (reviewed in Baker, 1998; Baker and Agard, 1994; Baker et al., 1993; Baker et al., 1992b; Shinde and Inouye, 1993). Near the end of the folding process, IMC propeptides are autoproteolytically excised. Propeptide excision triggers significant

conformational changes that cause the loss of hydrophobic surface exposure to solvent, thus marking the end of folding (Anderson et al., 1999; Eder et al., 1993a; Shinde et al., 1999). In the absence of the IMC propeptide, the enzyme will fold into an inactive and kinetically stable 'molten globule'-like intermediate (Baker et al., 1992b; Eder et al., 1993b). Addition of the propeptide *in trans* (Baker et al., 1992b; Eder et al., 1993b; Silen et al., 1989; Strausberg et al., 1993) causes rapid conversion of this folding intermediate to the native state, indicating that energy liberated from propeptide excision is not required for folding.

Following excision, IMCs remain non-covalently bound to their cognate enzymes, acting as tight binding autoinhibitors (Baker et al., 1992a; Li et al., 1995). Crystal structures reveal that the propeptide C-terminus occupies the cognate proteases' active site, while the rest of the propeptide is folded into a domain bound at a distance from the active site (Bryan et al., 1995; Gallagher et al., 1995; Sauter et al., 1998). Thus, propeptide-mediated inhibition is a result of the propeptide cleavage site sequence sterically occluding the active site (Sohl et al., 1997). The residues at the excision site play a critical role in mediating IMC action, possibly by guiding the folding of the active site (Baker, 1998; Peters et al., 1998). The use of these C-terminal residues may be a general mechanism for IMC action, as suggested by the observation that all protease propeptides that promote folding are autoinhibitors (Baker et al., 1993). Since IMCs bind and inhibit their cognate proteases, they must be degraded for enzyme activation. This degradation may be autoproteolytic, as has been proposed for subtilisin (Bryan et al., 1995). IMC degradation leaves the cognate protease locked into the native state, which can be metastable (Sohl et al., 1998), by a large kinetic barrier to unfolding (Baker, 1998). Interestingly, even after its IMC has been degraded, subtilisin 'remembers' steric information from its propeptide, and this 'memory' modulates the enzyme's biophysical and biochemical properties (Shinde et al., 1999; Shinde et al., 1997). Due to their role in imparting steric information, propeptides are also called 'steric chaperones' (Ellis, 1998).

The hypothesis that the furin propeptide is an IMC is consistent with recent work on the maturation of this endoprotease. Furin's propeptide is autoproteolytically excised at -Arg-Thr-Lys-Arg₁₀₇[↓]- in the ER, and excision is necessary for transport from the early secretory pathway (Creemers et al., 1995; Leduc et al., 1992; Molloy et al., 1994; Vey et al., 1994). However, propeptide excision is insufficient for activation, which requires transport to late secretory pathway compartments (Molloy et al., 1994; Vey et al., 1994). A recent *in vitro* study performed by our group elucidated the reason for this (Anderson et al., 1997). After excision, the propeptide remains non-covalently bound to furin, acting as a potent autoinhibitor ($K_{0.5}$ =14 nM). Exposure of the inactive furin•propeptide complex to a mildly acidic (pH 6.0) and calcium-containing (low millimolar) environment characteristic of the TGN results in a second cleavage within the propeptide at -Arg₇₀-Gly-Val-Thr-Lys-Arg₇₅[↓]-. Internal propeptide cleavage was found to require

both P1 and P6 arginines, suggesting that furin might catalyze this cleavage due to its pH-dependent cleavage site specificity. Concomitant with cleavage at -Arg₇₅[↓]-, the propeptide fragments dissociate from furin, permitting the enzyme to cleave substrates *in trans*. These *in vitro* findings were interpreted to suggest that furin becomes active *in vivo* within the TGN, the enzyme's compartment of residence (Molloy et al., 1994).

By a combination of *in vivo* and *in vitro* experimentation we found evidence that i) the furin propeptide has the properties of an IMC, and ii) after propeptide mediated folding, furin degrades the inhibitory propeptide via a transport-and pH-dependent, autoproteolytic, and intramolecular process. Three findings support the propeptide's role as an IMC: i) a furin construct lacking the propeptide, fur/fΔpro, is ER-retained and proteolytically inactive, ii) co-expression of fur/fΔpro with the propeptide *in trans* restores TGN-localization and activity, and iii) if the propeptide is not excised, furin accumulates in the ERGIC/CGN, suggesting incomplete folding and subsequent retention by the quality control system. We also found that after propeptide excision, the inactive furin•propeptide complex proceeds to the acidic compartments of the TGN/endosomal system, where it autoproteolytically and predominantly intramolecularly cleaves its propeptide at -Arg-Gly-Val-Thr-Lys-Arg₇₅[↓]-. This cleavage results in dissociation of the inhibitory propeptide ($t_{1/2}$ = ~105 minutes). Unlike propeptide excision, cleavage at -Arg₇₅[↓]- is not required for correct furin trafficking, suggesting that the enzyme, although inactive, is fully folded. The pH-modulated recognition of the internal propeptide cleavage site was demonstrated by the use of synthetic peptide substrates. Given that propeptide excision and internal cleavage are intramolecular, it suggests that the furin•propeptide complex undergoes rearrangement in order to permit furin's active site access to these two cleavage sites within the same propeptide. Interestingly, we found that the integrity of the P1/P6 Arg internal propeptide cleavage motif is essential for the correct folding of furin. Indeed, mutagenesis revealed that if the site of internal propeptide cleavage is changed to resemble the canonical (-Arg-X-Lys/Arg-Arg[↓]-) furin cleavage motif (-Arg-Gly-Val₇₂-Thr-Lys-Arg₇₅- → -Arg-Gly-Arg₇₂-Thr-Lys-Arg₇₅-), furin is predominantly ER-retained and remains a zymogen. A speculative model for furin folding based on the relative K_m 's of the propeptide excision site vs. the internal site of propeptide cleavage is discussed.

MATERIALS AND METHODS

Materials

All buffers and chemical reagents were purchased from Sigma (St. Louis, MO) unless otherwise specified. The peptide substrate pGlu-Arg-Thr-Lys-Arg-4-methyl-coumaryl-7-amide (MCA) was from Peptides International (Louisville, KY). The secreted soluble furin construct Fur713t was purified as described previously (Jean et al., 1998). Alkaline phosphatase-conjugated goat anti-mouse and goat anti-rabbit secondary antibodies were obtained from Southern Biotechnology Associates (SBA; Birmingham, AL). The anti-HA antibodies mAb HA.11 and mAb 12CA5 were obtained from the Berkeley Antibody Company (Berkeley, CA) and Boehringer-Mannheim Biochemicals (Indianapolis, IN), respectively. Purified mAbs M1 and M2 directed against the FLAG epitope were obtained from Kodak-IBI (Rochester, NY). The anti-signal sequence receptor (SSR) anti-serum was kindly provided by T. Rapoport and the anti-ERGIC-53 antiserum (G1/93) was kindly provided by H.-P. Hauri. Endoglycosidase H was purchased from Boehringer-Mannheim Biochemicals. Brefeldin A was purchased from Epicenter Technologies (Madison, WI). Decanoyl-Arg-Val-Lys-Arg-chloromethylketone (CMK) was purchased from Bachem (Torrance, CA). All amino acid derivatives (L-isomer) were purchased from Novabiochem (La Jolla, CA). The reagents and the solvents for solid-phase peptide synthesis were from Advanced Chemtech (Louisville, KY). The preloaded Fmoc-Ala-Wang resin was purchased from Synpep (La Jolla, CA), while the tert-butyloxycarbonyl (Boc)-anthranilic acid and the 9-fluorenylmethoxycarbonyl (Fmoc)-(3-nitro) Tyr were obtained from Bachem California (Torrance, CA). Peptide synthesis was carried out on an automated peptide synthesizer (Model 431A; Applied Biosystems, Mississauga, Ont., Canada) using procedures previously described (Jean et al., 1995).

Cell Culture

BSC-40 cells were maintained in minimal essential medium (MEM; GIBCO BRL, Gaithersburg, MD) containing 10% fetal bovine serum (FCS; HyClone, Logan, Utah) and 25 µg/ml gentamycin as described previously (Bresnahan et al., 1990; Thorne et al., 1989). In some experiments, following recombinant vaccinia infection, cells were fed in defined, serum-free medium (MCDB202; McKeehan and Ham, 1976).

Immunofluorescence

For immunofluorescence microscopy, cells were cultured on glass coverslips, and grown to 50-80% confluence before being used as described in the text. These cells were fixed in 4% paraformaldehyde and immunofluorescence analysis performed as described (Molloy et al., 1994). mAb M1 and mAb M2 (Kodak/IBI) were used at dilutions of 1:50 and 1:100 respectively, the signal sequence receptor peptide rabbit antiserum was used at 1:200, the ERGIC-53 mAb G1/93 was used at 1:250, the anti-furin tail PA1-062 rabbit antiserum was used at 1:300 (a dilution low enough to minimize ER staining), and the mAb HA.11 was used at 1:4000. Secondary antibodies included an IgG_{2b}-specific Texas Red (TxRd)-conjugated goat anti-mouse antibody (SBA) used at 1:400, an IgG₁ specific fluorescein isothiocyanate (FITC)-conjugated goat anti-mouse antibody (SBA) used at 1:150, and a TxRd-conjugated anti-rabbit antibody used at 1:400 (SBA).

Pulse-chase/immunoprecipitation

Metabolic labeling and immunoprecipitations to assess pro- β -NGF processing were performed as described previously (Bresnahan et al., 1990), except that the amount of processed β -NGF and unprocessed pro- β -NGF were quantitated using a PhosphorImager 445 SI (Molecular Dynamics; Sunnyvale, CA). The relative signal of the product was divided by the signal of the precursor, yielding a relative measure of processing efficiency.

For the analysis of furin glycosylation state, confluent BSC-40 cells (2×10^6 cells/sample) in 35 mm dishes were infected with recombinant VV at an m.o.i. of 10 and incubated at 37°C. At 4 hours post-infection, the medium was replaced with methionine- and cysteine-free MEM (ICN) supplemented with 1% dialyzed FCS and the cells were incubated for an additional 30 minutes at 37°C, after which they were pulse-labeled with [³⁵S]Met/Cys (NEN Express label, DuPont) at 200 μ Ci/ml for 30 minutes. Following the pulse, cells were either harvested or chased for varying intervals by replacing the labeling medium with MEM containing 10% FCS and supplemented with 150 μ g/ml each of methionine and cysteine. For harvesting, the plates were placed on ice, the medium removed and the cells lysed by trituration in 1 ml modified RIPA buffer (mRIPA, 50 mM Tris-HCl pH 8.0, 150 mM NaCl, 1% NP-40 and 1% sodium deoxycholate). The lysates were clarified by centrifugation at 16,000 g for 5 minutes and the supernatants transferred to fresh tubes for immunoprecipitation. Primary antibody PA1-062 (1:250) was added and the samples were incubated for 16 hours at 4°C with mixing. Following the primary incubation, protein A coupled to Sepharose CL4B (Zymed) was added (40 μ l of 50% slurry) and the incubation continued for an additional 2 hours, after which the beads were spun down, washed three times with mRIPA and resuspended in 30 μ l of 2 x SDS sample buffer. For determinations of endoglycosidase H sensitivity the washed immunoprecipitates were rinsed in D-PBS, then resuspended in 25 μ l of

reaction buffer (50 mM sodium citrate, pH 6.0, and 0.1 % SDS) and incubated for 18-24 hours at 37°C with or without endoglycosidase H (Boehringer-Mannheim) prior to addition of 30 µl 2 x SDS-PAGE loading buffer, and resolution by SDS-PAGE on an 8% gel.

Labeling of both furin and its propeptide was performed in essentially the same manner as described above. At 4 hours post-infection, the medium was replaced with arginine- and leucine-free MDCB202. After a 0.5 hour incubation at 37°C, the cells were pulse-labeled with 100 µCi each of [³H]Arg and [³H]Leu (NEN, Dupont) for 0.5 hours. Following the pulse, the cells were either harvested, or chased for varying intervals by replacing the labeling medium with MDCB202 supplemented with 150 µg/ml each of arginine and leucine. For harvesting, the cells were placed on ice, the medium removed and the cells lysed by trituration in 1 ml TX^{Ca2+} buffer (50 mM Tris-HCl, pH 8.0, 150 mM NaCl, 1% TX-100) supplemented with 10 µM decanoyl-Arg-Val-Lys-Arg-CMK to inhibit residual furin activity. For immunoprecipitation, the mAb M1 was added (100 µg/ml), and the samples incubated 16 hours at 4°C with mixing. Following the primary incubation, protein G coupled to Sepharose CL4B (Zymed) was added (40 µl of 50% slurry) and the incubation continued for an additional 2 hours, after which the beads were spun down, washed three times with TX^{Ca2+} and resuspended in 30 µl of 2 x SDS sample buffer. The samples were then separated on a 15% peptide gel using an SDS-Tris-tricine buffer system (Dayhuff et al., 1992; Schägger and von Jagow, 1987). The gel was stained with Coomassie blue, destained, incubated in dH₂O for 0.5 hour, then 1 M sodium salicylate for 0.5 hour, dried down and exposed to film. Radioactive bands representing furin and the propeptide were excised from the gel, treated with Solvable (Packard Biosciences; Meriden, Connecticut), and counted in the LSC cocktail Hionic Fluor (Packard) on a 1900 TR LS Analyzer (Packard). The counts obtained from corresponding gel regions of VV:WT infected cells were used for a background reading.

Membrane Fractionation, Furin Activity Assays and Titration Analysis

Crude preparations of cellular membranes were made as described previously (Anderson et al., 1997). Furin activity assays with 25 µl of the resuspended membrane pellets were carried out in 100 mM HEPES, pH 7.5, 1 mM 2-mercaptoethanol, 0.5% Triton X-100 and 1 mM CaCl₂. Fluorometric assays with pGlu-Arg-Thr-Lys-Arg-MCA containing peptides were performed as described previously (Jean et al., 1998) using a FluoroMax-2 spectrofluorometer equipped with a 96-well plate reader (Instrument SA, Edison, NJ). The excitation/emission wavelengths of 370/460 were used to measure released AMC (7-amino-4-methylcoumarin). To determine the number of furin active sites in both membrane preparations and Fur713t preparations, titration analysis was performed as described previously (Jean et al., 1998).

Furin Constructs and Vaccinia Virus (VV) Expression

The HA and FLAG epitope tagged furin construct fur/f/ha was generated using fur/f/ha Δ tc-k in pZvneo (Anderson et al., 1997). The BamHI/BamHI fragment from full length fur/f in pZvneo [described previously (Molloy et al., 1994)] was domain swapped into fur/f/ha Δ tc-k in order to restore both the transmembrane domain and cytoplasmic tail. The furin mutants V₇₂R: fur/f/ha, R₇₅A: fur/f/ha and fur/f Δ pro were based on the EcoRI/KpnI fragment of furin in pAlter-1 as a template, and generated by single primer mutagenesis using the primers V72R (5'- CTG GCA TCG AGG CCG GAC GAA GCG GTC -3', R75A (5'- GTG ACG AAG GCC TCC CTG TCG -3') and PROLO1 (5'- CTG CTA GCA GCT GAT GCT GAC TAC AAG GAC GAC GAT -3'). The V72R mutation introduced a diagnostic MspI, and the R75A mutation introduced a diagnostic StuI site (in boldface type). The full length furin constructs were then generated by triple-ligating the EcoRI/SacII fragment of the mutant furin with the EcoRI/XbaI and XbaI/SacII fragments of pZvneo: fur/f/ha. Pro/ha was generated by standard PCR from the construct fur/f/ha in pZvneo using the primers N.SS.PRO (5'- GAA GAT ATC ATG GAG CTG AGG CCC TGG -3') and C.PRO (5'- GTC GAT ATC TCA CCG TTT AGT CCG TCG CTT -3') followed by cloning of the fragments into the unique StuI site of pZVneo. This subcloning step was facilitated by the introduction of EcoRV sites (boldface type). In all primers, the nucleotides that are complementary to the furin sequence are underlined. All furin constructions were ultimately cloned into the pZVneo vector for generating recombinant vaccinia virus by marker transfer as previously described (VanSlyke et al., 1995).

Chemical Synthesis of Internally Quenched Fluorogenic Substrates.

Following coupling of Fmoc-(3-nitro) Tyr to the Ala-HMP resin, elongation of the peptide chain was accomplished using Fmoc solid phase peptide chemistry until the last step, whereupon Boc-anthranilic acid was added. The following side chain protecting groups were used: t-Boc for Lys, tert-butyl (tBut) for Ser and Asp, and 2,2,5,7,8-methylchroman-6-sulphonyl (Pmc) for Arg. Peptide derivatives were cleaved from the resin and deprotected by treating the resin for 3 hours with reagent K (King et al., 1990), followed by lyophilization and repeated washing with ether.

Purification and Characterization of Fluorescent Substrates.

The crude material from each synthesis was purified by reversed-phase high performance liquid chromatography (RP-HPLC), using first a 300 x 7.80 mm, 10 micron. Bondclone semipreparative C₁₈ column (Phenomenex, Torrance, CA) and then an analytical C₁₈ column (Vydac, Torrance, CA). The buffer system consisted of an aqueous 0.1 % (v/v) trifluoroacetic acid

Furin Constructs and Vaccinia Virus (VV) Expression

The HA and FLAG epitope tagged furin construct fur/f/ha was generated using fur/f/ha Δ tc-k in pZvneo (Anderson et al., 1997). The BamHI/BamHI fragment from full length fur/f in pZvneo [described previously (Molloy et al., 1994)] was domain swapped into fur/f/ha Δ tc-k in order to restore both the transmembrane domain and cytoplasmic tail. The furin mutants V₇₂R: fur/f/ha, R₇₅A: fur/f/ha and fur/f Δ pro were based on the EcoRI/KpnI fragment of furin in pAlter-1 as a template, and generated by single primer mutagenesis using the primers V72R (5'- CTG GCA TCG AGG CCG GAC GAA GCG GTC -3', R75A (5'- GTG ACG AAG GCC TCC CTG TCG -3') and PROLO1 (5'- CTG CTA GCA GCT GAT GCT GAC TAC AAG GAC GAC GAT -3'). The V72R mutation introduced a diagnostic MspI, and the R75A mutation introduced a diagnostic StuI site (in boldface type). The full length furin constructs were then generated by triple-ligating the EcoRI/SacII fragment of the mutant furin with the EcoRI/XbaI and XbaI/SacII fragments of pZvneo: fur/f/ha. Pro/ha was generated by standard PCR from the construct fur/f/ha in pZVneo using the primers N.SS.PRO (5'- GAA **GAT ATC** ATG GAG CTG AGG CCC TGG -3') and C.PRO (5'- GTC **GAT ATC** TCA CCG TTT AGT CCG TCG CTT -3') followed by cloning of the fragments into the unique StuI site of pZVneo. This subcloning step was facilitated by the introduction of EcoRV sites (boldface type). In all primers, the nucleotides that are complementary to the furin sequence are underlined. All furin constructions were ultimately cloned into the pZVneo vector for generating recombinant vaccinia virus by marker transfer as previously described (VanSlyke et al., 1995).

Chemical Synthesis of Internally Quenched Fluorogenic Substrates.

Following coupling of Fmoc-(3-nitro) Tyr to the Ala-HMP resin, elongation of the peptide chain was accomplished using Fmoc solid phase peptide chemistry until the last step, whereupon Boc-anthranilic acid was added. The following side chain protecting groups were used: t-Boc for Lys, tert-butyl (tBut) for Ser and Asp, and 2,2,5,7,8-methylchroman-6-sulphonyl (Pmc) for Arg. Peptide derivatives were cleaved from the resin and deprotected by treating the resin for 3 hours with reagent K (King et al., 1990), followed by lyophilization and repeated washing with ether.

Purification and Characterization of Fluorescent Substrates.

The crude material from each synthesis was purified by reversed-phase high performance liquid chromatography (RP-HPLC), using first a 300 x 7.80 mm, 10 micron. Bondclone semipreparative C₁₈ column (Phenomenex, Torrance, CA) and then an analytical C₁₈ column (Vydac, Torrance, CA). The buffer system consisted of an aqueous 0.1 % (v/v) trifluoroacetic acid

RESULTS

Furin propeptide has the properties of an IMC.

The furin propeptide has been proposed to be an IMC (reviewed in Molloy et al., 1999). Based on this hypothesis we can make three predictions regarding *in vivo* furin activation. First, truncation of the propeptide should result in misfolding of the protease with a subsequent loss of enzymatic activity, and possibly ER-retention by the quality control system. Second, co-expression of such a mutant with the propeptide *in trans* should restore both TGN localization and activity. Third, blocking propeptide excision should result in the accumulation of a furin folding intermediate, which may have exposed hydrophobic surfaces (see Introduction). This intermediate could be retained in the ER by the secretory pathway quality control system.

To test our first prediction, the epitope-tagged furin construct fur/f Δ pro was generated (Figure 1). Fur/f Δ pro contains an internal deletion of the entire proregion, with the furin signal peptide fused directly to the FLAG-tagged mature catalytic domain. For comparison, we generated fur/f/ha, a full-length furin construct containing an HA-tag within the proregion and a FLAG-tag on the catalytic domain (C-terminal to the propeptide excision site). This HA/FLAG epitope-tag strategy permitted simultaneous detection of furin's propeptide and mature domains. Neither epitope-tag had detectable effects on the enzyme (Anderson et al., 1997; Molloy et al., 1994).

Parallel plates of BSC-40 cells expressing either fur/f Δ pro or fur/f/ha were harvested and signal/pro-peptide removal from each construct verified by western blot using FLAG-specific mAbs (Figure 2A). mAb M2 recognizes all FLAG-tagged furin constructs, whereas mAb M1 requires the tag to be at the N-terminus (i.e., cleavage of the signal peptide in fur/f Δ pro and the propeptide in fur/f/ha, see Figure 1). The identical Mr and mAb M1 cross-reactivities of the fur/f Δ pro and fur/f/ha constructs are consistent with the mature proteins having the same primary amino acid sequences.

Quantitative enzyme activity assays revealed the importance of the propeptide to furin activity (Figure 2B). Extracts from control cells or cells expressing either fur/f/ha or fur/f Δ pro were incubated with a peptidyl furin substrate. Fur/f/ha displayed robust activity, whereas fur/f Δ pro was enzymatically inactive even though expressed at a comparable level.

The necessity of the propeptide for correct furin localization was demonstrated using glycosylation state analysis and immunofluorescence. Pulse-chase studies revealed that following a three hour chase, a significant percentage of pulse-labeled fur/f/ha becomes Endoglycosidase H (Endo H) resistant, revealing the addition of complex carbohydrate and hence transport to late Golgi compartments (Figure 3). By contrast, fur/f Δ pro remained fully Endo H sensitive (Figure 3), consistent with localization in the early secretory pathway. Next, BSC-40 cells expressing either fur/f/ha or fur/f Δ pro were fixed, permeabilized and stained with anti-FLAG mAbs.

Consistent with furin's previously demonstrated TGN localization (Molloy et al., 1994), fur/f/ha showed a paranuclear staining pattern (data not shown). By contrast, fur/f Δ pro showed a dispersed reticular stain that co-localized nearly completely with the signal sequence receptor (SSR), an ER marker (Figure 4). Thus, fur/f Δ pro's lack of activity and ER-localization is consistent with misfolding of the protein.

We then tested our second prediction: if the furin propeptide functions as an IMC, then co-expression of the propeptide *in trans* with fur/f Δ pro should facilitate protein folding, thereby rescuing fur/f Δ pro from ER localization as well as restoring enzymatic activity. A recombinant propeptide construct was generated consisting of the furin signal sequence followed by the HA epitope-tagged propeptide (pro/ha; see Figure 1). Replicate plates of BSC-40 cells expressing fur/f Δ pro alone or together with pro/ha were incubated with mAb M1. The cells were fixed and permeabilized, and the remaining fur/f Δ pro was stained with mAb M2. mAb M1 staining revealed that pro/ha restores TGN localization and cell surface cycling of fur/f Δ pro (Figure 5A). This rescue was inefficient, however, as most fur/f Δ pro remained in the ER.

We also determined whether pro/ha could rescue fur/f Δ pro activity. Due to the relative insensitivity of the *in vitro* fluorogenic assay (Figure 2), an *in vivo* assay was conducted using the furin substrate pro- β -NGF (Bresnahan et al., 1990). Parallel plates of BSC-40 cells were co-infected with vaccinia recombinants expressing pro- β -NGF and fur/f Δ pro and/or pro/ha. The cells were incubated with [³⁵S]Met/Cys and secreted pro- β -NGF products immunoprecipitated and processing efficiency quantified. Co-expression of pro- β -NGF with either pro/ha or fur/f Δ pro separately failed to enhance processing above control levels (Figure 5B, compare columns 1 and 2 with 3 and 4). Strikingly, co-expression of pro/ha and fur/f Δ pro resulted in significant pro- β -NGF processing (Figure 5B, column 5), although the extent of processing was less than native furin (>100 fold, data not shown). Thus, *in trans* propeptide expression restores fur/f Δ pro trafficking and activity consistent with a rescue of protein folding.

We then tested our third prediction: if the furin propeptide functions as an IMC, then failure to undergo propeptide excision should result in accumulation of a furin folding intermediate. Like fur/f Δ pro, this intermediate may be ER-retained by the quality control system. To test this prediction, we used fur/fD₁₅₃N, a FLAG-tagged furin with a mutation in the catalytic triad (Asp₁₅₃ → Asn) (Leduc et al., 1992; Molloy et al., 1994). As has been shown previously, fur/fD₁₅₃N i) does not undergo propeptide excision and thus fails to cross-react with mAb M1 (Figure 2A), ii) is inactive (Figure 2B), and iii) remains fully Endo H sensitive consistent with an early secretory pathway localization (Figure 3). Unexpectedly, and in contrast to fur/f Δ pro, fur/fD₁₅₃N displayed a dispersed, punctate stain with a paranuclear component that showed a limited overlap with mAb G1/93, an antibody against the ER-Golgi Intermediate Compartment (ERGIC) marker ERGIC-53 (Figure 4). The limited overlap between fur/fD₁₅₃N and ERGIC-53 was confirmed by confocal

microscopy (data not shown). The significant amount of fur/fD₁₅₃N that does not colocalize with ERGIC-53 could be in an unidentified subcompartment of the ERGIC or in the adjacent *cis*-Golgi Network. To further examine the localization of fur/fD₁₅₃N, cells were treated with brefeldin A (BFA) prior to fixation. In addition to causing fusion of Golgi with ER membranes, BFA also causes fusion of the ERGIC with *cis*-Golgi Network (CGN) membranes (Fullekrug et al., 1997). Consistent with localization of fur/fD₁₅₃N to the ERGIC/CGN, BFA treatment caused a nearly complete redistribution of fur/fD₁₅₃N to punctate ERGIC-53 containing structures (Figure 4).

Propeptide cleavage and furin activation.

Once an IMC has served its function in protein folding, this autoinhibitory domain must be degraded to permit protease activation (reviewed in Baker et al., 1993). Indeed, following autoproteolytic propeptide excision in the ER (-Arg-Thr-Lys-Arg₁₀₇[↓]-), furin is still enzymatically inactive due to stable association with the autoinhibitory propeptide ($K_{0.5}$ =14 nM; Anderson et al., 1997). *In vitro*, furin activation is concomitant with internal cleavage of the propeptide at the P1/P6 Arg motif at -Arg-Gly-Val-Thr-Lys-Arg₇₅[↓]-, and dissociation of the cleaved propeptide from furin. Cleavage at this site *in vitro* requires an acidic pH characteristic of the TGN [optimal cleavage at pH 6.0 (Anderson et al., 1997)], suggesting that furin becomes active in the acidic compartments of the late secretory pathway. In several studies, furin itself has been shown to cleave at P1/P6 Arg motifs, specifically at acidic pH (Brennan and Nakayama, 1994a; Brennan and Nakayama, 1994b), and both Arg residues are required for cleavage. Because both the P1 and P6 arginines at the internal cleavage site are required for furin activation at acidic pH (Anderson et al., 1997), it raised the possibility that internal propeptide cleavage is autoproteolytic. We next addressed this possibility as well as whether this cleavage is required *in vivo* for activation.

Autoproteolytic cleavage of the internal furin propeptide site.

To characterize the internal propeptide cleavage event, two sets of experiments were performed. First, the sensitivity of internal cleavage to furin inhibitors was investigated. An ER-localized furin construct, fur/fΔtc-k (see Figure 1), was expressed in cells. This construct undergoes propeptide excision, but remains proteolytically inactive due to stable association of the inhibitory propeptide (Anderson et al., 1997). Detergent solubilized membrane preparations containing fur/fΔtc-k were incubated at pH 6.0 in the absence or presence of two potent furin inhibitors; decanoyl-Arg-Val-Lys-Arg-CMK, a nM inhibitor of all PCs (Jean et al., 1998) and the selective furin inhibitor, α₁-PDX [K_i for furin = 0.6 nM (Jean et al., 1998)] (Figure 6A). Consistent with autoproteolysis, both inhibitors blocked the internal cleavage of the furin propeptide to yield the ~6 kDa HA-tagged, N-terminal fragment. Second, a dilutional analysis was performed in order to establish whether internal propeptide cleavage was inter- or intra-molecular.

Replicate samples containing fur/f Δ tc-k were sequentially diluted (up to 20-fold) and incubated at pH 6.0 for 3 hours, during which time furin becomes maximally active *in vitro* (Anderson et al., 1997). Relative furin activity was then determined, and the number of furin active sites was measured by titration analysis (Figure 6B). The observed regression line does not pass through the null point when approaching 0 nM of 'activateable' furin, indicating an intramolecular activation event. However, the rate of activation increases at higher furin concentrations, indicating some intermolecular activation as well. Thus, furin becomes active by autoproteolytically cleaving its propeptide, predominantly via an intramolecular process.

Autoproteolytic cleavage at -Arg-Gly-Val-Thr-Lys-Arg₇₅[↓]- has been proposed to be based on furin's pH-dependent cleavage site specificity (Anderson et al., 1997). To test this hypothesis, a kinetic analysis was performed using internally quenched fluorogenic peptide substrates corresponding to the sites of internal propeptide cleavage (QFS-1) and propeptide excision (QFS-8; see Table 1). Consistent with the processing of P1/P4 arginine-containing furin substrates, the QFS-8 peptide was cleaved slightly more efficiently at pH 7.5 than pH 6.0, with a low μ M K_m at both pH values and a 40% decrease in k_{cat} at pH 6.0. By contrast, the P1/P6 Arg-containing QFS-1 showed a marked preference for cleavage at pH 6.0. At neutral pH, a high K_m (71 μ M) for furin cleavage was observed, although the k_{cat} was nearly two-fold higher than that observed for QFS-8. Interestingly, at pH 6.0 a 3-fold lower K_m (23 μ M) for QFS-1 was observed. Even with a decrease in k_{cat} , the overall turnover number of QFS-1 at pH 6.0 was two-fold higher than pH 7.5 (Table I). These data support a model in which compartment-specific activation of furin is controlled, in part, by the different motifs of the two propeptide cleavage sites (see Discussion).

Autoproteolytic cleavage is necessary for *in vivo* furin activation.

We then examined the autoproteolytic cleavage and rate of propeptide dissociation from furin *in vivo* by pulse/chase analysis and co-immunoprecipitation. Plates of cells expressing fur/f/ha were pulse-labeled with [³H]Arg/Leu and harvested either immediately or following a chase. Furin•propeptide complexes were immunoprecipitated with mAb M1, resolved by SDS-PAGE, and processed for autoradiography. Dissociation of the propeptide from furin was quantitated by liquid scintillation counting of the relevant excised gel bands (Figure 7). Immediately after the pulse 100% of fur/f/ha molecules were associated with propeptide (Figure 7). The fraction of propeptide-associated furin decreased linearly for ~3.5 hours ($t_{1/2}$ = 105 minutes) culminating in 50% dissociation. Attempts to immunoprecipitate the ~6 kDa HA-tagged amino terminal propeptide fragment from either the cells or extracellular medium were not successful (data not shown), suggesting that it is labile. Longer chase times did not reveal further propeptide dissociation (data not shown; see Discussion). BFA treatment, which is known to block ER →

TGN transport, abolished propeptide dissociation from furin, indicating a requirement for transit of furin•propeptide complexes to late secretory pathway compartments for activation (Figure 7).

The importance of cleavage at -Arg₇₅[↓]- *in vivo* was addressed by comparing the activation and trafficking of fur/f/ha to that of an Arg₇₅ → Ala point mutant at the second propeptide cleavage site (R₇₅A: fur/f/ha). The R₇₅A mutation i) had no effect on the ER-localized initial propeptide excision (-Arg₁₀₇[↓]) (Figure 2A, lane 6 and Anderson et al., 1997), ii) did not alter export of the enzyme from the early secretory pathway (Figure 3), and iii) blocked furin activity as measured in cell extracts (Figure 2B, column 6). Next, BSC-40 cells infected with vaccinia recombinants expressing fur/f/ha or R₇₅A: fur/f/ha were treated for four hours with cycloheximide following an initial two hours of infection. The cells were then fixed, permeabilized and stained to detect furin mature domain (mAb M1) and propeptide (mAb HA.11). In untreated cells, fur/f/ha and R₇₅A: fur/f/ha displayed very similar staining patterns (Figure 8). The paranuclear staining pattern of the mature furin domains of both constructs co-localized with that of their respective propeptides, consistent with TGN localization and association with the autoinhibitory propeptide domain. [Propeptide staining was detected in the ER of both fur/f/ha and R₇₅A: fur/f/ha expressing cells (Figure 8)]. This ER staining likely represents nascent furin molecules, as it could be chased out by brief cycloheximide treatment (data not shown). Importantly, four hours of cycloheximide treatment revealed a striking difference between fur/f/ha and R₇₅A: fur/f/ha. Fur/f/ha showed a complete loss of paranuclear propeptide staining while maintaining staining of mature furin. In contrast, R₇₅A: fur/f/ha maintained prominent paranuclear staining that remained co-localized with the mature domain (Figure 8). Biochemical analysis revealed that in contrast to the native propeptide, R₇₅A propeptide remained largely associated with the enzyme throughout the chase (Figure 7). These data indicate that dissociation of the propeptide from furin requires the integrity of the -Arg₇₀-Gly-Val-Thr-Lys-Arg₇₅[↓]- cleavage site.

After establishing that inhibition of propeptide excision blocks transport of furin at the ERGIC/CGN (Figure 4), we investigated whether inhibition of internal propeptide cleavage similarly affects trafficking within the TGN/endosomal system. Cells expressing either fur/f/ha or R₇₅A: fur/f/ha were incubated with mAb M1 to detect furin cycling to the cell surface. The fixed and permeabilized cells were then incubated with antiserum directed against the furin cytoplasmic domain (PA1-062) to detect the steady state distribution of all furin molecules (Figure 9). (This is in contrast to the M2 post-fix staining used previously (Figure 5) which only detects furin molecules not already bound to mAb M1.) The highly similar staining patterns of mAb M1 and PA1-062 showed that, contrary to preventing propeptide excision, inhibition of internal propeptide cleavage had no apparent effect on trafficking of furin between the plasma membrane and the TGN. Further, a time course of mAb M1 uptake showed no apparent difference between the two

constructs (data not shown). These data suggest that furin folding is complete following propeptide excision, and that furin in the furin•propeptide complex is intrinsically active.

Modulation of internal propeptide cleavage.

Furin activation both *in vitro* and *in vivo* is a slow process, presumably due to inefficient internal propeptide cleavage at -Arg₇₅[↓]-, even at acidic pH (see Table I). We investigated whether we could accelerate the rate of furin activation by mutating this internal cleavage site to a consensus furin cleavage motif (-Arg-X-Lys/Arg-Arg[↓]-). We speculated that if internal propeptide cleavage in this mutant were efficient at neutral pH, furin might become active in the ER. To test this hypothesis, we examined the processing kinetics of a fluorogenic peptide substrate corresponding to the internal propeptide cleavage site, but with a P4 Arg (i.e. Val₇₂ → Arg) (QFS-3; see Table 1). Strikingly, introduction of the P4 Arg resulted in a dramatic drop in K_m relative to the native sequence at either pH, making it comparable to QFS-8, and a large increase in k_{cat} (8-11 fold). Intriguingly, we still observed a pH-dependent drop in K_m (5.17 μ M to 1.84 μ M), comparable to that seen with QFS-1 (~3 fold) (see Discussion).

The *in vivo* effects of the P4 Val → Arg substitution were analyzed by generating an epitope-tagged furin construct, V₇₂R:fur/f/ha, containing this mutation. Surprisingly, western blot analysis of V₇₂R:fur/f/ha expressed in BSC-40 cells revealed this construct failed to undergo efficient propeptide excision and remained largely a zymogen (Figure 2A). Further, pulse-chase studies showed V₇₂R:fur/f/ha remained predominantly Endo H sensitive, indicating retention in the early secretory pathway (Figure 3).

Immunofluorescence microscopy revealed that V₇₂R:fur/f/ha was predominantly ER-localized as it co-localized with the signal sequence receptor (Figure 10). This localization presumably reflects misfolding, as Fur/fD₁₅₃N, which also remains a zymogen, is able to escape the ER (Figure 4). Interestingly, a small amount of mAb M1-positive (i.e. propeptide excised) V₇₂R:fur/f/ha was visible by immunofluorescence as a paranuclear stain (Figure 10). This species i) did not disperse in the presence of BFA (data not shown), suggesting TGN localization, and ii) displayed TGN/cell surface cycling, as revealed by mAb M1 uptake (Figure 10). Although V₇₂R:fur/f/ha displayed no proteolytic activity *in vitro* against a peptide substrate (Figure 2B), *in vivo* proteolytic activity was observed by using the sensitive pro- β -NGF processing assay (data not shown). This suggested that a fraction of the material was indeed active. Clearly, however, the majority of V₇₂R:fur/f/ha is unable to transit out of the ER, implying misfolding and retention by the quality control system.

DISCUSSION

Furin activation is a multi-step process mediated by its IMC propeptide that requires an ordered pair of compartment-specific autoproteolytic propeptide cleavages to produce the mature, active endoprotease. That the propeptide functions as an IMC is suggested by the observations that: i) furin lacking the propeptide is inactive and ER-retained, ii) co-expression of the propeptide *in trans* rescues furin trafficking and endoproteolytic activity, and iii) blocking propeptide excision results in ERGIC/CGN localization, suggesting incomplete folding of furin. Following propeptide excision (-Arg-Thr-Lys-Arg₁₀₇[↓]-) and transport of the furin•propeptide complex to the acidic TGN/endosomal system, the propeptide undergoes a slower ($t_{1/2}$ = 105 minutes) autoproteolytic and predominantly intramolecular cleavage at -Arg-Gly-Val-Thr-Lys-Arg₇₅[↓]-. While propeptide excision is necessary for export from early secretory pathway compartments, blocking internal propeptide cleavage (Arg₇₅ → Ala) has no apparent effect on TGN/cell surface cycling. The importance of the propeptide cleavage site sequences for directing activation within the variable-pH environment of the secretory pathway was suggested by *in vitro* digests of synthetic peptides. This analysis revealed the preferential cleavage of the propeptide excision site sequence at neutral pH (similar to the ER) and the internal cleavage site sequence at mildly acidic pH (similar to the TGN). Analysis of a peptide substrate with the internal site of propeptide cleavage mutated to a consensus furin site (Val₇₂ → Arg) showed a greatly increased sensitivity to furin at neutral pH. Surprisingly, this mutation *in vivo* resulted in near complete inactivation and ER-localization of furin. Together, these results provide a rationale for the different sequences at the first and second sites of propeptide cleavage.

Furin transport out of the early secretory pathway.

Misfolded/unassembled secretory proteins are retained by the cellular quality control system (reviewed in Hammond and Helenius, 1995). While most of these proteins are ER retained, some escape the ER and transit to post-ER/pre-Golgi compartments, from which they may be retrieved (see Hammond and Helenius, 1994). Our analysis suggests that the ER and ERGIC/CGN may distinguish furin in different folding states. Presumably misfolded furin constructs (i.e. fur/fΔpro and V₇₂R:fur/f/ha) are retained in the ER, perhaps by virtue of chaperone binding. Indeed, preliminary co-immunoprecipitation studies show that fur/fΔpro and V₇₂R:fur/f/ha are associated with BiP (E.D.A. and G.T., unpublished results). Chaperone binding to fur/fΔpro could explain the poor recovery of activity by co-expressed pro/ha (Figure 5), as BiP could prevent interaction between fur/fΔpro and pro/ha.

In contrast to fur/fΔpro, the appearance of fur/fD₁₅₃N in the ERGIC/CGN suggests it is partially folded and is allowed to progress past the initial ER quality control machinery, only to be

prevented from trafficking further. It is currently unknown if fur/fD₁₅₃N is statically retained, or recycles between the ER and ERGIC/CGN, or whether fur/fD₁₅₃N and ERGIC-53, a potential transport receptor (Nichols et al., 1998; Vollenweider et al., 1998), are physically associated. Previously, Creemers et al. (1995) reported that furin constructs with mutations disrupting their propeptide excision site sequences were ER-retained zymogens. However, given the potential importance of the propeptide excision site sequence for IMC action (Li et al., 1995; Peters et al., 1998), mutation of this site may have resulted in misfolding, thus complicating analysis. By contrast, mutation of the catalytic triad of subtilisin has been shown not to result in misfolding (Carter and Wells, 1988; Eder et al., 1993a; Eder et al., 1993b), suggesting that fur/fD₁₅₃N represents a folding intermediate, rather than simply being misfolded.

The TGN/endosomal system and furin activation.

A requirement for exposure of the furin•propeptide complex to the acidic TGN/endosomal environment for activation is supported by three findings. First, previous work showed that ER-localized furin•propeptide complexes (i.e. fur/fΔtc-k; see Figure 1) fail to undergo internal propeptide cleavage (Anderson et al., 1997). This cleavage can be promoted, however, by *in vitro* exposure to mildly acidic pH, with maximal cleavage occurring at pH 6.0, in good agreement with the observed pH of the TGN (Demaurex et al., 1998; Seksek et al., 1995). Second, peptide substrates representing the internal propeptide cleavage site are more efficiently cleaved at pH 6.0 than at neutral pH (Table I). Third, internal cleavage can be blocked by BFA treatment, a compound that inhibits ER → TGN transport (Figure 7). However, our attempts to inhibit internal propeptide cleavage by treatment of cells with deacidifying agents (e.g. chloroquine and bafilomycin A) resulted in pleiotropic effects including i) molecular weight changes in furin [suggesting alteration of unknown secondary modifications (E.D.A. and G.T., unpublished results)], ii) disruption of furin trafficking (Chapman and Munro, 1994), and iii) disruption of shedding (Vey et al., 1994 and E.D.A. and G.T., unpublished results), all of which complicate data interpretation. Nonetheless, *in vitro* and *in vivo* data point to the pH of the TGN/endosomal system as key to governing propeptide cleavage at -Arg₇₅↓-.

The incomplete dissociation of the propeptide from furin during activation was surprising (Figure 7). Even at long time points (up to 7 hours), no propeptide dissociation past ~50% was observed (data not shown). This may be the result of some furin molecules misfolding due to over-expression, as suggested by the observations that many furin molecules that have undergone propeptide excision in BSC-40 cells remain Endo H sensitive, consistent with ER retention (Figure 3). Alternatively, it is possible that over-expression interferes with furin dimerization (Wolins et al., 1997) or an unknown but essential secondary modification.

Compared to the rapid ER-localized propeptide excision ($t_{1/2} < 10$ minutes), the rate of furin activation *in vitro* or *in vivo* is slow [$t_{1/2} \sim 90$ minutes (Anderson et al., 1997) and ~ 105 minutes (this study), respectively]. The relative efficiency of each propeptide cleavage may be partially explained by analysis of furin cleavage kinetics/ pH-sensitivity for peptide substrates representing the first and second propeptide cleavage sites (Table I). Characteristic of many -Arg-X-Lys/Arg-Arg[↓]- consensus furin sites, cleavage of QFS-8 (reflecting the site of propeptide excision) is relatively efficient at either neutral or acidic pH (low μM K_m , relatively high k_{cat}/K_m). By contrast, QFS-1 cleavage (reflecting the internal P1/P6 Arg propeptide cleavage site) is slower and pH-sensitive. Although the K_m of QFS-1 for furin is strikingly high at neutral pH (71 μM), it decreases three-fold at pH 6.0 (23 μM).

An additional contributor to the slow activation of furin may be a rearrangement of the furin•propeptide complex. Such a rearrangement may displace the propeptide excision site (-Arg₁₀₄-Thr-Lys-Arg₁₀₇[↓]-) from the furin active site, replacing it with the internal propeptide cleavage site (-Arg-Gly-Val-Thr-Lys-Arg₇₅[↓]-). This putative rearrangement may be triggered by the protonation of key His residues at sites of furin/propeptide contact, as is suggested by the existence of several closely positioned histidine residues flanking the internal furin propeptide cleavage site (His₆₉, His₈₀, His₈₄; see Figure 1) that are conserved between the PCs (see Anderson et al., 1997). At low pH these His residues may become protonated, resulting in destabilization of a possibly metastable furin•propeptide complex, thus triggering rearrangement. This rearrangement may be similar to the low pH-induced conformational change of the metastable influenza HA complex triggered, in part, by the protonation of a key His residue (Carr et al., 1997; Chen et al., 1998; Daniels et al., 1985). The role of His residues in modulating pH-dependent furin•propeptide interactions is consistent with our preliminary finding that a substitution of the P7 His residue in the QFS-1 sequence blocks the pH-dependent drop in K_m (E.D.A. and G.T., unpublished results). Thus, these data suggest that the ~ 3 -fold pH-dependent drop in K_m observed with the internal cleavage site sequence is not the result of the P1/P6 Arg motif, but rather the P7 His residue. [Indeed, this is consistent with the observation that QFS-3 displays a similar pH-dependent drop in K_m at pH 6.0 (see Table I).]

If not for pH-dependent cleavage, what is the reason for the P1/P6 Arg internal cleavage site sequence in the propeptide? The significance of the markedly different K_m 's at the first and second propeptide cleavage sites is suggested by two results. First, analysis of QFS-3 cleavage revealed a sharp drop in K_m (nearly 15-fold) coupled with a dramatic increase in k_{cat}/K_m (nearly 160-fold; see Table I). Indeed, the k_{cat}/K_m of QFS-3 was nearly 10-fold greater than that of QFS-8, which represents the propeptide excision site. Second, when this mutation (i.e. Val₇₂ → Arg) was introduced into furin (V₇₂R:fur/f/ha), it inhibited propeptide excision and resulted in ER-retention (Figures 2, 3 and 10).

One explanation for V₇₂R:fur/f/ha's disrupted activation is based on studies of α -lytic protease and subtilisin. For both bacterial proteases, the integrity of the propeptide excision site sequence is crucial for IMC activity (Li et al., 1995; Peters et al., 1998). Additionally, subtilisin's propeptide is largely unstructured, and folds only by interacting with the protease domain (Bryan et al., 1995; Strausberg et al., 1993). It may be that the internal propeptide cleavage site of V₇₂R:fur/f/ha, being a much better substrate than the propeptide excision site (see Table I), is able to outcompete the excision site for access to the partially folded furin active site. This may be facilitated by furin's lack of propeptide structure early in the folding process. This inappropriate binding would prevent furin from folding properly, leaving the bulk of the enzyme as a misfolded, ER-retained zymogen. In a minority of V₇₂R:fur/f/ha molecules, the propeptide excision site binds correctly to the active site, resulting in the folding of a small component of V₇₂R:fur/f/ha (Figure 10 and data not shown). Unfortunately, the scarcity of this species precluded biochemical characterization (data not shown).

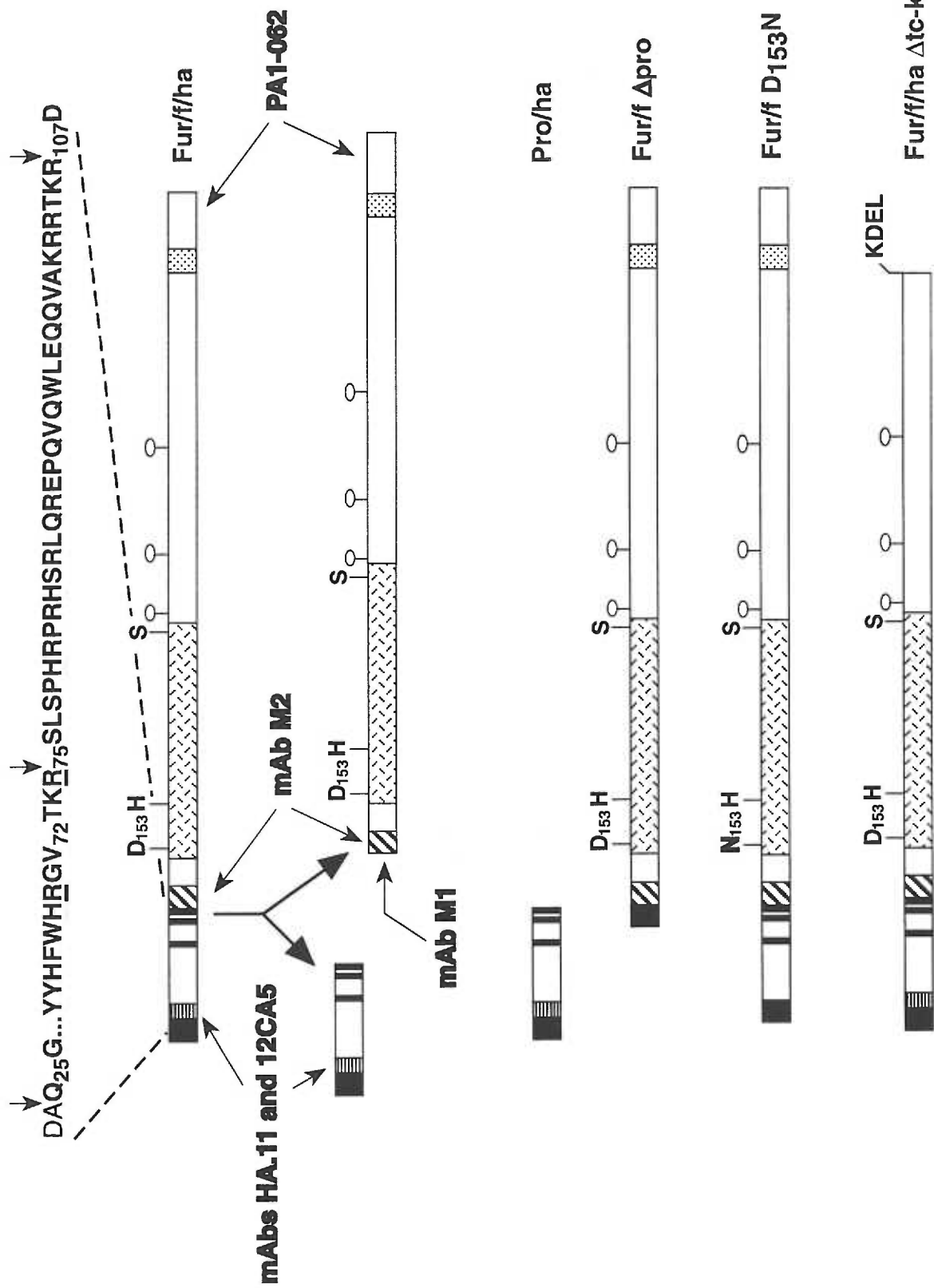
These data may explain why the site of propeptide excision (-Arg-Thr-Lys-Arg₁₀₇[↓]-) and the internal site of propeptide cleavage (-Arg-Gly-Val-Thr-Lys-Arg₇₅[↓]-) have such different cleavage motifs. The amino acids at the site of propeptide excision must bind the active site of the folding furin catalytic domain in order for the propeptide to exert its IMC action. The internal site of propeptide cleavage in an unstructured propeptide might compete with the site of propeptide excision for access to the active site. This non-productive interaction is prevented by the unusual P1/P6 Arg motif in the internal propeptide cleavage site, which conveys a very high K_m in the neutral environment of the ER (Table I). Thus, furin folding is aided by the relative K_m's of the sites of propeptide excision and internal propeptide cleavage.

The study of furin folding/activation not only enhances our understanding of furin, but also of other PCs and IMC-mediated folding generally. Accumulating evidence demonstrates that other PCs undergo propeptide and pH-dependent activation processes (Lamango et al., 1999; Zhou et al., 1995 and E.D.A. and G.T., unpublished results), suggesting that the results of our studies on furin may inform research on the activation of other PCs. Additionally, the rapidity with which the prokaryotic IMCs are degraded following folding makes the study of late events in this process technically difficult (e.g. see Bryan et al., 1995). The slow and pH-dependent process of furin activation allows the study of late events in IMC-mediated folding that cannot be observed in any other known system.

ACKNOWLEDGMENTS

We are grateful to L. Thomas and S. Molloy for expert technical assistance throughout all stages of this work. We thank S. Molloy for critical reading of the manuscript and members of the Thomas lab for helpful discussions. We thank T. Rapoport and H.-P. Hauri for generously providing reagents. We thank S. Kuman for performing mass spectrometry on the peptide substrates. E.D.A. is the recipient of a Tartar Trust Fellowship. F.J. is the recipient of an MRC (Canada) fellowship.

Figure 1. Schematic of furin constructs. To explore the role of the propeptide in furin folding/activation, a number of recombinant constructs were generated using loop-in, loop-out or site-directed mutagenesis. In construct fur/fD₁₅₃N the aspartic acid residue of the catalytic triad has been changed to an asparagine, resulting in inactivation of the protease. Fur/f/ha, fur/fΔpro, fur/fD₁₅₃N, fur/f/haΔtc-k, V₇₂R:fur/f/ha and R₇₅A:fur/f/ha all have the FLAG epitope tag inserted directly after the propeptide cleavage site (*diagonal bars*), so the N-terminus of the FLAG sequence is exposed upon excision. The anti-FLAG mAb M2 can recognize either the blocked or exposed forms of the FLAG epitope. The anti-FLAG mAb M1 can only recognize the FLAG epitope if it has a free amino-terminus. Hence mAb M1 is only able to detect furin after the propeptide has been excised. In fur/f/ha, pro/ha, V₇₂R:fur/f/ha and R₇₅A:fur/f/ha the HA epitope tag (*vertical bars*) has been inserted directly after the signal sequence (*black*). The HA epitope is recognized by the mAbs 12CA5 and HA.11. The cytoplasmic tail of furin is recognized by the polyclonal rabbit antiserum PA1-062. The subtilisin-like catalytic domain of furin is denoted by hatchmarks. The residues of the catalytic triad are indicated (Asp, His, Ser). Potential glycosylation sites are denoted by 'lollipops.' Pairs of basic amino acids in the propeptide are indicated by thick vertical bars. Arg residues known to be required for internal propeptide cleavage (Arg₇₀, Arg₇₅) are underlined in black. His residues believed to be involved in furin•propeptide rearrangement (His₆₉, His₈₀, His₈₄) are underlined in gray.



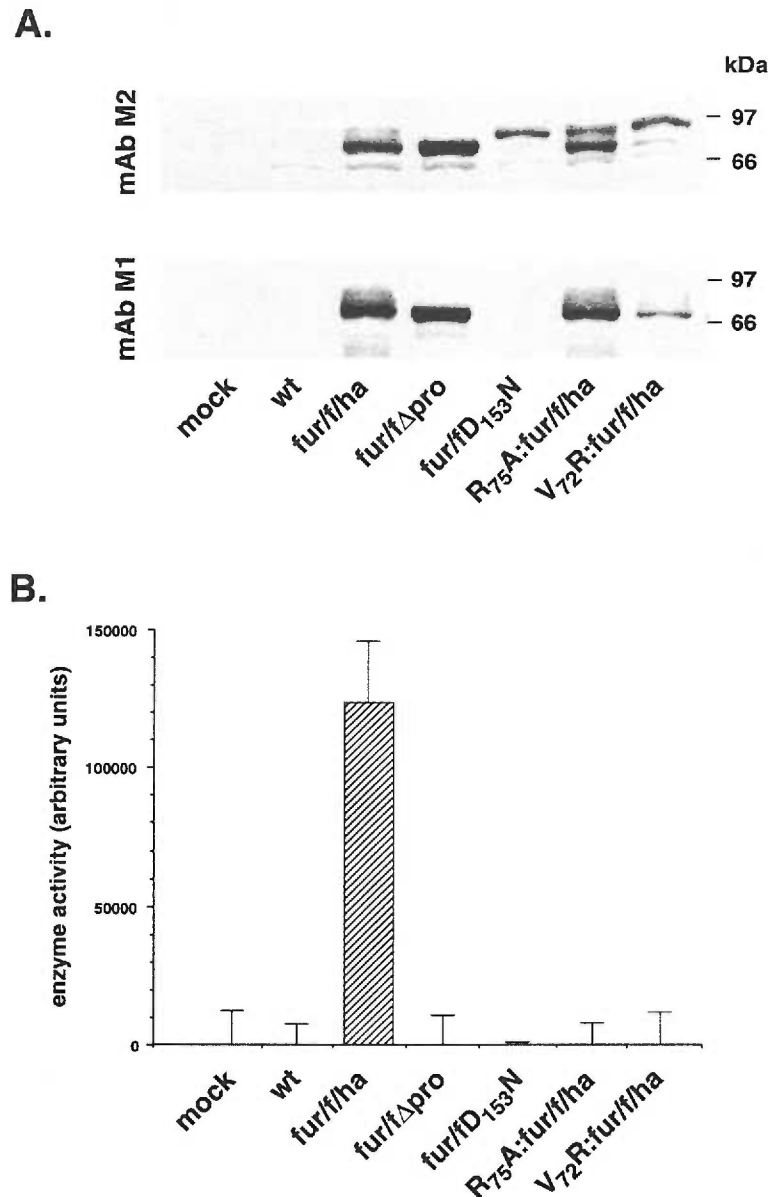


Figure 2. Expression, immunoreactivity and *in vitro* activity of furin constructs.

(A) Samples of crude membrane preparations (15 μ l/lane) of mock infected BSC-40 cells, or BSC-40 cells infected with VV:WT, VV:hFur/f/ha, VV:hFur/fΔpro, VV:hFur/fD₁₅₃N, VV:R₇₅A:hFur/f/ha or VV:V₇₂R:hFur/f/ha were analyzed by SDS-PAGE followed by immunoblotting, using either mAb M1 or mAb M2. The blots were developed with an alkaline phosphatase-conjugated goat anti-mouse secondary antibody. (B) Proteolytic activity of the same crude membrane preparations against pGlu-Arg-Thr-Lys-Arg-MCA (30 μ l/assay). Each column represents the average of two samples assayed in duplicate. Furin activity is shown in arbitrary units of fluorescence. Bars indicate standard deviations.

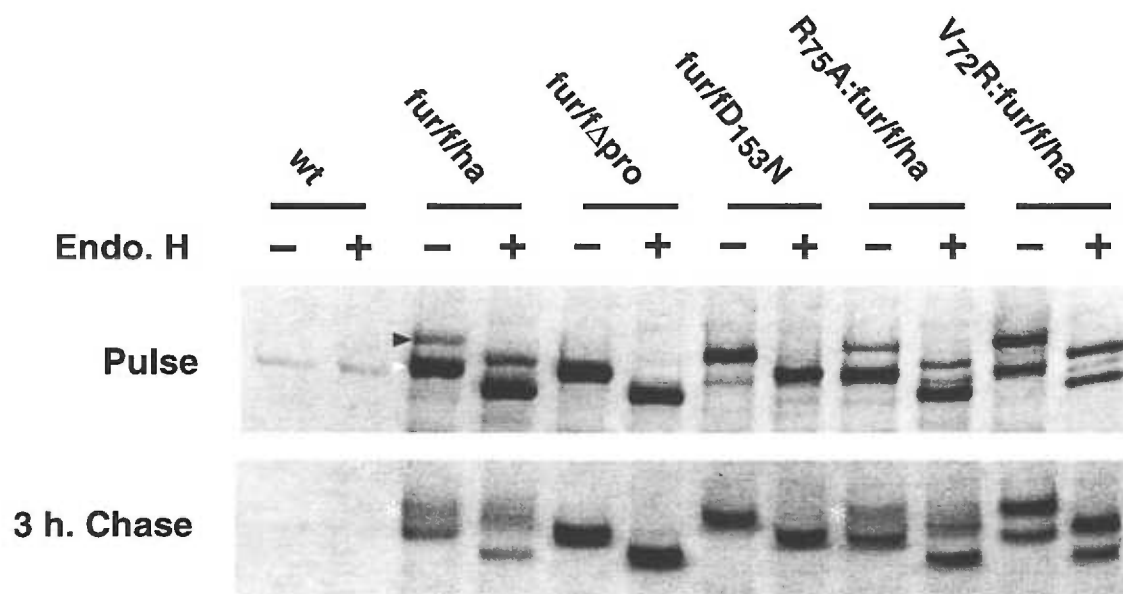


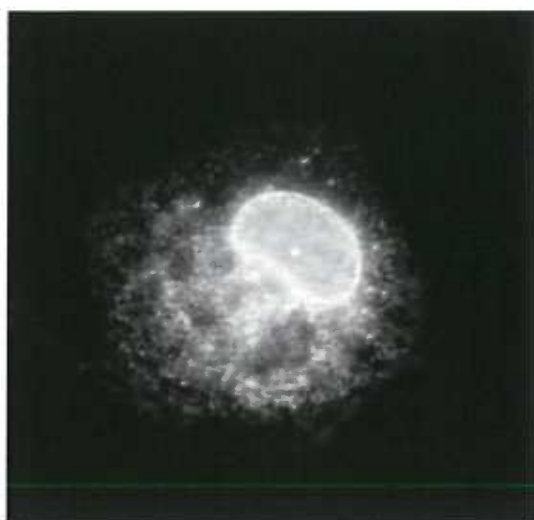
Figure 3. Glycosylation analysis of furin constructs. Replicate plates of BSC-40 cells were infected with VV:WT, VV:hFur/f/ha, VV:hFur/fΔpro, VV:hFur/fD₁₅₃N, VV:R₇₅A:hFur/f/ha or VV:V₇₂R:hFur/f/ha, and incubated at 37°C for 4 hours. The cells were pulse labeled with [³⁵S]Met/Cys for 30 minutes, and chased for 3 hours in complete medium with an 150 μg/ml each of cold methionine and cysteine at 37°C. Cells were then harvested in mRIPA and furin immunoprecipitated with PA1-062 (1:250). Immunoprecipitates were incubated for 16-24 hours in reaction buffer (50 mM sodium citrate pH 6.0, and 0.1% SDS) or buffer with 2.5 mU of endoglycosidase H. Following digestion, the samples were resolved by an 8% SDS-PAGE gel which was then processed for fluorography. Furin zymogen (*black arrow*), mature furin with an excised propeptide (*white arrow*), and sialated furin (*white asterisk*) are indicated. The intensity of the chase autoradiograph was increased to make it comparable to the pulse autoradiograph.

Figure 4. Retention of fur/f Δ pro and fur/fD₁₅₃N in the early secretory pathway. Replicate plates of subconfluent BSC-40 cells were infected with VV:hFur/f Δ pro or VV:hFur/fD₁₅₃N. Following inoculation the cells were incubated at 37°C for a total of 5 hours. Cells expressing fur/fD₁₅₃N were treated with brefeldin A and cycloheximide (both at 10 μ g/ml) for 2 hours prior to fixation. All cells were fixed with paraformaldehyde, permeablized and incubated with either mAb M1 or PA1-062 to detect furin. Cells were also incubated either with an anti-signal sequence receptor rabbit antiserum (SSR), or with an anti-ERGIC-53 mouse mAb (G1/93). Examples of structures containing co-localizing fur/fD₁₅₃N and ERGIC-53 are marked by arrowheads. mAb M1 was detected using a goat anti-mouse IgG_{2b}-FITC secondary antibody, the signal-sequence receptor antiserum using a goat anti-rabbit-TxRd antibody, PA1-062 with goat anti-rabbit-TxRd, and G1/93 with goat anti-mouse IgG₁-FITC.

Furin

SSR

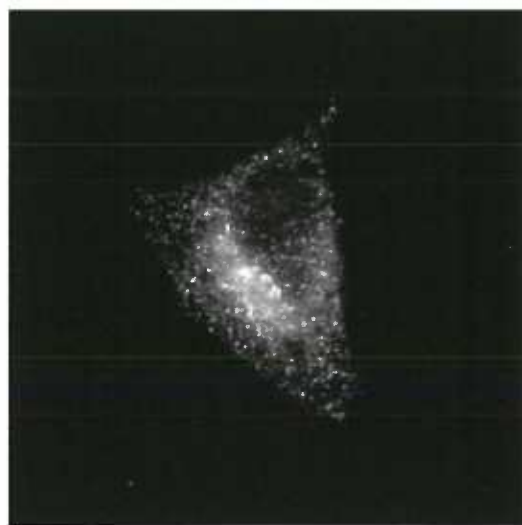
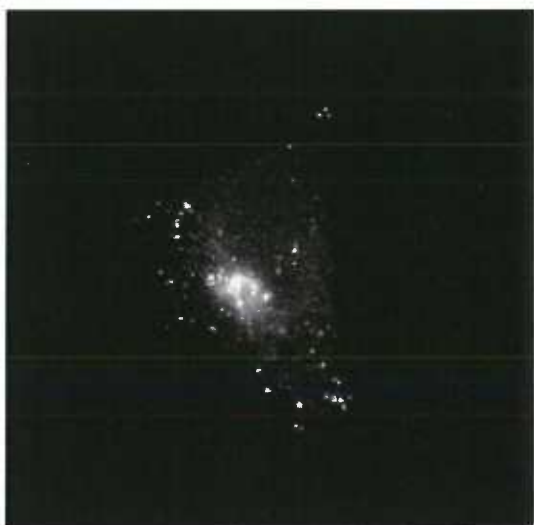
Fur/fΔpro



Furin

G1/93

Fur/fD₁₅₃N



Furin

G1/93

**2 h.
BFA + CHX
Fur/fD₁₅₃N**

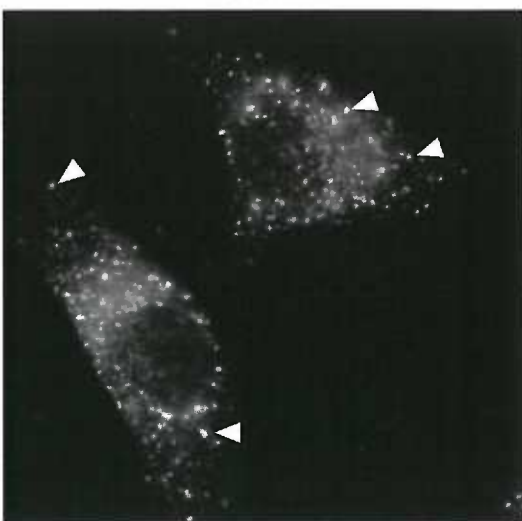
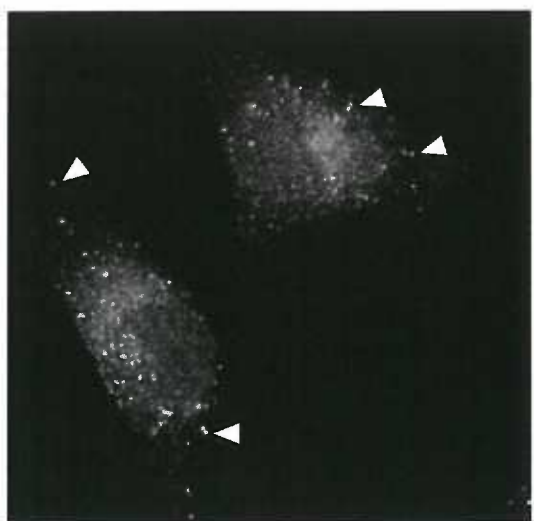
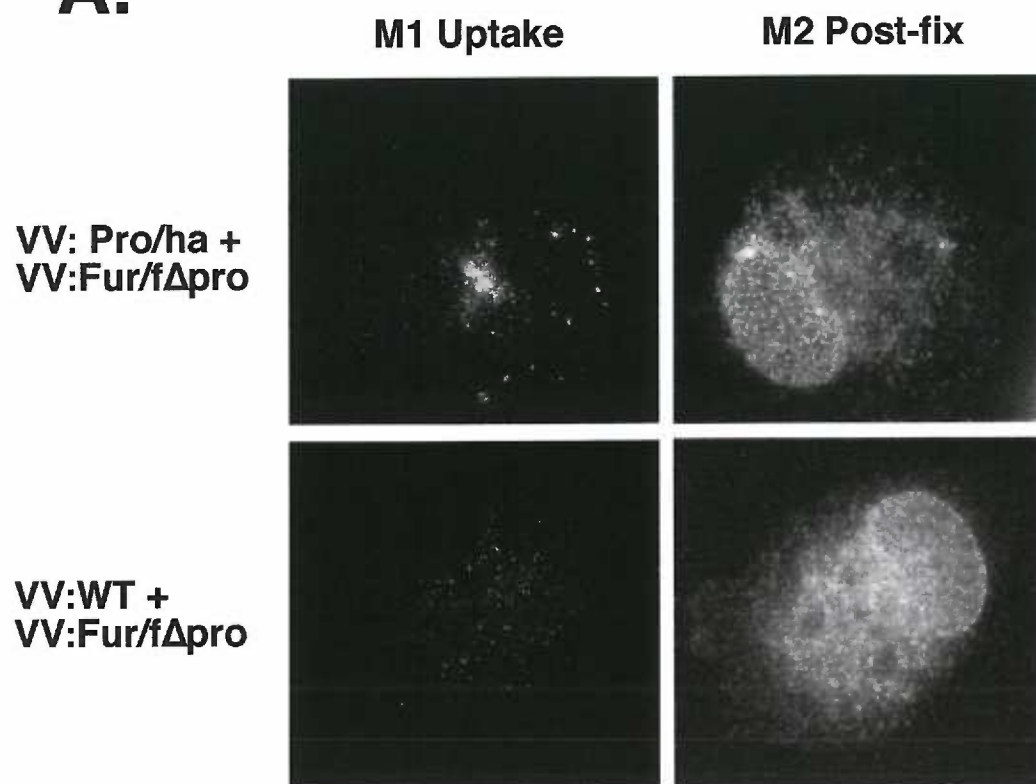
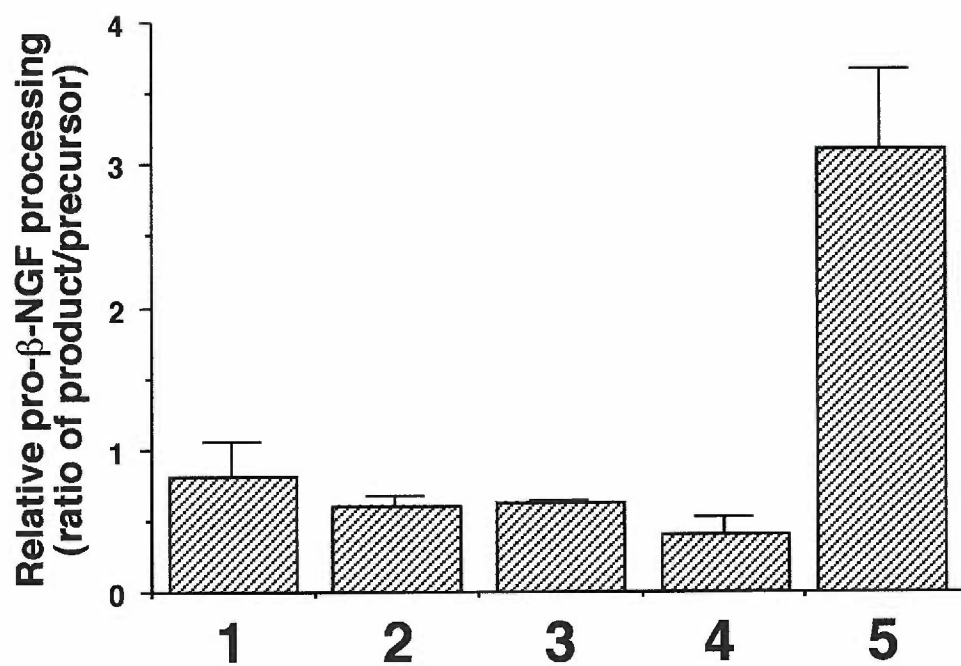


Figure 5. *In trans* restoration of activity and trafficking to fur/fΔpro by the furin propeptide. (A) Replicate plates of subconfluent BSC-40 cells grown on coverslips were infected with VV:hFur/fΔpro (m.o.i. = 6) and VV:WT (m.o.i. = 4) or VV:hPro/ha (m.o.i. = 4). Following inoculations, mAb M1 was added to the medium (30 μg/ml) and the cells incubated at 37°C for 5 hours. The cells were then fixed with paraformaldehyde, permeablized and incubated with mAb M2 to detect the remaining furin. mAb M1 was detected using a goat anti-mouse IgG_{2b}-FITC antibody, and mAb M2 was visualized using a goat anti-mouse IgG₁-TxRd antibody. (B) Replicate plates of BSC-40 cells were infected with either VV:mNGF (*column 1*; multiplicity of infection [m.o.i.] = 5) or co-infected with VV:mNGF (m.o.i. = 5) and VV:WT (*column 2*; m.o.i. = 2; m.o.i. = 7 total). Additional samples were triple-infected with VV:mNGF, VV:hFur/fΔpro/ha and VV:WT (*column 3*), VV:mNGF, VV:WT and VV:hPro/ha (*column 4*), or with VV:mNGF, VV:hFur/fΔpro and VV:hPro/ha (*column 5*; all m.o.i.'s = 2, 3 and 3, respectively). The signal from the precursor (pro-β-NGF) and product (β-NGF) were quantitated, and the ratio of product to precursor determined. Each reading represents the average of two separate samples. Bars indicate standard deviations.

A.



B.



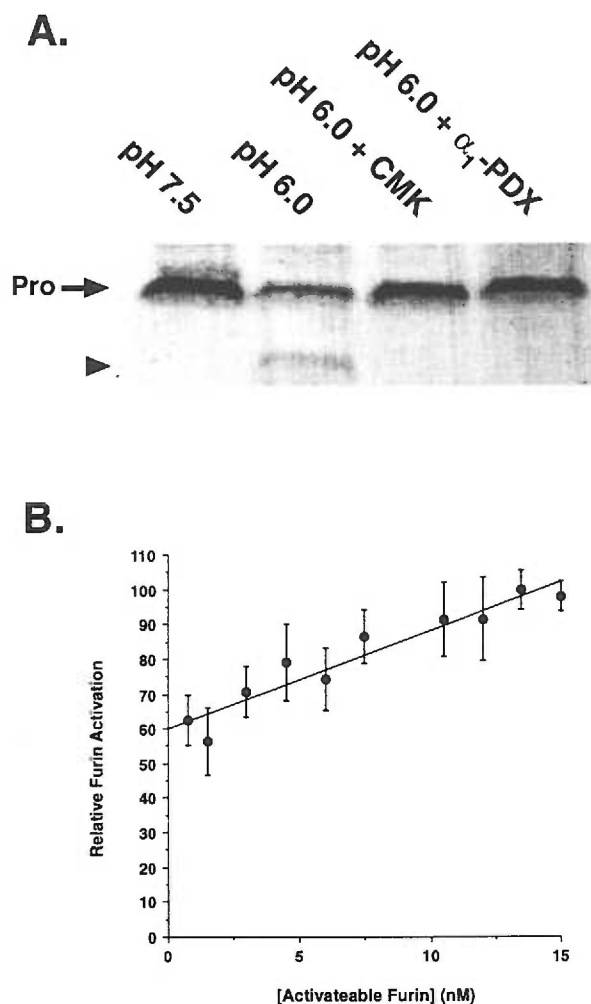


Figure 6. Autoproteolytic, intramolecular activation of furin. Replicate 15 cm plates of BSC-40 cells were infected with either VV:WT or VV:hFur/f Δ tc-k (m.o.i. = 5). At 16-18 hours post-infection the cells were harvested and crude membrane preparations were made. The membrane pellets were resuspended in pH 6.0 or pH 7.5 activation buffer (10 mM Bis-Tris, pH 6.0/pH 7.5 with 5 mM CaCl₂ and 1 mM β -ME) as indicated. In (A) 200 μ M α_1 -PDX or 200 μ M decanoyl-Arg-Val-Lys-Arg-CMK was added to experimental samples in pH 6.0 activation buffer prior to incubation at 30°C for 3 hrs. Following incubation the samples were analyzed by SDS-PAGE and western blotting for the propeptide using mAb 12CA5. The intact propeptide (*arrow*) and cleaved ~6 kDa HA-tagged N-terminal propeptide fragment (*arrowhead*) are indicated. In (B) the samples were diluted in pH 6.0 activation buffer on ice, and subsequently incubated at 30°C for 3 hours. Following incubation, furin activity was determined against the pGlu-Arg-Thr-Lys-Arg-MCA substrate. Background activity from VV:WT infected cells was subtracted from the activity of VV:hFur/f Δ tc-k infected cells, and relative activity computed. Finally, the amount of active furin in the membrane preparation was determined by titration with decanoyl-Arg-Val-Lys-Arg CMK. The data points indicate the mean of five separate experiments. Bars indicate standard deviation.

Table I: Furin processing of native and mutant propeptide cleavage motifs. Kinetic values are averages of at least two separate trials, and were determined as described (see Materials and Methods). All errors were 15% or less.

Peptidyl Substrate									
P7 P6 P5 P4 P3 P2 P1 P'1 P'2									
						</			

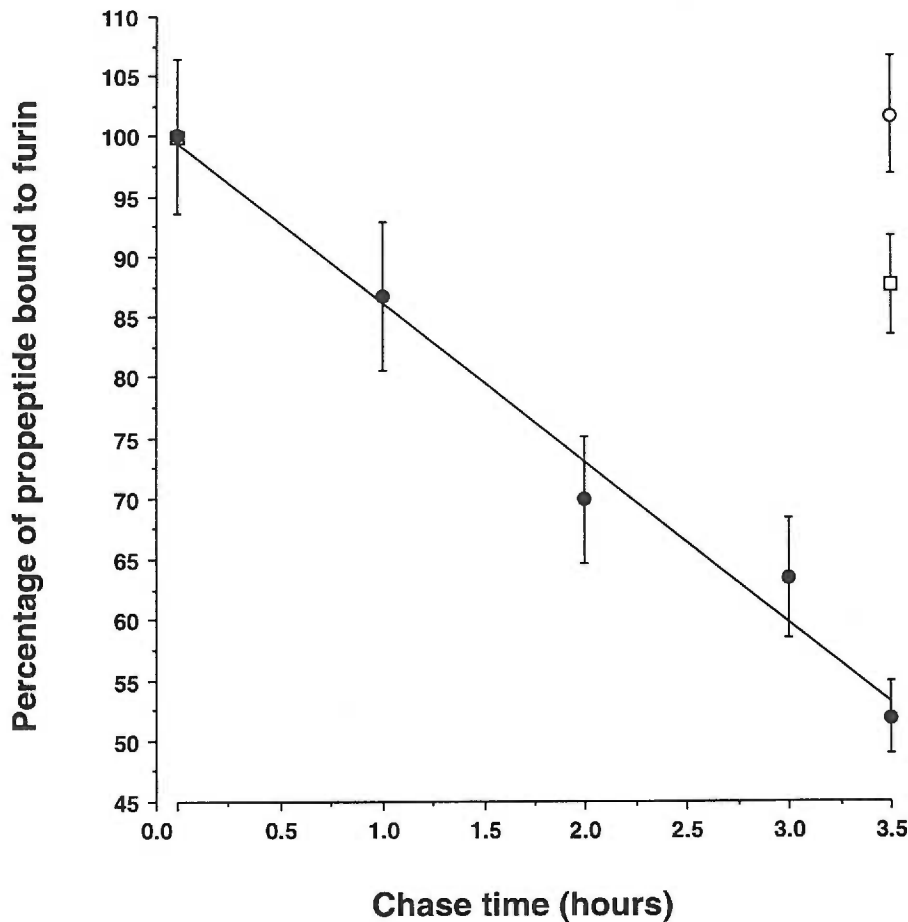


Figure 7. *In vivo* furin activation. Replicate 35 mm plates of confluent BSC-40 cells were infected with VV:hFur/f/ha or VV:R₇₅A:hFur/f/ha. The cells were infected for 4 hours at 37°C, and then pulse labeled for 0.5 hours with 100 μ Ci each of [³H]Arg and [³H]Leu. The cells were refed with medium containing 150 μ g/ml cold Arg and Leu, and harvested after the indicated chase times in TXCa²⁺ buffer supplemented with 10 μ M decanoyl-Arg-Val-Lys-Arg-CMK to inhibit residual furin activity. mAb M1 was added (100 μ g/ml) and furin immunoprecipitated overnight at 4°C. The immunoprecipitates were run on a 15% SDS-PAGE gel and processed for autoradiography. Furin and propeptide bands were excised, dissolved, and counted in LSC cocktail. The relative propeptide signal is presented as a percentage of the furin signal (*closed circles*). In an additional experiment, cells infected with VV:hFur/f/ha were treated with brefeldin A (10 μ g/ml) during labeling and chase times (*open circle*). R₇₅A:fur/f/ha is represented by an open square. R₇₅A:fur/f/ha and BFA treated fur/f/ha data points were taken after a seven hour chase to illustrate the long-term stability of propeptide association. Each experiment was repeated at least 3 times, and error bars indicate SEM.

Figure 8: Furin•propeptide localization and propeptide dissociation. Replicate plates of BSC-40 cells grown on glass coverslips were infected with either VV:hFur/f/ha or VV:R₇₅A:hFur/f/ha as indicated. Following inoculation, the cells were incubated at 37°C. At two hours post-infection, cycloheximide (10 µg/ml) was added to the treated cultures (bottom four panels). All cells were incubated at 37°C for a total of six hours post-infection. The cells were then fixed with paraformaldehyde, permeablized, and incubated with mAb M1, to detect furin mature domain localization, and with HA.11, to detect propeptide localization. The cells were then processed for immunofluorescence microscopy. mAb M1 was detected using a goat anti-mouse IgG_{2b}-FITC secondary antibody, and mAb HA.11 was visualized using a goat anti-mouse IgG₁-TxRd antibody.

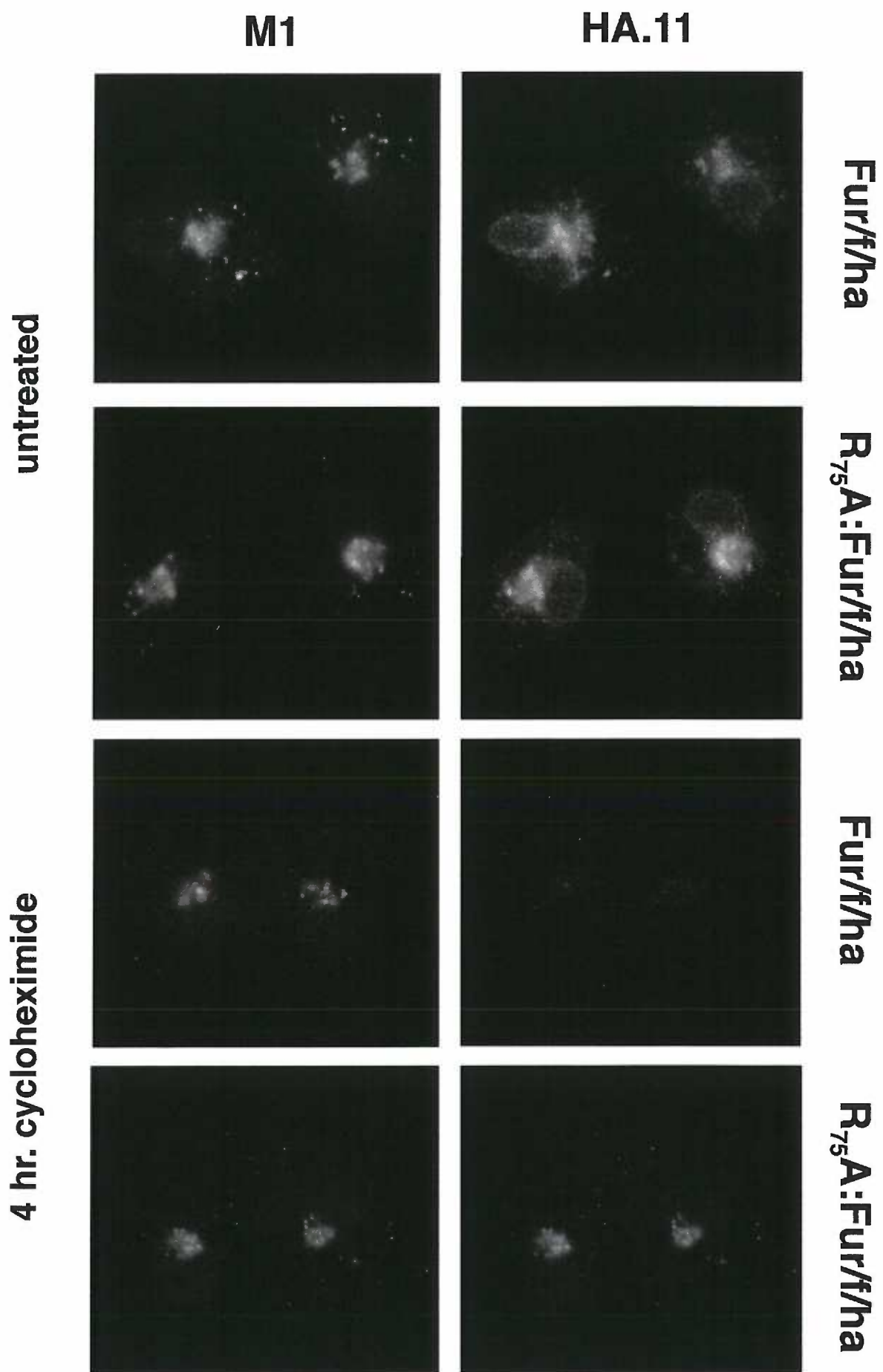
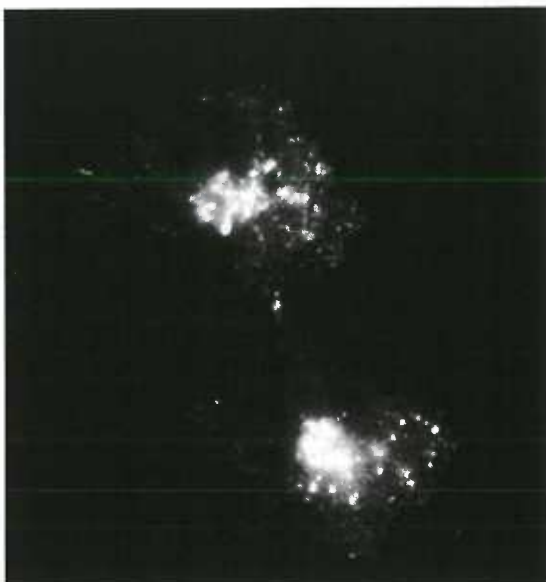


Figure 9: Antibody uptake and internal propeptide cleavage. Replicate plates of BSC-40 cells grown on glass coverslips were infected with VV:hFur/f/ha or VV:R₇₅A:hFur/f/ha and incubated at 37°C. At four hours post-infection, mAb M1 (30 µg/ml) was added to the culture medium and the cells were incubated for an additional hour to assess furin cycling between the TGN and plasma membrane. The cells were then fixed with paraformaldehyde, permeabilized, and incubated with PA1-062 to detect the total pool of furin. mAb M1 was detected using a goat anti-mouse IgG_{2b}-FITC, and PA1-062 using a goat anti-rabbit-TxRd antibody.

mAb M1 Uptake

PA1-062 Post-Fix

Fur/f/ha



R75A:Fur/f/ha

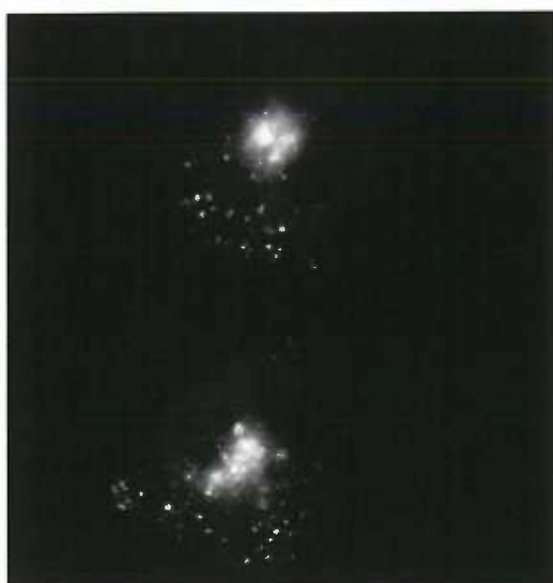
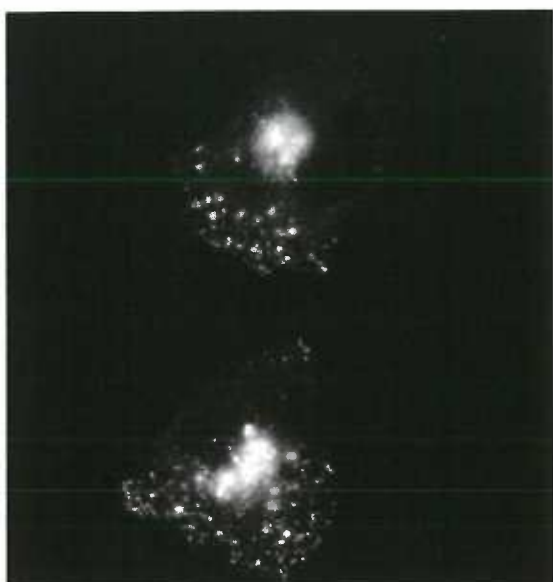
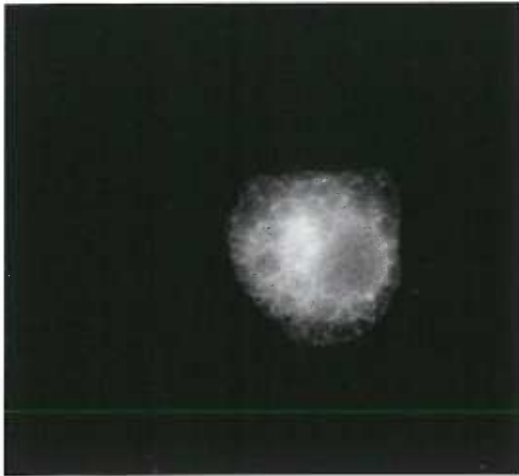
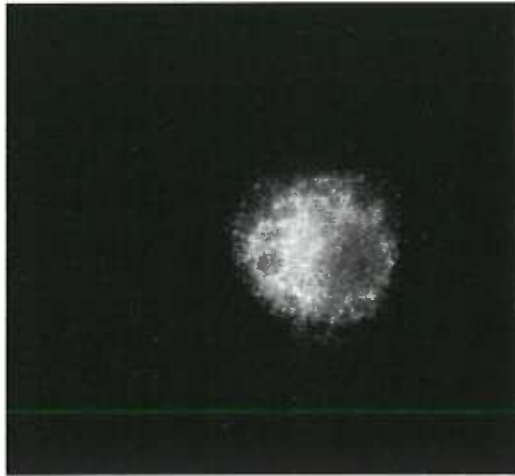


Figure 10. V₇₂R:fur/f/ha subcellular localization. Replicate plates of BSC-40 cells grown on glass coverslips were infected with VV:V₇₂R:hFur/f/ha. All cells were fixed after 5 hours of incubation at 37°C. mAb M1 (30 µg/ml) was added to the extracellular medium of indicated samples 1 hour prior to fixation. The fixed cells were permeablized and incubated with mAb HA.11 to detect furin, and also with either an anti-signal sequence receptor rabbit antiserum, or with mAb M1 to detect furin that has undergone propeptide excision. mAb M1 was detected using a goat anti-mouse IgG_{2b}-FITC secondary antibody, the signal-sequence receptor antiserum was visualized using a goat anti-rabbit-TxRd mAb, and HA.11 using a goat anti-mouse IgG₁-TxRd antibody.

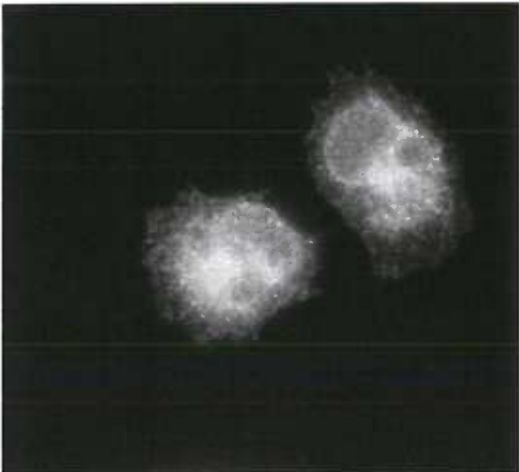
HA.11



SSR



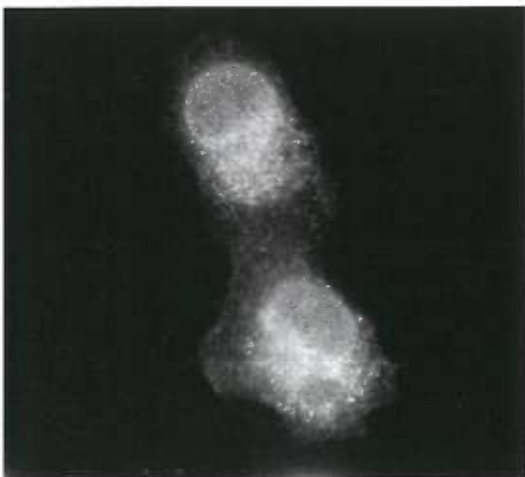
HA.11



mAb M1 Post-fix



HA.11



mAb M1 Uptake



SUMMARY AND CONCLUSIONS

Research presented in this thesis demonstrates that furin undergoes a multi-step pH-dependent activation process during transport from the ER to the TGN. Furin is synthesized as an inactive zymogen with an 83 residue N-terminal propeptide that is autoproteolytically excised within the ER (Creemers et al., 1995; Leduc et al., 1992; Molloy et al., 1994; Vey et al., 1994). The furin propeptide probably acts as an IMC, as suggested by the observations that i) a furin construct lacking the propeptide is inactive and ER-localized, suggesting misfolding, ii) co-expression of the propeptide *in trans* restores trafficking and activity, and iii) failure to excise the propeptide results in ERGIC/CGN localization, suggesting that this construct is trapped in an intermediate folding state and is being selectively retained by the quality control system. Following excision, the propeptide remains non-covalently bound to furin, acting as an autoinhibitor. *In vitro* exposure of the inactive furin•propeptide complex to an acidic (pH 6.0) and calcium-containing (low millimolar) environment characteristic of TGN/endosomal compartments results in autoproteolytic and predominantly intramolecular cleavage within the propeptide at -Arg₇₀-Gly-Val-Thr-Lys-Arg₇₅[↓]-. The pH-modulated cleavage of the internal propeptide cleavage site was demonstrated by the use of synthetic peptide substrates. Following internal cleavage, the propeptide fragments dissociate from furin, permitting the enzyme to cleave substrates *in trans*. This process occurs slowly both *in vitro* ($t_{1/2}$ = 90 minutes) and *in vivo* ($t_{1/2}$ = 105 minutes). *In vivo* activation can be blocked with BFA, consistent with the necessity for transport of furin to acidic late secretory pathway compartments for activation. Unlike excision, blocking internal propeptide cleavage does not result in a trafficking defect. Surprisingly, the integrity of the P1/P6 Arg internal cleavage site motif is essential for the correct folding of furin. Introduction of a P4 Arg into the site of internal propeptide cleavage to generate an -Arg-X-Lys/Arg-Arg[↓]- consensus cleavage motif (-Arg-Gly-Val₇₂-Thr-Lys-Arg₇₅- → -Arg-Gly-Arg₇₂-Thr-Lys-Arg₇₅-) was unexpectedly found to block propeptide excision and prevent export from the ER. This may be due to the existence of a furin folding pathway involving the differential binding of the propeptide excision and internal cleavage sites, based on their dissimilar K_m 's, to the folding protease's substrate binding pockets.

While the studies described in this thesis served to discern the general outline for the processes of furin folding and activation, many important questions remain unanswered. These questions include: i) can the furin propeptide be directly demonstrated to be an IMC?, ii) is the furin•propeptide complex metastable, and does it undergo a pH-induced rearrangement triggered by protonation of key His residues?, iii) does V₇₂R:fur/f/ha misfold due to non-productive binding of the mutant internal cleavage site to the folding proteases' substrate binding pockets?, and iv) is

fur/fD₁₅₃N in an intermediate folding state, and, if so, how does the quality control system recognize this and prevent transport past the ERGIC/CGN?

The most direct way to begin addressing these questions would be by *in vitro* reconstitution of furin folding and activation from purified components. This could be performed in a manner similar to that described for subtilisin and α -lytic protease. Generally, folding of these proteases is reconstituted *in vitro* by denaturing the catalytic domain, removing/diluting the denaturant, and adding back propeptide *in trans* (Baker et al., 1992b; Zhu et al., 1989). *In vitro* folding and activation of a truncated furin construct lacking the non-essential cytoplasmic tail, transmembrane domain, and cysteine-rich region (Introduction, Figure 5) could be studied by the use of circular dichroism and other techniques in conjunction with protease activity assays with synthetic peptide substrates.

A potential complication, however, distinguishes the *in vitro* reconstitution of furin folding from that of either subtilisin or α -lytic protease. It has been suggested that the furin P domain, which is essential for PC activity, folds into a domain separate from the catalytic/propeptide domains (Lipkind et al., 1998; Zhou et al., 1998). The multidomain structure of eukaryotic furin may make *in vitro* reconstitution of global folding technically difficult, as hydrophobic residues in the different furin domains may interact non-productively with each other, resulting in misfolding and aggregation. Indeed, aggregation during global folding *in vitro* is a problem frequently encountered with multidomain eukaryotic proteins (Netzer and Hartl, 1997). It may be possible to prevent aggregation by adding purified chaperone(s) to *in vitro* furin folding reactions. Preliminary evidence indicates that BiP binds to misfolded furin mutants *in vivo* (E.D.A. and G.T., unpublished results), suggesting that this molecular chaperone could prove useful for furin folding *in vitro*.

In vitro reconstitution of furin folding/activation will not only enhance our understanding of furin, but also of other PCs and IMC-mediated folding generally. Accumulating evidence shows that other PCs undergo propeptide and pH-dependent activation processes (Lamango et al., 1999; Zhou et al., 1995 and E.D.A. and G.T., unpublished results), suggesting that the model established for furin activation may serve as an archetype for the other PCs. Additionally, the rapidity with which the prokaryotic IMCs are degraded following folding makes the study of late events in this process technically difficult (e.g. see Bryan et al., 1995). The slow and pH-dependent process of furin activation will allow the study of late events in IMC-mediated folding that cannot be observed in any other known system.

REFERENCES

- Adeli, K., J. Macri, A. Mohammadi, M. Kito, R. Urade, and D. Cavallo. 1997. Apolipoprotein B is intracellularly associated with an ER-60 protease homologue in HepG2 cells. *J Biol Chem.* 272:22489-22494.
- Anderson, D.E., R.J. Peters, B. Wilk, and D.A. Agard. 1999. alpha-lytic protease precursor: characterization of a structured folding intermediate. *Biochemistry.* 38:4728-4735.
- Anderson, E.D., L. Thomas, J.S. Hayflick, and G. Thomas. 1993. Inhibition of HIV-1 gp160-dependent membrane fusion by a furin-directed alpha1-antitrypsin variant. *J. Biol. Chem.* 268:24887-24891.
- Anderson, E.D., J.K. VanSlyke, C.D. Thulin, F. Jean, and G. Thomas. 1997. Activation of the furin endoprotease is a multiple-step process: requirements for acidification and internal propeptide cleavage. *EMBO J.* 16:1508-1518.
- Anfinsen, C.B. 1973. Principles that govern the folding of protein chains. *Science.* 181:223-230.
- Anglikar, H., U. Neumann, S.S. Molloy, and G. Thomas. 1995. Internally quenched fluorogenic substrate for furin. *Anal. Biochem.* 224:409-412.
- Baker, D. 1998. Metastable states and folding free energy barriers. *Nat Struct Biol.* 5:1021-1024.
- Baker, D., and D.A. Agard. 1994. Kinetics versus thermodynamics in protein folding. *Biochem.* 33:7505-7509.
- Baker, D., A.K. Shiau, and D.A. Agard. 1993. The role of pro regions in protein folding. *Curr. Opin. Cell Biol.* 5:966-970.
- Baker, D., J.L. Silen, and D.A. Agard. 1992a. Protease pro region required for folding is a potent inhibitor of the mature enzyme. *Proteins.* 12:339-344.
- Baker, D., J.L. Sohl, and D.A. Agard. 1992b. A protein-folding reaction under kinetic control. *Nature.* 356:263-265.
- Baldwin, R.L., and G.D. Rose. 1999a. Is protein folding hierarchic? I. Local structure and peptide folding. *Trends Biochem Sci.* 24:26-33.
- Baldwin, R.L., and G.D. Rose. 1999b. Is protein folding hierarchic? II. Folding intermediates and transition states. *Trends Biochem Sci.* 24:77-83.
- Balow, J.P., J.D. Weissman, and K.P. Kearse. 1995. Unique expression of major histocompatibility complex class I proteins in the absence of glucose trimming and calnexin association. *J Biol Chem.* 270:29025-29029.
- Bannykh, S.I., N. Nishimura, and W.E. Balch. 1998. Getting into the Golgi. *Trends Cell Biol.* 8:21-25.
- Beggah, A., P. Mathews, P. Beguin, and K. Geering. 1996. Degradation and endoplasmic reticulum retention of unassembled alpha- and beta-subunits of Na,K-ATPase correlate with interaction of BiP. *J Biol Chem.* 271:20895-20902.

- Bergeron, J.J., M.B. Brenner, D.Y. Thomas, and D.B. Williams. 1994. Calnexin: a membrane-bound chaperone of the endoplasmic reticulum. *Trends Biochem Sci.* 19:124-128.
- Blond-Elguindi, S., S.E. Cwirla, W.J. Dower, R.J. Lipshutz, S.R. Sprang, J.F. Sambrook, and M.J. Gething. 1993. Affinity panning of a library of peptides displayed on bacteriophages reveals the binding specificity of BiP. *Cell.* 75:717-728.
- Bonifacino, J.S., and A.M. Weissman. 1998. Ubiquitin and the control of protein fate in the secretory and endocytic pathways. *Annu Rev Cell Dev Biol.* 14:19-57.
- Braks, J.A., and G.J. Martens. 1994. 7B2 is a neuroendocrine chaperone that transiently interacts with prohormone convertase PC2 in the secretory pathway. *Cell.* 78:263-273.
- Brennan, S.O., and K. Nakayama. 1994a. Cleavage of proalbumin peptides by furin reveals unexpected restrictions at the P2 and P'1 sites. *FEBS Lett.* 347:80-84.
- Brennan, S.O., and K. Nakayama. 1994b. Furin has the proalbumin substrate specificity and serpin inhibitory properties of an in situ hepatic convertase. *FEBS Lett.* 338:147-151.
- Bresnahan, P.A., R. Leduc, L. Thomas, J. Thorner, H.L. Gibson, A.J. Brake, P.J. Barr, and G. Thomas. 1990. Human fur gene encodes a yeast KEX2-like endoprotease that cleaves pro-beta-NGF in vivo. *J. Cell Biol.* 111:2851-2859.
- Bresnahan, P.A., J.S. Hayflick, S.S. Molloy, and G. Thomas. 1993. Endoproteolysis of Growth Factors and Other Nonendocrine Precursor Proteins. In *Mechanisms of Intracellular Trafficking and Processing of Proteins*. Y.P. Loh, editor. CRC Press, Boca Raton, FL. 225-250.
- Broglia, R.A., G. Tiana, S. Pasquali, H.E. Roman, and E. Vigezzi. 1998. Folding and aggregation of designed proteins. *Proc Natl Acad Sci U S A.* 95:12930-12933.
- Bruzzaniti, A., K. Goodge, P. Jay, S.A. Taviaux, M.H. Lam, P. Berta, T.J. Martin, J.M. Moseley, and M.T. Gillespie. 1996. C8, a new member of the convertase family. *Biochem. J.* 314:727-731.
- Bryan, P., L. Wang, J. Hoskins, S. Ruvinov, S. Strausberg, P. Alexander, O. Almog, G. Gilliland, and T. Gallagher. 1995. Catalysis of a protein folding reaction: mechanistic implications of the 2.0 Å structure of the subtilisin-prodomain complex. *Biochemistry.* 34:10310-10318.
- Buchberger, A., H. Schroder, T. Hesterkamp, H.J. Schonfeld, and B. Bukau. 1996. Substrate shuttling between the DnaK and GroEL systems indicates a chaperone network promoting protein folding. *J Mol Biol.* 261:328-333.
- Bukau, B., and A.L. Horwich. 1998. The Hsp70 and Hsp60 chaperone machines. *Cell.* 92:351-366.
- Carr, C.M., C. Chaudhry, and P.S. Kim. 1997. Influenza hemagglutinin is spring-loaded by a metastable native conformation. *Proc Natl Acad Sci U S A.* 94:14306-14313.
- Carter, P., and J.A. Wells. 1988. Dissecting the catalytic triad of a serine protease. *Nature.* 332:564-568.
- Chanat, E., and W.B. Huttner. 1991. Milieu-induced, selective aggregation of regulated secretory proteins in the trans-Golgi network. *J. Cell Biol.* 115:1505-1519.

- Chandra, S., E.P. Kable, G.H. Morrison, and W.W. Webb. 1991. Calcium sequestration in the Golgi apparatus of cultured mammalian cells revealed by laser scanning confocal microscopy and ion microscopy. *J. Cell Sci.* 100:747-752.
- Chapman, R., C. Sidrauski, and P. Walter. 1998. Intracellular signaling from the endoplasmic reticulum to the nucleus. *Annu Rev Cell Dev Biol.* 14:459-485.
- Chapman, R.E., and S. Munro. 1994. Retrieval of TGN proteins from the cell surface requires endosomal acidification. *EMBO J.* 13:2305-2312.
- Chen, J., K.H. Lee, D.A. Steinhauer, D.J. Stevens, J.J. Skehel, and D.C. Wiley. 1998. Structure of the hemagglutinin precursor cleavage site, a determinant of influenza pathogenicity and the origin of the labile conformation. *Cell.* 95:409-417.
- Chen, W., J. Helenius, I. Braakman, and A. Helenius. 1995. Cotranslational folding and calnexin binding during glycoprotein synthesis. *Proc Natl Acad Sci U S A.* 92:6229-6233.
- Chevet, E., H.N. Wong, D. Gerber, C. Cochet, A. Fazel, P.H. Cameron, J.N. Gushue, D.Y. Thomas, and J.J. Bergeron. 1999. Phosphorylation by CK2 and MAPK enhances calnexin association with ribosomes. *EMBO J.* 18:3655-3666.
- Clague, M.J. 1998. Molecular aspects of the endocytic pathway. *Biochem J.* 336:271-282.
- Clairmont, C.A., A. De Maio, and C.B. Hirschberg. 1992. Translocation of ATP into the lumen of rough endoplasmic reticulum- derived vesicles and its binding to luminal proteins including BiP (GRP 78) and GRP 94. *J Biol Chem.* 267:3983-3990.
- Creemers, J.W., M. Vey, W. Schafer, T.A. Ayoubi, A.J. Roebroek, H.D. Klenk, W. Garten, and W.J. Van de Ven. 1995. Endoproteolytic cleavage of its propeptide is a prerequisite for efficient transport of furin out of the endoplasmic reticulum. *J. Biol. Chem.* 270:2695-2702.
- Creighton, T.E. 1993. *Proteins: Structures and Molecular Properties.* W. H. Freeman and Company, New York. 507 pp.
- Cresswell, P., and E.A. Hughes. 1997. Protein degradation: the ins and outs of the matter. *Curr Biol.* 7:R552-555.
- Daniels, R.S., J.C. Downie, A.J. Hay, M. Knossow, J.J. Skehel, M.L. Wang, and D.C. Wiley. 1985. Fusion mutants of the influenza virus hemagglutinin glycoprotein. *Cell.* 40:431-439.
- Dayhuff, T.J., R.F. Gesteland, and J.F. Atkins. 1992. Electrophoresis, Autoradiography and Electroblotting of Peptides: T4 Gene 60 Hopping. *BioTechniques.* 13:500- 503.
- DeFelippis, M.R., L.A. Alter, A.H. Pekar, H.A. Havel, and D.N. Brems. 1993. Evidence for a self-associating equilibrium intermediate during folding of human growth hormone. *Biochemistry.* 32:1555-1562.
- Demaurex, N., W. Furuya, S. D'Souza, J.S. Bonifacino, and S. Grinstein. 1998. Mechanism of acidification of the trans-Golgi network (TGN). In situ measurements of pH using retrieval of TGN38 and furin from the cell surface. *J Biol. Chem.* 273:2044-2051.
- Dobson, C.M., and M. Karplus. 1999. The fundamentals of protein folding: bringing together theory and experiment. *Curr Opin Struct Biol.* 9:92-101.

- Duan, Y., and P.A. Kollman. 1998. Pathways to a protein folding intermediate observed in a 1-microsecond simulation in aqueous solution. *Science*. 282:740-744.
- Eaton, W.A. 1999. Searching for "downhill scenarios" in protein folding. *Proc Natl Acad Sci U S A*. 96:5897-5899.
- Eaton, W.A., V. Munoz, P.A. Thompson, C.K. Chan, and J. Hofrichter. 1997. Submillisecond kinetics of protein folding. *Curr Opin Struct Biol*. 7:10-14.
- Eder, J., M. Rheinhecker, and A.R. Fersht. 1993a. Folding of subtilisin BPN': characterization of a folding intermediate. *Biochemistry*. 32:18-26.
- Eder, J., M. Rheinhecker, and A.R. Fersht. 1993b. Folding of subtilisin BPN': role of the pro-sequence. *J Mol Biol*. 233:293-304.
- Ellis, R.J. 1998. Steric chaperones. *Trends Biochem Sci*. 23:43-45.
- Ellis, R.J. 1999. Molecular chaperones: pathways and networks. *Curr Biol*. 9:R137-139.
- Ellis, R.J., and F.U. Hartl. 1999. Principles of protein folding in the cellular environment. *Curr Opin Struct Biol*. 9:102-110.
- Farquhar, M.G., and G.E. Palade. 1998. The Golgi apparatus: 100 years of progress and controversy. *Trends Cell Biol*. 8:2-10.
- Farr, G.W., E.C. Scharl, R.J. Schumacher, S. Sondek, and A.L. Horwich. 1997. Chaperonin-mediated folding in the eukaryotic cytosol proceeds through rounds of release of native and nonnative forms. *Cell*. 89:927-937.
- Fedorov, A.N., and T.O. Baldwin. 1997. Cotranslational protein folding. *J Biol. Chem*. 272:32715-32718.
- Ferrari, D.M., and H.D. Soling. 1999. The protein disulphide-isomerase family: unravelling a string of folds. *Biochem J*. 339:1-10.
- Fersht, A.R. 1995. Optimization of rates of protein folding: the nucleation-condensation mechanism and its implications. *Proc Natl Acad Sci U S A*. 92:10869-10873.
- Fersht, A.R. 1997. Nucleation mechanisms in protein folding. *Curr Opin Struct Biol*. 7:3-9.
- Field, M.C., P. Moran, W. Li, G.A. Keller, and I.W. Caras. 1994. Retention and degradation of proteins containing an uncleaved glycosylphosphatidylinositol signal. *J Biol. Chem*. 269:10830-10837.
- Fink, A.L. 1995. Compact intermediate states in protein folding. *Annu Rev Biophys Biomol Struct*. 24:495-522.
- Flynn, G.C., J. Pohl, M.T. Flocco, and J.E. Rothman. 1991. Peptide-binding specificity of the molecular chaperone BiP. *Nature*. 353:726-730.
- Fourie, A.M., J.F. Sambrook, and M.J. Gething. 1994. Common and divergent peptide binding specificities of hsp70 molecular chaperones. *J Biol. Chem*. 269:30470-30478.

- Freskgard, P.O., N. Bergenheim, B.H. Jonsson, M. Svensson, and U. Carlsson. 1992. Isomerase and chaperone activity of prolyl isomerase in the folding of carbonic anhydrase. *Science*. 258:466-468.
- Fujishige, A., K.R. Smith, J.L. Silen, and D.A. Agard. 1992. Correct folding of alpha-lytic protease is required for its extracellular secretion from *Escherichia coli*. *J Cell Biol*. 118:33-42.
- Fullekrug, J., B. Sonnichsen, U. Schafer, P. Nguyen Van, H.D. Soling, and G. Mieskes. 1997. Characterization of brefeldin A induced vesicular structures containing cycling proteins of the intermediate compartment/cis-Golgi network. *FEBS Lett*. 404:75-81.
- Fuller, R.S., A.J. Brake, and J. Thorner. 1989. Intracellular targeting and structural conservation of a prohormone-processing endoprotease. *Science*. 246:482-486.
- Gahmberg, C.G., and M. Tolvanen. 1996. Why mammalian cell surface proteins are glycoproteins [published erratum appears in *Trends Biochem Sci* 1996 Dec;21(12):491]. *Trends Biochem Sci*. 21:308-311.
- Gallagher, T., G. Gilliland, L. Wang, and P. Bryan. 1995. The prosegment-subtilisin BPN' complex: crystal structure of a specific 'foldase'. *Structure*. 3:907-914.
- Gaynor, E.C., T.R. Graham, and S.D. Emr. 1998. COPI in ER/Golgi and intra-Golgi transport: do yeast COPI mutants point the way? *Biochim Biophys Acta*. 1404:33-51.
- Gluschankof, P., and R.S. Fuller. 1994. A C-terminal domain conserved in precursor processing proteases is required for intramolecular N-terminal maturation of pro-Kex2 protease. *EMBO J*. 13:2280-2288.
- Goodman, L.J., and C.M. Gorman. 1994. Autoproteolytic activation of the mouse prohormone convertase mPC1. *Biochem. Biophys. Res. Commun*. 201:795-804.
- Hammond, C., and A. Helenius. 1994. Quality control in the secretory pathway: retention of a misfolded viral membrane glycoprotein involves cycling between the ER, intermediate compartment, and Golgi apparatus. *J Cell Biol*. 126:41-52.
- Hammond, C., and A. Helenius. 1995. Quality control in the secretory pathway. *Curr Opin Cell Biol*. 7:523-529.
- Hartl, F.U. 1996. Molecular chaperones in cellular protein folding. *Nature*. 381:571-579.
- Hatsuzawa, K., K. Murakami, and K. Nakayama. 1992a. Molecular and enzymatic properties of furin, a Kex2-like endoprotease involved in precursor cleavage at Arg-X-Lys/Arg-Arg sites. *J. of Biochem*. 111:296-301.
- Hatsuzawa, K., M. Nagahama, S. Takahashi, K. Takada, K. Murakami, and K. Nakayama. 1992b. Purification and characterization of furin, a Kex2-like processing endoprotease, produced in Chinese hamster ovary cells. *J. Biol. Chem*. 267:16094-16099.
- Helenius, A. 1994. How N-linked oligosaccharides affect glycoprotein folding in the endoplasmic reticulum. *Mol Biol. Cell*. 5:253-265.
- Helenius, A., T. Marquardt, and I. Braakman. 1992. The Endoplasmic Reticulum as a Protein-Folding Compartment. *Trends in Cell Biol*. 2:227-231.

- Helenius, A., E.S. Trombetta, D. Hebert, and J.F. Simons. 1997. Calnexin, Calreticulin and the Folding of Glycoproteins. *Trends in Cell Biol.* 7:193-200.
- Herrmann, J.M., P. Malkus, and R. Schekman. 1999. Out of the ER--outfitters, escorts and guides. *Trends Cell Biol.* 9:5-7.
- Hsu, V.W., L.C. Yuan, J.G. Nuchtern, J. Lippincott-Schwartz, G.J. Hammerling, and R.D. Klausner. 1991. A recycling pathway between the endoplasmic reticulum and the Golgi apparatus for retention of unassembled MHC class I molecules. *Nature.* 352:441-444.
- Huppa, J.B., and H.L. Ploegh. 1998. The eS-Sence of -SH in the ER. *Cell.* 92:145-148.
- Hurtley, S.M., and A. Helenius. 1989. Protein oligomerization in the endoplasmic reticulum. *Annual Review of Cell Biology.* 5:277-307.
- Hwang, C., A.J. Sinskey, and H.F. Lodish. 1992. Oxidized redox state of glutathione in the endoplasmic reticulum. *Science.* 257:1496-1502.
- Ikemura, H., and M. Inouye. 1988. In vitro processing of pro-subtilisin produced in Escherichia coli. *J. Biol. Chem.* 263:12959-12963.
- Infante, C., F. Ramos-Morales, C. Fedriani, M. Bornens, and R.M. Rios. 1999. GMAP-210, A cis-Golgi network-associated protein, is a minus end microtubule-binding protein. *J Cell Biol.* 145:83-98.
- Isidoro, C., C. Maggioni, M. Demoz, A. Pizzagalli, A.M. Fra, and R. Sitia. 1996. Exposed thiols confer localization in the endoplasmic reticulum by retention rather than retrieval. *J Biol. Chem.* 271:26138-26142.
- Itin, C., M. Foguet, F. Kappeler, J. Klumperman, and H.P. Hauri. 1995. Recycling of the endoplasmic reticulum/Golgi intermediate compartment protein ERGIC-53 in the secretory pathway. *Biochem Soc Trans.* 23:541-544.
- Jackson, M.R., M.F. Cohen-Doyle, P.A. Peterson, and D.B. Williams. 1994. Regulation of MHC class I transport by the molecular chaperone, calnexin (p88, IP90). *Science.* 263:384-387.
- Jaenicke, R. 1987. Folding and association of proteins. *Prog Biophys Mol Biol.* 49:117-237.
- Jaenicke, R. 1991. Protein folding: local structures, domains, subunits, and assemblies. *Biochemistry.* 30:3147-3161.
- Jean, F., A. Basak, J. DiMaio, N.G. Seidah, and C. Lazure. 1995. An internally quenched fluorogenic substrate of prohormone convertase 1 and furin leads to a potent prohormone convertase inhibitor. *Biochem J.* 307:689-695.
- Jean, F., K. Stella, L. Thomas, G. Liu, Y. Xiang, A.J. Reason, and G. Thomas. 1998. alpha1-Antitrypsin Portland, a bioengineered serpin highly selective for furin: application as an antipathogenic agent. *Proc Natl Acad Sci U S A.* 95:7293-7298.
- Johnson, R.T., and C.J. Gibbs, Jr. 1998. Creutzfeldt-Jakob disease and related transmissible spongiform encephalopathies. *N Engl J Med.* 339:1994-2004.

- Jones, B.G., L. Thomas, S.S. Molloy, C.D. Thulin, M.D. Fry, K.A. Walsh, and G. Thomas. 1995. Intracellular trafficking of furin is modulated by the phosphorylation state of a casein kinase II site in its cytoplasmic tail. *EMBO J.* 14:5869-5883.
- Kaiser, C., and S. Ferro-Novick. 1998. Transport from the endoplasmic reticulum to the Golgi. *Curr Opin Cell Biol.* 10:477-482.
- Kaushal, S., and H.G. Khorana. 1994. Structure and function in rhodopsin. 7. Point mutations associated with autosomal dominant retinitis pigmentosa. *Biochemistry.* 33:6121-6128.
- Kendall, J.M., M.N. Badminton, R.L. Dormer, and A.K. Campbell. 1994. Changes in free calcium in the endoplasmic reticulum of living cells detected using targeted aequorin. *Anal. Biochem.* 221:173-181.
- Kim, J.H., L. Johannes, B. Goud, C. Antony, C.A. Lingwood, R. Daneman, and S. Grinstein. 1998. Noninvasive measurement of the pH of the endoplasmic reticulum at rest and during calcium release. *Proc Natl Acad Sci U S A.* 95:2997-3002.
- Kim, P.S., and P. Arvan. 1995. Calnexin and BiP act as sequential molecular chaperones during thyroglobulin folding in the endoplasmic reticulum. *J Cell Biol.* 128:29-38.
- Kim, P.S., and P. Arvan. 1998. Endocrinopathies in the family of endoplasmic reticulum (ER) storage diseases: disorders of protein trafficking and the role of ER molecular chaperones. *Endocr Rev.* 19:173-202.
- King, D.S., C.G. Fields, and G.B. Fields. 1990. A cleavage method which minimizes side reactions following Fmoc solid phase peptide synthesis. *Int J Pept Protein Res.* 36:255-266.
- Knittler, M.R., S. Dirks, and I.G. Haas. 1995. Molecular chaperones involved in protein degradation in the endoplasmic reticulum: quantitative interaction of the heat shock cognate protein BiP with partially folded immunoglobulin light chains that are degraded in the endoplasmic reticulum. *Proc Natl Acad Sci U S A.* 92:1764-1768.
- Koch, G.L. 1987. Reticuloplasmins: a novel group of proteins in the endoplasmic reticulum. *J Cell Sci.* 87:491-492.
- Kopito, R.R. 1999. Biosynthesis and degradation of CFTR. *Physiol Rev.* 79:S167-173.
- Krause, K.H., and M. Michalak. 1997. Calreticulin. *Cell.* 88:439-443.
- Krishna, R.G., and F. Wold. 1993. Post-Translational Modification of Proteins. In *Advances in Enzymology and Related Areas of Molecular Biology*. Vol. 67. A. Meister, editor. John Wiley and Sons, Inc., New York. 265-298.
- Kuznetsov, G., and S.K. Nigam. 1998. Folding of secretory and membrane proteins. *N Engl J Med.* 339:1688-1695.
- Lamango, N.S., E. Apletalina, J. Liu, and I. Lindberg. 1999. The proteolytic maturation of prohormone convertase 2 (PC2) is a pH- driven process. *Arch Biochem Biophys.* 362:275-282.
- Lansbury, P.T., Jr. 1999. Evolution of amyloid: what normal protein folding may tell us about fibrillogenesis and disease. *Proc Natl Acad Sci U S A.* 96:3342-3344.

- Leduc, R., S.S. Molloy, B.A. Thorne, and G. Thomas. 1992. Activation of human furin precursor processing endoprotease occurs by an intramolecular autoproteolytic cleavage. *J. Biol. Chem.* 267:14304-14308.
- Li, Y., Z. Hu, F. Jordan, and M. Inouye. 1995. Functional analysis of the propeptide of subtilisin E as an intramolecular chaperone for protein folding. Refolding and inhibitory abilities of propeptide mutants. *J. Biol. Chem.* 270:25127-25132.
- Li, Y., and M. Inouye. 1994. Autoprocessing of prothiolsubtilisin E in which active-site serine 221 is altered to cysteine. *J. Biol. Chem.* 269:4169-4174.
- Lin, P., H. Le-Niculescu, R. Hofmeister, J.M. McCaffery, M. Jin, H. Hennemann, T. McQuistan, L. De Vries, and M.G. Farquhar. 1998. The mammalian calcium-binding protein, nucleobindin (CALNUC), is a Golgi resident protein. *J Cell Biol.* 141:1515-1527.
- Lin, P., Y. Yao, R. Hofmeister, R.Y. Tsien, and M.G. Farquhar. 1999. Overexpression of CALNUC (nucleobindin) increases agonist and thapsigargin releasable Ca^{2+} storage in the Golgi. *J Cell Biol.* 145:279-289.
- Lindberg, I. 1994. Evidence for cleavage of the PC1/PC3 pro-segment in the endoplasmic reticulum. *Mol. Cel. Neurosci.* 5:263-268.
- Lipkind, G.M., A. Zhou, and D.F. Steiner. 1998. A model for the structure of the P domains in the subtilisin-like prohormone convertases. *Proc Natl Acad Sci U S A.* 95:7310-7315.
- Liu, G., L. Thomas, R.A. Warren, C.A. Enns, C.C. Cunningham, J.H. Hartwig, and G. Thomas. 1997. Cytoskeletal protein ABP-280 directs the intracellular trafficking of furin and modulates proprotein processing in the endocytic pathway. *J Cell Biol.* 139:1719-1733.
- Liu, Y., P. Choudhury, C.M. Cabral, and R.N. Sifers. 1999. Oligosaccharide modification in the early secretory pathway directs the selection of a misfolded glycoprotein for degradation by the proteasome. *J Biol. Chem.* 274:5861-5867.
- Lyman, S.K., and R. Schekman. 1997. Binding of secretory precursor polypeptides to a translocon subcomplex is regulated by BiP. *Cell.* 88:85-96.
- Marquardt, T., and A. Helenius. 1992. Misfolding and aggregation of newly synthesized proteins in the endoplasmic reticulum. *J Cell Biol.* 117:505-513.
- Matlack, K.E., B. Misselwitz, K. Plath, and T.A. Rapoport. 1999. BiP acts as a molecular ratchet during posttranslational transport of prepro- α factor across the ER membrane. *Cell.* 97:553-564.
- Matlack, K.E., W. Mothes, and T.A. Rapoport. 1998. Protein translocation: tunnel vision. *Cell.* 92:381-390.
- Matthews, C.R. 1993. Pathways of protein folding. *Annu Rev Biochem.* 62:653-683.
- Matthews, D.J., L.J. Goodman, C.M. Gorman, and J.A. Wells. 1994a. A survey of furin substrate specificity using substrate phage display. *Protein Sci.* 3:1197-1205.
- Matthews, G., K.I. Shennan, A.J. Seal, N.A. Taylor, A. Colman, and K. Docherty. 1994b. Autocatalytic maturation of the prohormone convertase PC2. *J. Biol. Chem.* 269:588-592.

- McCracken, A.A., and J.L. Brodsky. 1996. Assembly of ER-associated protein degradation in vitro: dependence on cytosol, calnexin, and ATP. *J Cell Biol.* 132:291-298.
- McKeehan, W.L., and R.G. Ham. 1976. Methods for reducing the serum requirement for growth in vitro of nontransformed diploid fibroblasts. *Dev. Biol. Stand.* 37:97-98.
- Meerabux, J., M.L. Yaspo, A.J. Roebroek, W.J. Van de Ven, T.A. Lister, and B.D. Young. 1996. A new member of the proprotein convertase gene family (LPC) is located at a chromosome translocation breakpoint in lymphomas. *Canc. Res.* 56:448-451.
- Meldolesi, J., and T. Pozzan. 1998. The endoplasmic reticulum Ca^{2+} store: a view from the lumen. *Trends Biochem Sci.* 23:10-14.
- Mellman, I., R. Fuchs, and A. Helenius. 1986. Acidification of the endocytic and exocytic pathways. *Annu. Rev. Biochem.* 55:663-700.
- Melnick, J., J.L. Dul, and Y. Argon. 1994. Sequential interaction of the chaperones BiP and GRP94 with immunoglobulin chains in the endoplasmic reticulum. *Nature.* 370:373-375.
- Misselwitz, B., O. Staack, and T.A. Rapoport. 1998. J proteins catalytically activate Hsp70 molecules to trap a wide range of peptide sequences. *Mol Cell.* 2:593-603.
- Miyazono, K., U. Hellman, C. Wernstedt, and C.H. Heldin. 1988. Latent high molecular weight complex of transforming growth factor beta 1. Purification from human platelets and structural characterization. *J. Biol. Chem.* 263:6407-6415.
- Molloy, S.S., E.D. Anderson, F. Jean, and G. Thomas. 1999. Bi-cycling the furin pathway: from TGN localization to pathogen activation and embryogenesis. *Trends Cell Biol.* 9:28-35.
- Molloy, S.S., P.A. Bresnahan, S.H. Leppla, K.R. Klimpel, and G. Thomas. 1992. Human furin is a calcium-dependent serine endoprotease that recognizes the sequence Arg-X-X-Arg and efficiently cleaves anthrax toxin protective antigen. *J. Biol. Chem.* 267:16396-16402.
- Molloy, S.S., L. Thomas, J.K. VanSlyke, P.E. Stenberg, and G. Thomas. 1994. Intracellular trafficking and activation of the furin proprotein convertase: localization to the TGN and recycling from the cell surface. *EMBO J.* 13:18-33.
- Moran, P., and I.W. Caras. 1992. Proteins containing an uncleaved signal for glycosylphosphatidylinositol membrane anchor attachment are retained in a post-ER compartment. *J Cell Biol.* 119:763-772.
- Moriyama, T., S.K. Sather, T.P. McGee, and R.D. Simoni. 1998. Degradation of HMG-CoA reductase in vitro. Cleavage in the membrane domain by a membrane-bound cysteine protease. *J Biol. Chem.* 273:22037-22043.
- Nakayama, K. 1997. Furin: a mammalian subtilisin/Kex2p-like endoprotease involved in processing of a wide variety of precursor proteins. *Biochem J.* 327:625-635.
- Netzer, W.J., and F.U. Hartl. 1997. Recombination of protein domains facilitated by co-translational folding in eukaryotes. *Nature.* 388:343-349.
- Nichols, W.C., U. Seligsohn, A. Zivelin, V.H. Terry, C.E. Hertel, M.A. Wheatley, M.J. Moussalli, H.P. Hauri, N. Ciavarella, R.J. Kaufman, and D. Ginsburg. 1998. Mutations in the

ER-Golgi intermediate compartment protein ERGIC-53 cause combined deficiency of coagulation factors V and VIII. *Cell*. 93:61-70.

Nishimura, N., S. Bannykh, S. Slabough, J. Matteson, Y. Altschuler, K. Hahn, and W.E. Balch. 1999. A di-acidic (DXE) code directs concentration of cargo during export from the endoplasmic reticulum. *J Biol. Chem.* 274:15937-15946.

Noda, T., and M.G. Farquhar. 1992. A non-autophagic pathway for diversion of ER secretory proteins to lysosomes. *J Cell Biol.* 119:85-97.

Oberg, K., B.A. Chrnyk, R. Wetzel, and A.L. Fink. 1994. Nativelike secondary structure in interleukin-1 beta inclusion bodies by attenuated total reflectance FTIR. *Biochemistry*. 33:2628-2634.

Onuchic, J.N., P.G. Wolynes, Z. Luthey-Schulten, and N.D. Socci. 1995. Toward an outline of the topography of a realistic protein-folding funnel. *Proc Natl Acad Sci U S A*. 92:3626-3630.

Pahl, H.L., and P.A. Baeuerle. 1997. Endoplasmic-Reticulum-Induced Signal Transduction and Gene Expression. *Trends in Cell Biol.* 7:50-55.

Peters, R.J., A.K. Shiau, J.L. Sohl, D.E. Anderson, G. Tang, J.L. Silen, and D.A. Agard. 1998. Pro region C-terminus:protease active site interactions are critical in catalyzing the folding of alpha-lytic protease. *Biochemistry*. 37:12058-12067.

Pilon, M., R. Schekman, and K. Romisch. 1997. Sec61p mediates export of a misfolded secretory protein from the endoplasmic reticulum to the cytosol for degradation. *EMBO J*. 16:4540-4548.

Plempner, R.K., S. Bohmler, J. Bordallo, T. Sommer, and D.H. Wolf. 1997. Mutant analysis links the translocon and BiP to retrograde protein transport for ER degradation. *Nature*. 388:891-895.

Plempner, R.K., and D.H. Wolf. 1999. Retrograde protein translocation: ERADication of secretory proteins in health and disease. *Trends Biochem Sci.* 24:266-270.

Power, S.D., R.M. Adams, and J.A. Wells. 1986. Secretion and autoproteolytic maturation of subtilisin. *Proc. Natl Acad. Sci. USA*. 83:3096-3100.

Prabakaran, D., P.S. Kim, V.M. Dixit, and P. Arvan. 1996. Oligomeric assembly of thrombospondin in the endoplasmic reticulum of thyroid epithelial cells. *Eur J Cell Biol.* 70:134-141.

Prusiner, S.B. 1998. Prions. *Proc Natl Acad Sci U S A*. 95:13363-13383.

Prusiner, S.B., M.R. Scott, S.J. DeArmond, and F.E. Cohen. 1998. Prion protein biology. *Cell*. 93:337-348.

Ptitsyn, O.B., R.H. Pain, G.V. Semisotnov, E. Zerovnik, and O.I. Razgulyaev. 1990. Evidence for a molten globule state as a general intermediate in protein folding. *FEBS Lett.* 262:20-24.

Qu, D., J.H. Teckman, S. Omura, and D.H. Perlmutter. 1996. Degradation of a mutant secretory protein, alpha1-antitrypsin Z, in the endoplasmic reticulum requires proteasome activity. *J Biol. Chem.* 271:22791-22795.

- Radford, S.E., and C.M. Dobson. 1999. From computer simulations to human disease: emerging themes in protein folding. *Cell*. 97:291-298.
- Ramirez, F. 1996. Fibrillin mutations in Marfan syndrome and related phenotypes. *Curr Opin Genet Dev*. 6:309-315.
- Rapoport, T.A., M.M. Rolls, and B. Jungnickel. 1996. Approaching the mechanism of protein transport across the ER membrane. *Curr Opin Cell Biol*. 8:499-504.
- Reddy, P.S., and R.B. Corley. 1998. Assembly, sorting, and exit of oligomeric proteins from the endoplasmic reticulum. *Bioessays*. 20:546-554.
- Rehemtulla, A., A.J. Dorner, and R.J. Kaufman. 1992. Regulation of PACE propeptide-processing activity: requirement for a post-endoplasmic reticulum compartment and autoprolytic activation. *Proc. Natl Acad. Sci. USA*. 89:8235-8239.
- Roos, N. 1988. A possible site of calcium regulation in rat exocrine pancreas cells: an X-ray microanalytical study. *Scan. Micro*. 2:323-329.
- Rothman, J.E. 1989. Polypeptide chain binding proteins: catalysts of protein folding and related processes in cells. *Cell*. 59:591-601.
- Sambrook, J.F. 1990. The involvement of calcium in transport of secretory proteins from the endoplasmic reticulum. *Cell*. 61:197-199.
- Sauter, N.K., T. Mau, S.D. Rader, and D.A. Agard. 1998. Structure of alpha-lytic protease complexed with its pro region. *Nat Struct Biol*. 5:945-950.
- Sawyer, J.T., T. Lukaczyk, and M. Yilla. 1994. Dithiothreitol treatment induces heterotypic aggregation of newly synthesized secretory proteins in HepG2 cells. *J Biol. Chem*. 269:22440-22445.
- Scales, S.J., R. Pepperkok, and T.E. Kreis. 1997. Visualization of ER-to-Golgi transport in living cells reveals a sequential mode of action for COPII and COPI. *Cell*. 90:1137-1148.
- Schafer, W., A. Stroh, S. Berghofer, J. Seiler, M. Vey, M.L. Kruse, H.F. Kern, H.D. Klenk, and W. Garten. 1995. Two independent targeting signals in the cytoplasmic domain determine trans-Golgi network localization and endosomal trafficking of the proprotein convertase furin. *EMBO J*. 14:2424-2435.
- Schägger, H., and G. von Jagow. 1987. Tricine-sodium dodecyl sulfate-polyacrylamide gel electrophoresis for the separation of proteins in the range from 1 to 100 kDa. *Anal. Biochem*. 166:369-379.
- Seidah, N.G., and M. Chretien. 1997. Eukaryotic protein processing: endoproteolysis of precursor proteins. *Curr Opin Biotechnol*. 8:602-607.
- Seidah, N.G., M. Chretien, and R. Day. 1994. The family of subtilisin/kexin like pro-protein and pro-hormone convertases: divergent or shared functions. *Biochimie*. 76:197-209.
- Seidah, N.G., J. Hamelin, M. Mamarbachi, W. Dong, H. Tardos, M. Mbikay, M. Chretien, and R. Day. 1996. cDNA structure, tissue distribution, and chromosomal localization of rat PC7, a novel mammalian proprotein convertase closest to yeast kexin-like proteinases. *Proc. Natl Acad. Sci. USA*. 93:3388-3393.

- Seksek, O., J. Biwersi, and A.S. Verkman. 1995. Direct measurement of trans-Golgi pH in living cells and regulation by second messengers. *J. Biol. Chem.* 270:4967-4970.
- Shakhnovich, E., V. Abkevich, and O. Ptitsyn. 1996. Conserved residues and the mechanism of protein folding. *Nature.* 379:96-98.
- Shakhnovich, E.I. 1997. Theoretical studies of protein-folding thermodynamics and kinetics. *Curr Opin Struct Biol.* 7:29-40.
- Shinde, U., X. Fu, and M. Inouye. 1999. A pathway for conformational diversity in proteins mediated by intramolecular chaperones. *J Biol. Chem.* 274:15615-15621.
- Shinde, U., and M. Inouye. 1993. Intramolecular chaperones and protein folding. *Trends Biochem Sci.* 18:442-446.
- Shinde, U.P., J.J. Liu, and M. Inouye. 1997. Protein memory through altered folding mediated by intramolecular chaperones. *Nature.* 389:520-522.
- Sidrauski, C., R. Chapman, and P. Walter. 1998. The unfolded protein response: an intracellular signalling pathway with many surprising features. *Trends Cell Biol.* 8:245-249.
- Siezen, R.J., J.W. Creemers, and W.J. Van de Ven. 1994. Homology modelling of the catalytic domain of human furin. A model for the eukaryotic subtilisin-like proprotein convertases. *Eur J Biochem.* 222:255-266.
- Siezen, R.J., J.A.M. Leunissen, and U. Shinde. 1995. Homology Analysis of the Propeptides of Subtilisin-Like Serine Proteases (Subtilases). In *Intramolecular Chaperones and Protein Folding*. U. Shinde and M. Inouye, editors. R. G. Landes Company, Austin, TX. 233-252.
- Silen, J.L., D. Frank, A. Fujishige, R. Bone, and D.A. Agard. 1989. Analysis of prepro-alpha-lytic protease expression in *Escherichia coli* reveals that the pro region is required for activity. *J. Bact.* 171:1320-1325.
- Smeeckens, S.P. 1993. Processing of protein precursors by a novel family of subtilisin-related mammalian endoproteases. *Bio/Technology.* 11:182-186.
- Sohl, J.L., S.S. Jaswal, and D.A. Agard. 1998. Unfolded conformations of alpha-lytic protease are more stable than its native state. *Nature.* 395:817-819.
- Sohl, J.L., A.K. Shiau, S.D. Rader, B.J. Wilk, and D.A. Agard. 1997. Inhibition of alpha-lytic protease by pro region C-terminal steric occlusion of the active site. *Biochemistry.* 36:3894-3902.
- Sommer, T., and D.H. Wolf. 1997. Endoplasmic reticulum degradation: reverse protein flow of no return. *FASEB J.* 11:1227-1233.
- Song, L., and L.D. Fricker. 1995. Calcium- and pH-dependent aggregation of carboxypeptidase E. *J. Biol. Chem.* 270:7963-7967.
- Sorensen, S.O., H.B. van den Hazel, M.C. Kielland-Brandt, and J.R. Winther. 1994. pH-dependent processing of yeast procarboxypeptidase Y by proteinase A in vivo and in vitro. *Eur. J. of Biochem.* 220:19-27.

- Sousa, M., and A.J. Parodi. 1995. The molecular basis for the recognition of misfolded glycoproteins by the UDP-Glc:glycoprotein glucosyltransferase. *EMBO J.* 14:4196-4203.
- Steiner, D.F. 1998. The proprotein convertases. *Curr Opin Chem Biol.* 2:31-39.
- Steiner, D.F., S.P. Smekens, S. Ohagi, and S.J. Chan. 1992. The new enzymology of precursor processing endoproteases. *J. Biol. Chem.* 267:23435-23438.
- Strausberg, S., P. Alexander, L. Wang, F. Schwarz, and P. Bryan. 1993. Catalysis of a protein folding reaction: thermodynamic and kinetic analysis of subtilisin BPN' interactions with its propeptide fragment. *Biochem.* 32:8112-8119.
- Suter, U., J.V. Heymach, Jr., and E.M. Shooter. 1991. Two conserved domains in the NGF propeptide are necessary and sufficient for the biosynthesis of correctly processed and biologically active NGF. *EMBO J.* 10:2395-2400.
- Takahashi, S., T. Nakagawa, T. Banno, T. Watanabe, K. Murakami, and K. Nakayama. 1995. Localization of furin to the trans-Golgi network and recycling from the cell surface involves Ser and Tyr residues within the cytoplasmic domain. *J. Biol. Chem.* 270:28397-28401.
- Teasdale, R.D., and M.R. Jackson. 1996. Signal-mediated sorting of membrane proteins between the endoplasmic reticulum and the golgi apparatus. *Annu Rev Cell Dev Biol.* 12:27-54.
- Thomas, G., S.S. Molloy, E.D. Anderson, and L. Thomas. 1995a. Multi-Step Activation of Furin: A Model for the Eukaryotic Proprotein Convertases. In *Intramolecular Chaperones and Protein Folding*. U. Shinde and M. Inouye, editors. R. G. Landes Company, Austin, TX. 157-179.
- Thomas, P.J., B.H. Qu, and P.L. Pedersen. 1995b. Defective protein folding as a basis of human disease. *Trends Biochem Sci.* 20:456-459.
- Thorne, B.A., L.W. Caton, and G. Thomas. 1989. Expression of mouse proopiomelanocortin in an insulinoma cell line. Requirements for beta-endorphin processing. *J. Biol. Chem.* 264:3545-3552.
- Thorne, B.A., and G.D. Plowman. 1994. The heparin-binding domain of amphiregulin necessitates the precursor pro-region for growth factor secretion. *Mol. Cell. Biol.* 14:1635-1646.
- Valls, L.A., J.R. Winther, and T.H. Stevens. 1990. Yeast carboxypeptidase Y vacuolar targeting signal is defined by four propeptide amino acids. *J. Cell Biol.* 111:361-368.
- Van de Ven, W.J., A.J. Roebroek, and H.L. Van Duijnhoven. 1993. Structure and function of eukaryotic proprotein processing enzymes of the subtilisin family of serine proteases. *Critical Reviews in Oncogenesis.* 4:115-136.
- VanSlyke, J.K., L. Thomas, and G. Thomas. 1995. Use of Vaccinia Virus Vectors to Study Neuropeptide Processing. In *Peptidases and Neuropeptide Processing*. Vol. 23. A.I. Smith, editor. Academic Press, San Diego. 45-64.
- Vey, M., W. Schafer, S. Berghofer, H.D. Klenk, and W. Garten. 1994. Maturation of the trans-Golgi network protease furin: compartmentalization of propeptide removal, substrate cleavage, and COOH-terminal truncation. *J. Cell Biol.* 127:1829-1842.

- Vidricaire, G., J.B. Denault, and R. Leduc. 1993. Characterization of a secreted form of human furin endoprotease. *Biochem Biophys Res Commun.* 195:1011-1018.
- Vindrola, O., and I. Lindberg. 1992. Biosynthesis of the prohormone convertase mPC1 in AtT-20 cells. *Mol. Endo.* 6:1088-1094.
- Vollenweider, F., F. Kappeler, C. Itin, and H.P. Hauri. 1998. Mistargeting of the lectin ERGIC-53 to the endoplasmic reticulum of HeLa cells impairs the secretion of a lysosomal enzyme. *J Cell Biol.* 142:377-389.
- Voorhees, P., E. Deignan, E. van Donselaar, J. Humphrey, M.S. Marks, P.J. Peters, and J.S. Bonifacino. 1995. An acidic sequence within the cytoplasmic domain of furin functions as a determinant of trans-Golgi network localization and internalization from the cell surface. *EMBO J.* 14:4961-4975.
- Wagner, C., and T. Kiefhaber. 1999. Intermediates can accelerate protein folding. *Proc Natl Acad Sci U S A.* 96:6716-6721.
- Wan, L., S.S. Molloy, L. Thomas, G. Liu, Y. Xiang, S.L. Rybak, and G. Thomas. 1998. PACS-1 defines a novel gene family of cytosolic sorting proteins required for trans-Golgi network localization. *Cell.* 94:205-216.
- Warren, G., and I. Mellman. 1999. Bulk flow redux? *Cell.* 98:125-127.
- Watanabe, M., A. Hirano, S. Stenglein, J. Nelson, G. Thomas, and T.C. Wong. 1995. Engineered serine protease inhibitor prevents furin-catalyzed activation of the fusion glycoprotein and production of infectious measles virus. *J. of Virology.* 69:3206-3210.
- Wiertz, E.J., D. Tortorella, M. Bogoy, J. Yu, W. Mothes, T.R. Jones, T.A. Rapoport, and H.L. Ploegh. 1996. Sec61-mediated transfer of a membrane protein from the endoplasmic reticulum to the proteasome for destruction. *Nature.* 384:432-438.
- Wolins, N., H. Bosshart, H. Kuster, and J.S. Bonifacino. 1997. Aggregation as a determinant of protein fate in post-Golgi compartments: role of the luminal domain of furin in lysosomal targeting. *J Cell Biol.* 139:1735-1745.
- Wu, X., N. Sakata, K.M. Lele, M. Zhou, H. Jiang, and H.N. Ginsberg. 1997. A two-site model for ApoB degradation in HepG2 cells. *J Biol. Chem.* 272:11575-11580.
- Zapun, A., S.M. Petrescu, P.M. Rudd, R.A. Dwek, D.Y. Thomas, and J.J. Bergeron. 1997. Conformation-independent binding of monoglucosylated ribonuclease B to calnexin. *Cell.* 88:29-38.
- Zhou, A., S. Martin, G. Lipkind, J. LaMendola, and D.F. Steiner. 1998. Regulatory roles of the P domain of the subtilisin-like prohormone convertases. *J Biol. Chem.* 273:11107-11114.
- Zhou, A., L. Paquet, and R.E. Mains. 1995. Structural elements that direct specific processing of different mammalian subtilisin-like prohormone convertases. *J Biol. Chem.* 270:21509-21516.
- Zhu, X.L., Y. Ohta, F. Jordan, and M. Inouye. 1989. Pro-sequence of subtilisin can guide the refolding of denatured subtilisin in an intermolecular process. *Nature.* 339:483-484.